치의과학 박사학위논문

Analysis of surface characteristics of ceramic and tooth structures by plasma treatment and its effect on adhesion

플라즈마 처리가 세라믹 및 치질의 표면 특성과 접착력에 미치는 효과 분석

2017 년 8 월

서울대학교 대학원

치의과학과 치과생체재료과학 전공

한 금 준

Analysis of surface characteristics of ceramic and tooth structures by plasma treatment and its effect on adhesion

지도교수 조 병 훈

이 논문을 치의과학 박사학위논문으로 제출함
2017 년 4 월

서울대학교 대학원
치의과학과 치과생체재료과학 전공
한 금 준

한금준의 박사학위논문을 인준함
2017년 6 월

위 원 장 _____ (인)

부위원장 _____ (인)

위 원 _____ (인)

위 원 _____ (인)

위 원 _____ (인)

Abstract

Analysis of surface characteristics of ceramic and tooth structures by plasma treatment and its effect on adhesion

Geum-Jun Han

Division of Dental Biomaterials Science,

Department of Dental Science,

The Graduate School, Seoul National University

(Directed by Prof. Byeong-Hoon Cho, D.D.S., Ph D.)

Objective : Atmospheric pressure plasma can easily change the surface properties of substrates using a low cost and environment-friendly dry process of a simple system. For adhesion, plasma can also be used to implement chemically active species on the substrate surface by inducing polar functional groups or through ion bombardment. The purpose of this study is to evaluate the effectiveness of plasma polymer coating on the bond strength of composite resin to ceramic, as well as the direct effects of plasma on the adhesion of resin composite to tooth structures and the durability of the bond.

Methods : The effect of plasma polymer coating was evaluated using shear bond strength (SBS) and micro-shear bond strength (MSBS) tests. The plasma coated

surfaces were characterized using Fourier transform infra-red (FTIR) spectrophotometer in an attenuated total reflectance (ATR) mode, X-ray photoelectron spectroscopy (XPS), and contact angle measurements. The fractured surfaces were evaluated using a stereomicroscope and scanning electron microscopy (SEM) with energy dispersive spectroscopy (EDS), and also the chemical structure and composition of the surface were verified using Focused ion beam (FIB), transmission electron microscopy (TEM) and EDS respectively.

The direct effect of plasma on the adhesion of resin composite to dentin was evaluated using micro-tensile bond strength (MTBS) tests, before and after thermocycling (TC). The bond strength data were interpreted using Weibull analysis. The hybrid layer formation at the adhesive/dentin interface was characterized by micro-Raman spectroscopy and SEM analyses.

Results : Among the groups treated with plasma polymer coating, the SBS of the adhesive to the ceramic surface pre-treated sequentially with water and triethyleneglycol dimethacrylate (TEGDMA) plasma in helium gas was significantly higher than that of the adhesive to the untreated surface ($p < 0.05$). Also, the SBS obtained with the plasma deposition of TEGDMA at the highest input voltage was statistically similar to the gold standard by HF etching and silane coupling agent coating. Plasma deposition of 1,3-butadiene was effective at flow rates of more than 2 standard cubic centimeters (sccm). The SBS obtained with the sequential plasma deposition of hexamethyldisiloxane (HMDSO) and benzene was statistically similar to the gold standard by HF etching and silane coupling agent coating. The sequential plasma deposition of TMS and benzene also showed about two times higher bond strength values than that of Z-Prime Plus.

The plasma polymer deposition of benzene and 1,3-butadiene improved the

MSBS of resin composite to enamel ($p < 0.05$). The procedure improved enamel adhesion but failed to improve durability in terms of mean bond strength. However, the plasma polymer deposition increased the Weibull modulus (*m)* after TC, which indicated that the scatter of the bond strength was narrowed with respect to durability. However, future studies to evaluate solubility of the plasma-deposited polymers will be necessary in the point of toxicity.

In the dentin, the plasma-drying groups presented significantly higher bond strength than the wet bonding and dry bonding groups, either with or without rewetting ($p < 0.05$). Micro-Raman spectral analysis indicated that plasma-drying improved the penetration and polymerization efficacy of the adhesive. Even after TC, the bond strength of plasma-drying group did not reduce.

Conclusion : Plasma polymer coating technique could contribute to enhance the bonding of conventional dental adhesives on the surface of ceramic and tooth structures. In particular, 1,3-butadiene or benzene enhanced the adhesion of composite resin through the simple deposition of C=C double bonds.

On the dentin surface, the plasma treatment using a He gas, with or without rewetting, improved the adhesion of resin composite to dentin and its durability.

Plasma application in adhesion of resin composite to the ceramic and tooth structures will be a promising method.

Keywords : Plasma treatment, Ceramic, Tooth structures, Adhesion, Polymer deposition, Durability

Student Number : 2013-21808

Contents

Acknowledgement: As a graduate student of Seoul National University, I declare that the contents of this PhD thesis were compiled from those of eight following publications of the research results during my degree program and re-organized in view-points of adhesion substrates and plasma equipments.

1. Cho BH, Han GJ, Oh KH, Chung SN, Chun BH. The effect of plasma polymer coating using atmospheric-pressure glow discharge on the shear bond strength of composite resin to ceramic. J Mater Sci 2011;46:2755-2763.
2. Han GJ, Chung SN, Chun BH, Kim CK, Oh KH, Cho BH. Effect of the applied power of atmospheric pressure plasma on the adhesion of composite resin to dental ceramic. J Adhes Dent 2012;14:461-469.
3. Han GJ, Chung SN, Chun BH, Kim CK, Oh KH, Cho BH. 1,3-Butadiene as an Adhesion Promoter Between Composite Resin and Dental Ceramic in a Dielectric Barrier Discharge Jet. Plasma Chem Plasma Process 2013;33:539-551.
4. Han GJ, Kim JH, Kim CK, Chung SN, Chun BH, Cho BH. Sequential deposition of Hexamethyldisiloxane and benzene in non-thermal plasma adhesion to dental ceramic. Macromol Res 2013;21:1118-1126.
5. Han GJ, Kim JH, Chung SN, Chun BH, Kim CK, Cho BH. Effect of plasma deposition using low-power/non-thermal atmospheric pressure plasma on promoting adhesion of composite resin to enamel. Plasma Chem Plasma Process 2014;34:933-947.
6. Han GJ, Kim JH, Chung SN, Chun BH, Kim CK, Seo DG, Son HH, Cho BH. Effect of non-thermal atmospheric pressure pulsed plasma on the adhesion and durability of resin composite to dentin. Eur J Oral Sci 2014;122:417-423.

7. Kim JH, Han GJ, Kim CK, Oh KH, Chung SN, Chun BH, Cho BH. Promotion of adhesive penetration and resin bond strength to dentin using non-thermal atmospheric pressure plasma. Eur J Oral Sci 2016;124:89-95.
8. Han GJ, Kim JH, Cho BH, Oh KH, Jeong JJ. Promotion of resin bonding to dental zirconia ceramic using plasma deposition of tetramethylsilane and benzene. Eur J Oral Sci. 2017;125:81-87.

1. Introduction

The interest in aesthetics, biological safety, cost and the efficacy of dental care is becoming greater with time. Feldspathic ceramic has excellent esthetic properties, and biocompatibility, and major emphasis in research have been directed toward the enhancement of its strength and aesthetic properties. So many ceramic restorations are still the most commonly used restorations in fixed prosthodontics.[1] In order to adhesive the feldspathic ceramic in oral cavity, etching of the feldspathic ceramic surface with hydrofluoric acid (HF) and coating with silane coupling agent on it has been recommended as a reliable protocol for ceramic bonding of resin composites and cements.[2,3] However, because the procedure was complicated and required toxic chemicals, various ceramic bonding techniques such as silica coating were introduced.[4,5] Also, it has also been shown to have a weakening effect on the flexural strength which is in contrast to state of the rough feldspathic ceramic surface after HF surface treatment.[6]

Zirconia ceramics have been increasingly used for dental crowns and bridges due to their superior mechanical properties and good esthetics.[52] In addition, the development in dental computer-aided design and manufacturing (CAD/CAM) technology has contributed to the popularity of zirconia ceramics as substitutions for dental metal alloys.[53] Zirconia prostheses can be cemented with conventional luting cements such as glass-ionomer cements. However, the expanded application of zirconia, e.g. partial coverage crown and resin-bonded fixed partial denture, requires a reliable bond of resin-based materials to zirconia surface for improving retention and marginal seal.[54] A limitation of zirconia restorations is poor resin bonding to their surfaces due to the chemical inertness and low surface energy.[55-57]

Various methods for improving resin bonding to zirconia surfaces have been proposed, such as glass micro-pearls coating,[80] selective infiltration etching,[58] and a vapor phase deposition technique,[57] but these methods have still not been adopted for practical applications. In clinical practice, the use of airborne-particle abrasion and primers containing phosphate ester has been recommended for improving resin bonding to zirconia restorations.[55,59,60,61] However, there is still clinical concern about obtaining a reliable bond to zirconia.

Since Buonocore introduced enamel bonding technique using a phosphoric acid etching procedure, various adhesion strategies have evolved with the development of esthetic restorative materials and dental adhesive systems. Because restorative materials such as ceramics and resin composites and tooth substrates that consist of enamel and dentin are heterogenic in their structures and compositions, complicated and substrate-specific adhesion strategies have been contemplated.[2,74,75,76] The complexity of the substrates, restorative materials, and adhesion procedures makes dental adhesion difficult and the bonding technique sensitive. There are also problems in durability under the harsh oral environment, where the bonding is continually exposed to thermal and mechanical stresses as well as to hydrolytic attacks from wet conditions.[77,78,79] As an adherend, enamel mainly consists of highly mineralized inorganic hydroxyapatite crystals with a small portion of organic components and water. It is more similar to ceramic than dentin.

Most current dental adhesive systems show favorable immediate results in terms of bond strength.[90] However, the adhesive interface is the weakest link within the adhesion complex of tooth-colored restorations, and the durability of aged resin-dentin adhesion is questionable. Previous long-term studies have shown that the

bond strength of resin to dentin decreases over time.[90,107] A new strategy to produce a long-term durable dentin adhesion is needed.

Dentin adhesive systems include the physical and chemical modifications of tooth substrates using either acids (etch-and-rinse technique) or acidic monomers (self-etch technique).[121, 122] The etch-and-rinse technique is the most common technique used by dental practitioners and provides a reliable adhesion to enamel.[90] However, dentin adhesion with etch-and-rinse adhesive systems has proved to be less predictable and more sensitive to the clinician's technique due to the morphological and physiological heterogeneity of dentin.[90,92,122,123] After acid etching, the demineralized dentin surface should be kept hydrated to prevent the exposed collagen network from collapsing prior to an adequate infiltration of adhesive monomers; this clinical technique is referred to as the wet bonding technique. [124,125] However, the extent of hydration of demineralized dentin is difficult to standardize for optimal performance of adhesive systems in clinical practice. Therefore, adjunctive approaches, such as the use of an electric device and collagen cross-linking agents, have been investigated to improve the adhesive penetration into the dentin surface and stabilize the hybrid layer.[126-128]

Plasma is recognized as a state of matter together with gases, liquids, and solids.[7] More or less ionized gas in plasma consists of electrons, ions, and neutral components in fundamental and excited states.[8,9] Plasmas are electrically neutral, but they contain free charge carriers and are electrically conductive and chemically active. They are classified as either cold or thermal, depending on their activation method and working power.[8] Due to the wide range of temperatures they emit, plasma technology has been used for various applications such as surface treatments and coatings, waste destruction, gas treatments, chemical synthesis,

machining, and high-precision mass spectrometric analysis by plasma-source.[7,8,10] Thermal plasmas, especially arc plasma, have been extensively industrialized[8]. In the dental field, non-thermal atmospheric pressure plasma (NT-APP) have been studied for the purposes of modifying titanium implant surfaces,[13,14] improving mechanical properties of fiber-reinforced acrylic resin materials,[15] and increasing bond strength between fiber posts and core resin (16) and between composite luting agents and ceramics.[17] Recently, plasma has attracted attention in the biomedical field.[108,109] The term 'plasma' refers to a partially ionized gas and is also known as the fourth state of matter.[110] Plasma is widely used in modern industries for surface treatments, which include cleaning, activation, and deposition of thin films.[111] Among various types of artificially generated plasmas, NT-APP, which has a relatively low temperature and does not require a vacuum system, has garnered attention in the biomedical field.

The floating-electrode dielectric barrier discharge (FE-DBD) is one of the most prevalent types of plasma-chemical reactors used to generate NT-APP since the self-pulsed discharges from the dielectric layers prevent the discharge current from increasing to a level that induces arcing.[18,19] Since the first report of NT-APP in 1968, FE-DBD in atmospheric air has been explored in many applied fields ranging from industry to biology and medicine.[20] FE-DBD in air at atmospheric pressure can also easily make a polymer surface hydrophilic by increasing surface roughness and the content of oxygen-containing functional groups using a simple system, low cost, and an environment-friendly dry process, because it needs no water.[21] FE-DBD treatment using gases such as He, O_2, and N_2 can improve adhesion between polymer and metal and between polymers.[4,21]

Plasmas can be used to modify the chemical characteristics of the exposed

topmost surface without affecting the material properties.[8,22] For adhesion, plasma can also be used to implement chemically active species on the substrate surface by inducing polar functional groups or through ion bombardment.[23-25] Ritts *et al*. introduced a dentin surface treatment technique using a non-thermal argon plasma brush for dentin bonding.[26] They ascribed the 64% increase of micro-tensile dentin bond strength after 30 seconds of plasma treatment to an increase in carbonyl groups. Nishigawa *et al*. showed that for the repair of a fractured denture base, the plasma treatment of the heat-cured acrylic resin surface exhibited significantly higher shear bond strength than that of the control group, even though the plasma equipment was operated under atmospheric pressure and with no special gas.[27] They also reported that surface treatment of conventional polymers in an inert-gas glow discharge reactor results in chemical changes of the substrate surface; plasma surface modification procedures allow formation of stronger bonds, improve wettability, and produce chemically active sites for adhesion of other molecules.[9,28,29] They also reported on the long-term reliability of the adhesion.[82]

The physical surface etching and chemical grafting of oxygen-containing groups to substrate surfaces,[4,21,30] the deposition process known as 'plasma enhanced chemical vapor deposition (PECVD)' has also been widely used to enhance adhesion in micro- and nano-fabrication fields.[2,29,31] The excellent adhesion imparted by the deposition mechanism of a plasma polymer to a substrate can be utilized to improve the adhesion characteristics of other materials.[2] Plasma polymers have been suggested to be adhesion promoters for any kind of substrate materials and to provide water resistivity of adhesion.[2] Therefore, NT-APP may be used to improve the adhesion effectiveness and durability between various restoratives and tooth substrates. However, only a few studies have attempted to

use the NT-APP for dental applications such as cavity preparation and bleaching.[9,32] In our laboratory, a small pencil-type plasma torch that can be used to apply plasma or plasma polymers directly to teeth or restoratives in a patient's mouth and to modify the surfaces of restoratives or implants at chair-side was designed.

Parameters of plasma operation such as electrode configuration, gas flow rate, gas type, applied power, and the distance between the plasma applicator nozzle and the substrate surface are known to influence the properties of the deposited coating.[31,33] By altering the process parameters, a wide range of thicknesses, surface activities, solubilities, dielectric properties, and cross-linking densities of polymer coatings can be obtained.[21,31,29] Several adhesion mechanisms in PECVD, such as diffusion of polymer chains and functional groups for chemical reactions and formation of a stable interfacial adhesion layer and strong bonds, need to be induced at the interface.[9,29]

Using plasma polymerization and surface deposition of specific monomers, adhesion promotion was also suggested to be mediated by the plasma polymers containing functional groups.[17,80,81] Non-thermal atmospheric pressure helium plasmas to dental ceramic adhesion with or without monomers and observed increased bond strengths through increases in the number of hydrophilic groups and in the chemical interaction of C=C double bonds. Previously, Derand *et al*. and Piascik *et al*. improved the bond strengths of resin composite cements to alumina and zirconia ceramics with plasma spray coating of hexamethyldisiloxane (HMDSO) using radiofrequency plasma devices in vacuum reactors.[17,80,81] The plasma polymers deposited on a substrate surface are known to be densely cross-linked and water resistant,[83] and as a result, may contribute to the durability of the

plasma adhesion.

FE-DBD is a “direct” plasma method, in which both excited species and charged species can be transferred directly to the substrate surface in atmospheric conditions.[34] This makes the equipment more flexible for depositing films on various types of surfaces and particularly suitable for local film deposition with low temperature, high plasma stability, efficient reaction chemistry, and low energy consumption.[34,35] They also need to evaporate easily due to their low molecular weight. 1,3-butadiene, a small hydrocarbon, is in a gas state at room temperature and has two aliphatic C=C double bonds that are easily broken by plasma energy to yield active radicals. Also, adhesion promotion has been enhanced using PECVD with organosilicons such as HMDSO, tetraethyl orthosilicate, and octamethylcyclotetrasiloxane.[28,36] Using atmospheric PECVD, HMDSO was suggested to deposit layers which contained Si-O-Si components and -$[CH_2$-CH_2-$]_n$ units, where the former provided stability and the latter provided polymeric chains for subsequent chemical-crosslinking reactions.[28] In the dental field, plasma treatment with HMDSO in a radiofrequency plasma reactor was also reported to improve the adhesion to aluminum oxide ceramic surfaces, although they failed to confirm siloxane (-Si-O-Si-O-) networks[17]. Plasma deposition in FE-DBD was highly system-dependent, so that parameters including the design of plasma jet, applied power, process gas and precursor monomers must be investigated for each system.[31,33,37]

Plasma, the fourth state of matter, has been adopted to modern industries for surface engineering such as cleaning, etching, adhesion enhancement, and deposition of thin films.[129] Recently, NT-APP has a relatively low temperature and thus, when optimally controlled, can induce changes in the surface characteristics

of substrates without heat damage[131]. The non-destructive property of NT-APP is particularly attractive for dental applications in which heat sensitive substrates, such as teeth, ceramics, and resin composites, are frequently involved. Plasma treatment could increase the hydrophilicity of dentin and allow for better penetration of the adhesive into the demineralized dentin surface.[26,120,132]

Plasma treatments are widely used for the surface activation of polymers prior to coating, painting, and bonding processes.[131] A large amount of chemically active species in plasmas are able to increase the surface energy and optimize the surface chemistry of substrates without affecting their bulk properties. In dentistry, several researchers have attempted to apply plasma treatments for improving resin bonding to glass fibers, fiber-reinforced composites, glass ceramics, and polycrystalline ceramics.[17,114,115] However, there have been few attempts to use plasma treatment to improve bonding to zirconia by chemically functionalizing its surface.[80,81] Organosilane coating is a well-established method to improve adhesion between inorganic substrates (e.g., metals and ceramics) and organic polymers (e.g., resin composites). However, conventional silane chemistry is not effective for zirconia because it is more chemically stable than silica-containing ceramics and not readily hydrolyzed.

Therefore, the purpose of this study is:

*Adhesion to ceramic

First, to evaluate the effectiveness of plasma polymer coating using NT-APP jet on the shear bond strength of composite resin to feldspathic porcelain. Second, to investigate the effect of the applied audiofrequency (a.f.) power on the chemical composition of the plasma polymer on the ceramic surface and the adhesive strength between the composite resin and the feldspathic porcelain. Third, to

investigated the effects of adhesion enhancement of plasma deposition with 1,3-butadiene on the ceramic surface using an experimental FE-DBD jet. Fourth, to investigate whether HMDSO and benzene were effective precursor monomers in dental ceramic adhesion, when they were deposited using a FE-DBD jet. Fifth, to investigate the effect of plasma deposition of an organosilane and benzene on resin bonding to a dental zirconia ceramic.

*Adhesion to tooth

First, to investigate the effect of monomer deposition using a low-power, non-thermal atmospheric pressure plasma on adhesion of resin composite to enamel and its durability. Second, to investigate the effects of low-power, NT-APP treatments in pulsed and conventional modes on the adhesion of resin composite to dentin and the durability of the bond. Third, to investigate the effect of plasma-drying on the bond strength of an etch-and-rinse adhesive to dentin as compared to that of the contemporary wet bonding technique.

Based on these research objectives, we have studied a plasma processing technique that maintains durability in high humid environment, maintains excellent adhesive power, and has high biocompatibility even in the oral environment with high temperature changes. For the purpose, we evaluated the effect of plasma treatment on the adhesion and its durability by measuring adhesion strength immediately and after thermocycling, and the effect was interpreted by characterizing surface changes with microscopic and chemical analyses.

For the purpose, the effect of plasma adhesion on the bond strength of composite resin to ceramic was evaluated by measuring shear bond strength (SBS) using the iris method.[38] In case of enamel and dentin, they were evaluated by measuring microshear bond strength (MSBS) and microtensile bond strength (MTBS),

respectively. The effect of plasma treatment was also compared with that of a commercially available primer for zirconia using MSBS measurements. The durability of the bond strengths were also compared using Weibull analysis. The hydrophilicity of plasma coated ceramic surfaces were characterized using contact angle measurements. The chemical composition of the plasma polymer deposited on ceramic surfaces was evaluated using Fourier transform infra-red spectrophotometer (FTIR) in an attenuated total reflectance (ATR) mode and X-ray photoelectron spectroscopy (XPS). The fractured surfaces were observed under a stereomicroscope and for selected specimens they were evaluated using scanning electron microscopy (SEM) and energy dispersive spectroscopy (EDS). From the specimens prepared using a focused ion beam (FIB) technique, the structure and composition were also verified with transmission electron microscopy (TEM) and energy dispersive spectroscopy (EDS), respectively. The plasma treated zirconia surfaces were also characterized by XPS, and the plasma-polymerized layers were verified with a TEM using FIB micromachining and EDS. The hybrid layer formation at the adhesive/dentin interface was also characterized by micro-Raman spectroscopy and SEM analyses.

2. MATERIALS AND METHODS

1) ADHESION TO CERAMIC

1.1 The effect of plasma polymer coating using non-thermal atmospheric pressure plasma (NT-APP) jet on the shear bond strength of composite resin to ceramic

1.1.1 Equipment Set-up

The NT-APP shown in Figure1a is composed of three parts: a mass flow system, a plasma torch, and a reactor for plasma polymer deposition. The pencil-type plasma torch is composed of an outer ceramic tube (4 mm in inner diameter) wrapped with a ground electrode and an inner ceramic needle tube (2 mm in diameter) containing a hot metal rod electrode that passes through the center of the outer tube. Helium (He) was delivered into the tube at a flow rate of 2 L/min as a carrier gas, carrying vaporized distilled water (DW) for cleaning and HMDSO or triethyleneglycol dimethacrylate (TEGDMA) for plasma polymerization, after passing through a glass bubbler. Between the metal rod electrode and the ground electrode connected around the tip of the ceramic tube, a radio frequency (RF) voltage of 2 kV was applied at 15 kHz. For standardization, the flow rate of the vaporized water and monomers was controlled at a rate of 50 standard cubic centimeters (sccms) using a mass flow controller (FC7700C, Aera Japan, Hachioji, Japan). The distance between the surface of the porcelain sample and the tip of the plasma torch could be adjusted according to the deposition rate of the plasma polymer and the cleaning effects.

1.1.2 Adhesion Test

Fifty pressed CAD/CAM ceramic blocks (8 x 10 x 15 mm) of feldspathic porcelain (VITABlOCS Mark II for CEREC/inLab, 2M2C I10, Lot No. 14800; Vita Zahfabrik, Bad Sackingen, Germany) were embedded in acrylic molds with self-curing acrylic resin. In order to create uniform surface roughness and parallel surface geometry for shear loading, the top surfaces of the ceramic blocks were polished with 500 grit silicon carbide abrasive paper (Buehler Ltd, Lake Bluff, IL, USA) under running water using an automatic polishing machine (Rotopol-V;

Struers Ltd, Glasgow G60 5EU, UK). Before the assigned treatment, the polished surfaces of all ceramic specimens were cleaned with 10% citric acid, rinsed with distilled water and then ultrasonically cleaned for 5 minutes to remove surface contamination and the smear layer. They were dried in a vacuum jar overnight. The samples were stored in a chamber of 100% relative humidity at room temperature from the beginning of the experiment until the shear bond strength (SBS) test.[7,17] Prepared ceramic blocks were randomly divided into five groups (Table 1). In group 1, the control group, the Adper Scotchbond Multi-Purpose (SBMP, Lot No. 9RL; 3M ESPE, St. Paul, MN, USA) adhesive was applied to the polished surfaces of ceramic blocks with no treatment. The adhesive was light-cured for 20 seconds using a halogen light source (VIP, light intensity 600 mW/cm2; Bisco Inc, Schaumburg, IL, USA). In the experimental groups, the ceramic specimen was placed on a stand in an atmospheric pressure acrylic chamber which had a passive outlet for He gas. The stand was used to position the polished top surface of the specimen 0.5 cm below the tip of the plasma torch (Figure 1b). In group 2, the polished ceramic surface was exposed to NT-APP carrying vaporized TEGDMA in helium gas. The SBMP adhesive was immediately applied to the plasma polymer-coated surface and light-cured for 20 seconds. In group 3, an additional step of plasma surface treatment with vaporized DW in helium gas was applied to clean the adherent surface. After the cleaning step, the plasma polymer coating step with vaporized TEGDMA in helium gas with consecutive adhesive application and light-curing were completed, as in group 2. In group 4, HMDSO was additionally used as a precursor monomer since the plasma polymer from HMDSO had siloxane and silane groups for bonding with ceramic. The procedures were performed sequentially in the order of plasma cleaning with water, plasma polymer coating

with HMDSO, plasma polymer coating with TEGDMA, adhesive application, and adhesive light-curing for 20 seconds. In group 5, the polished surfaces of the ceramic blocks were treated according to a routine clinical protocol for bonding feldspathic porcelain, consisting of surface etching with 4% buffered hydrofluoric acid gel (HF, Porcelain Etchant, Lot No. 0800003209; Bisco Inc.) for 4 minutes, washing, drying with compressed air from a three-way syringe, coating the surface with a silane coupling agent (Monobond-S, Lot No. M08100; Ivoclar Vivadent AG, Liechtenstein), drying, adhesive application, and light curing for 20 seconds. A metal iris, a stainless steel coin (8 mm in diameter and 1.5 mm in height) with a concentric hole (3 mm in diameter) in the center, was used as a mold for packing composite[38]. The iris was coated with Teflon to prevent it from adhering to the cured adhesive of the ceramic surface. The iris was pressed against the treated ceramic surface, and a composite resin (Filtek Z-250, A3 shade, Lot No. N111413; 3M ESPE) was filled into the hole. It was then light-cured for 40 seconds. All the specimens were stored in a humid chamber at room temperature (22℃) for 24 hours before testing.

Shear bond strength was measured at a crosshead speed of 1.0 mm/min using a universal testing machine (UTM, LF Plus; Lloyd Instruments LTD, Fareham Hampshire, UK). After debonding, fracture analysis was performed using a stereomicroscope (SZ40, Olympus Corp, Tokyo, Japan), and photographs of both sides of the fracture surfaces were taken. The failure modes were classified as adhesive fracture (A), fracture between the polished ceramic surface and the cured adhesive layer; mixed fracture (M), fracture meandering from the adhesive interface to the ceramic surface, where as a result, small fragments of ceramic were observed on the adhesively fractured flat adhesive surface; or cohesive fracture of

ceramic (C), an oblique fracture of the ceramic adherend.

1.1.3 Surface Characterization

The microscopic images at various magnifications and constituting elements of the fractured surfaces in the selected debonded specimens from each group were evaluated using a field-emission scanning electron microscope (FE-SEM, S-4700, HITACHI high technologies Co, Tokyo, Japan) operating at 15 kV and an embedded energy dispersive spectrometer (EDS, EX-220, Horiba, Kyoto, Japan).

In order to verify the effects of plasma cleaning with DW and plasma polymer coating with HMDSO or TEGDMA, a contact angle meter (Phoenix 150; Surface Electro Optics, Seoul, Korea) was used to measure the water contact angles on a series of ceramic surfaces, such as those polished with #500 SiC paper, those plasma-treated with water after polishing, those plasma polymer coated with TEGDMA on the polished and water plasma-treated surface, those plasma polymer coated with TEGDMA on the polished surface, those plasma polymer coated with HMDSO on the polished and water plasma-treated surface, those plasma polymer coated with TEGDMA on the polished, water plasma-treated, and HMDSO plasma-coated surface, and those surfaces on which the adhesive was applied and cured after plasma treatment (Table 2). By gently dropping a deionized water droplet onto the treated surface using a micro-syringe, the static contact angle was automatically obtained from the photo image collected by the embedded software.

1.1.4 Statistical Analysis

The data obtained from the SBS test were analyzed statistically using a Kruskal–Wallis non-parametric test, and post hoc multiple comparison tests were also conducted with a Dunnett test at a 5% level of significance. Failure mode data were analyzed using a Chi-square test.

1.2 The effect of the applied power of non-thermal atmospheric pressure plasma (NT-APP) jet on the adhesion of composite resin to dental ceramic

1.2.1 Equipment Set-up

The NT-APP consisted of three parts: a mass flow system, a plasma torch, and a power supply. The pencil-type plasma torch was composed of an outer ceramic tube (4 mm in inner diameter and 6 mm in outer diameter) wrapped in a ground electrode and an inner ceramic needle tube (2 mm in diameter) containing a hot metal rod electrode that passed through the center of the outer tube. Helium (He) was delivered into the tube at a flow rate of 2 L/min as a carrier gas after passing through a glass bubbler, where it carried TEGDMA vapor for plasma polymerization. The applied a.f. power was transformed using a power supply from an input voltage of 9 ~ 18 V at 60 Hz AC to an output voltage of 1.13 ~ 1.98 kV in V_{rms} and an output current of 7.07 ~ 14.14 mA in I_{rms} at 15 kHz. These parameters were monitored using high voltage (P6015A and TM502A, Tektronix Inc., Beaverton, OR, USA) connected to an oscilloscope. The flow rate of the monomer vapor was controlled at a rate of 50 sccm using a mass flow controller (FC7700C, Aera Japan). The distance between the surface of the ceramic specimen and the tip of the plasma torch was fixed at 0.5 cm, and the treatment time was fixed at 60 seconds.

1.2.2 Adhesion Test

Pressed computer-aided design and computer-aided manufacturing (CAD/CAM) ceramic blocks (8 x 10 x 15 mm) of feldspathic porcelain (VITABlOCS Mark II for CEREC/inLab, 2M2C I10, Vita Zahfabrik) were embedded in acrylic molds with self-curing acrylic resin. To create uniform surface roughness and parallel surface

geometry for shear loading, the top surfaces of the ceramic blocks were ground with 500 grit silicon carbide abrasive paper (Buehler Ltd.) under running water using an automatic polishing machine (Rotopol-V; Struers Ltd.). Before the assigned treatment, the polished surfaces of all ceramic specimens were cleaned with 10% citric acid, rinsed with distilled water and then ultrasonically cleaned for 5 minutes to remove surface contamination and the smear layer. They were dried in a vacuum jar overnight. The samples were stored in a chamber at 100% relative humidity at room temperature from the beginning of the experiment until the SBS test.

Prepared ceramic blocks were randomly divided into five groups (n = 20): three experimental groups with plasma polymerization at an output voltage of 1.13, 1.70, and 1.98 kV, a negative control group, and a positive control group (Table 4). In the negative control group (Group 1), the adhesive of Adper Scotchbond Multi-Purpose adhesive system (SBMP adhesive, Lot No. 9RL; 3M ESPE) was applied to the ground surface of the ceramic block with no treatment. The adhesive was light-cured for 20 seconds using a halogen light source (VIP, light intensity 600 mW/cm^2, Bisco Inc.). In the experimental groups, the ceramic specimen was placed on a stand 0.5 cm below the tip of the plasma torch. The ground ceramic surface was exposed to NT-APP carrying TEGDMA vapor in helium gas. The input power for plasma polymerization was 9, 15, and 18 V in Groups 2, 3, and 4, respectively. The SBMP adhesive was immediately applied to the plasma polymer-deposited ceramic surface and light-cured for 20 seconds. In the positive control group (Group 5) using HF etching and silane application, the ground ceramic surface was etched with hydrofluoric acid (Porcelain Etchant, Bisco Inc.) for 4 minutes, rinsed with copious amount of running water, dried with compressed air, and then a silane

coupling agent (Monobond-S, Ivoclar Vivadent AG,) was applied to the etched surface and completely dried with compressed air. The same adhesive was immediately applied and light-cured as in the other groups.

A metal iris, namely a stainless steel coin (8 mm in diameter and 1.5 mm in height) with a concentric hole (3 mm in diameter) in the center, was used as a mold for packing composite. The iris was coated with Teflon to prevent it from adhering to the cured adhesive of the ceramic surface. The iris was pressed against the treated ceramic surface, and a composite resin (Filtek Z-250, A3 shade, 3M ESPE) was filled into the hole. The specimen was then light-cured for 40 seconds. All specimens were stored in a humid chamber at room temperature for 24 hours prior to testing. SBS was measured at a crosshead speed of 1.0 mm/min using a universal testing machine (UTM, LF Plus; Lloyd Instruments Ltd.).

1.2.3 Fracture Analysis

After the debonding test, fracture analysis was performed using a stereomicroscope (SZ40, Olympus Corp.). Photographs of both sides of the fractured surfaces were taken. The fractures of ceramic were classified as adhesive fracture (A), mixed fracture (M), and cohesive fracture (C): A, fracture between the ground ceramic surface and the cured adhesive layer; M, fracture meandering from the adhesive interface to the ceramic surface, where as a result, small ceramic fragments were observed on the adhesively-fractured flat adhesive surface or an irregularly reflected white opacity was observed just beneath the adhesively-fractured flat ceramic surface due to a subsurface-crack propagation and incomplete fracture; C, an oblique fracture of the ceramic adherend (Table 4 and Figure 4). The fractured surfaces and cross-sections of selected debonded specimens were evaluated using a field-emission scanning electron microscope

(FE-SEM, S-4700, HITACHI high technologies Co.) operated at 15 kV.

1.2.4 Surface Characterization

To investigate the effect of different applied powers on chemical changes of the plasma polymer deposited onto the ceramic surface, the hydrophilicity and chemical composition of the treated ceramic surfaces were evaluated using a contact angle meter (Phoenix 150, Surface Electro Optics) and an XPS (Sigma Probe, Thermo VG, East Grinstead, UK), respectively. The polished surfaces of all ceramic specimens were cleaned with 10% citric acid, rinsed with distilled water and then ultrasonically cleaned for 5 minutes to remove surface contamination and the smear layer. They were dried in a vacuum jar overnight before the treatments. The hydrophilicity of a series of treated ceramic surfaces was evaluated by measuring the contact angle between deionized water and the following treated ceramic surfaces: G, ground with #500 SiC paper; S, HF etching and silane coupling agent coating onto the ground surface; T9, TEGDMA plasma-deposited at an input power of 9 V after grinding; T15, TEGDMA plasma-deposited at an input power of 15 V after grinding; T18, TEGDMA plasma-deposited at an input power of 18 V after grinding (Table 5). By gently dropping a droplet of deionized water onto the treated surface using the sessile drop method at room temperature, the static contact angle values were obtained by a goniometric method (n = 7). From the contact angle measurements, the work of adhesion for the corresponding treated surface was calculated using the following equation:[39]

$\omega_A = \gamma_W(1+\cos\theta)$

where γ_W is the surface tension of water (7.28×10^{-2} N/m). Values of ω_A (work of adhesion) for different substrate surfaces indicate their hydrophilicity.

The chemical composition and the functional groups of the plasma polymer

deposited onto ceramic surfaces were characterized by XPS using a monochromatized Al Kα X-ray source at 15 kV and 100 W. The surface composition was obtained from the areas of the C1s, O1s, and Si2p peaks, obtained in high resolution mode with a 20 eV pass energy and 0.1 eV step size. All binding energies were calibrated to carbon (C1s) at 284.5 eV. The measurements were carried out in a vacuum around 2 x 10^{-9} mB

1.2.5 Statistical Analysis

The data obtained from the SBS test were analyzed statistically using one-way analysis of variance (ANOVA), and *post hoc* multiple comparison tests were conducted with a Dunnett T3 test at a 5% level of significance. A normality test and an equal variance test were also performed using the Kolmogorov-Smirnov test and Shapiro-Wilks test ($p > 0.05$) and with Levene's test ($p = 0.018$), respectively. Failure mode data were analyzed using the Kruskal-Wallis non-parametric test. Because Levene's test for the rank of fracture mode failed to assume the homogeneity of variances, *post hoc* multiple comparison tests were also conducted with a Dunnett T3 test at a 5% level of significance.

1.3 1,3-Butadiene as adhesion promoter between composite resin and dental ceramic in a floating electrode dielectric barrier discharge (FE-DBD) jet

1.3.1 Equipment Set-up

An experimental floating electrode dielectric barrier discharge (FE-DBD) jet equipment was designed by modifying the previously reported NT-APP jet, especially in the position of the ground electrode of the plasma torch.[34] The pencil-type plasma torch was composed of a ceramic tube (4 mm in inner diameter and 6 mm in outer diameter) wrapped in a hot electrode. A ground electrode was connected to the specimen stand. As a carrier gas, a flow rate of 2 L/min of Helium

(He) was mixed with various amount of 1,3-butadiene gas for PECVD and delivered into the tube. The applied a.f. power was transformed using a power supply from an input voltage of 15 V at 60 Hz AC to an output voltage of 2.0 kV in V_{rms} and an output current of 2.86 mA in I_{rms} at 15 kHz; these parameters were monitored using high voltage and current probes (P6015A and TM502A, Tektronix Inc., Beaverton, OR, USA) connected to an oscilloscope (DPO2000, Tektronix, Inc., Table 8 and Figure 8). The distance between the surface of the ceramic specimen and the tip of the FE-DBD torch was fixed at 0.5 cm, and the treatment time was fixed at 10 seconds. As the variable of this study, the flow rate of 1,3-butadiene gas was controlled in sccm using a home-made ball flow meter.

1.3.2 Adhesion Test

Pressed ceramic blocks (8 x 10 x 15 mm) of feldspathic porcelain (VITABlOCS Mark II for CEREC/inLab, 2M2C I10, Vita Zahfabrik) for CAD/CAM milling were embedded in acrylic molds with self-curing acrylic resin. To create uniform surface roughness and parallel surface geometry for shear loading, the top surfaces of the ceramic blocks were ground with 500 grit silicon carbide abrasive paper (Buehler Ltd.) under running water using an automatic polishing machine (Rotopol-V; Struers Ltd.). Before the assigned treatment, the polished surfaces of all ceramic specimens were cleaned with 10% citric acid, rinsed with distilled water and then ultrasonically cleaned for 5 minutes to remove surface contamination and the smear layer. They were dried in a vacuum jar overnight.

Prepared ceramic blocks were randomly divided into five groups (n = 10): four experimental groups with PECVD of 1,3-butadiene at flow rates of 0.5, 2.0, 3.0 and 6.0 sccm, and a negative control group (Table 8). In the negative control group (Group 1), the adhesive of Adper Scotchbond Multi-Purpose adhesive system

(SBMP adhesive, Lot No. 9RL; 3M ESPE) was applied to the prepared ceramic surface with no treatment. The adhesive was light-cured for 20 seconds using a halogen light source (VIP, light intensity 600 mW/cm^2, Bisco Inc.). In the experimental groups, the ceramic specimen was placed on a specimen stand, with the surface of ceramic specimen being 0.5 cm below the tip of the FE-DBD ceramic tube. The prepared ceramic surface was exposed to FE-DBD jet carrying a mixture of 1,3-butadiene gas and helium gas for 10 seconds. The output power for plasma polymerization was a RF voltage of 2 KV at 15 kHz,, and the flow rates of precursor monomer gas in Groups 2, 3, 4, and 5 was 0.5, 2.0, 3.0, and 6.0 sccm, respectively. The SBMP adhesive was immediately applied to the PECVD deposited ceramic surface and light-cured for 20 seconds.

A Teflon-coated coin-shaped stainless steel iris with a concentric hole (3 mm in diameter) at the center was used as a mold for packing composite. The iris was pressed against the treated ceramic surface, and a composite resin (Filtek Z-250, A3 shade, 3M ESPE) was filled into the hole. The specimen was then light-cured for 40 seconds. All specimens were stored in a humid chamber at room temperature for 24 hours prior to testing. SBS was measured at a crosshead speed of 1.0 mm/min using a universal testing machine (UTM, LF Plus; Lloyd Instruments Ltd.).

1.3.3 Fracture Analysis

After debonding test, fracture analysis was performed using a stereomicroscope (SZ40, Olympus Corp.). Photographs of both sides of the fractured surfaces were taken. For selected cases, the fracture modes were confirmed using a field-emission scanning electron microscope (FE-SEM, S-4700, HITACHI high technologies Co.) operated at 15 kV. The fractures of ceramic were classified as adhesive fracture (A),

mixed fracture (M), and cohesive fracture (C): A, fracture between the prepared ceramic surface and the cured adhesive layer; M, fracture meandering from the adhesive interface to the ceramic surface, where as a result, small ceramic fragments were observed on the adhesively-fractured flat adhesive surface or an irregularly reflected white opacity was observed just beneath the adhesively-fractured flat ceramic surface due to a subsurface-crack propagation and incomplete fracture; C, an oblique fracture of the ceramic adherend (Table 8).

1.3.4 Surface Characterization

The chemical composition of the PECVD deposited onto ceramic surfaces was characterized by XPS (Sigma Probe, Thermo VG Scientific) using a monochromatized Al Kα X-ray source at 15 kV and 100 W. The surface composition was analyzed from the areas of the C1s, O1s, and Si2p peaks, obtained in high resolution mode with 20 eV pass energy and 0.1 eV step size. All of the binding energies were calibrated to carbon (C1s) at 284.5 eV. The measurements were carried out in a vacuum at approximately 2 x 10^{-9} mB.

In order to differentiate C=C double bonds from C-C groups, chemical changes of the PECVD deposited on the ceramic surfaces were also compared using FT-IR (Nicolet 6700, Thermo Nicolet, Madison, WI, USA) in an ATR mode. Due to nanometer-scale deposition, the relative height of each functional group was compared using the FTIR spectra of the PECVD specimens deposited for extremely long deposition time of 15 minutes with different flow rates of precursor monomer gas. They were obtained in a transmission mode from 32 scans at a resolution of 4 cm^{-1}.

To verify the structure and composition of the PECVD on the ceramic surface, a thin cross-section of the interface coated with 6 sccm of 1,3-butadiene for 15

minutes was prepared using a focused ion beam (FIB, Nova 200 Nanolab, FEI Company, Hillsboro, OR, USA). After deposition of Pt to protect its top portion, the FIB sample was prepared with a 30 kV Ga liquid-metal ion source. The sample was transferred to a transmission electron microscope (TEM) sample grid with a micro-manipulator. To remove damaged layers created by the FIB, final milling was carried out with low-energy Ga milling at 10 kV and approximately 30 to 50 pA. The sample was observed under a TEM (JEOL 3000F, JEOL Ltd., Tokyo, Japan) at 200 kV equipped with an EDS.

1.3.5 Statistical Analysis

The data obtained from the SBS test were analyzed statistically using one-way ANOVA and the failure mode data were analyzed using the Kruskal-Wallis non-parametric test. *Post hoc* multiple comparison tests were conducted with a Dunnett T3 test at a 5% level of significance for both analyses.

1.4 Sequential deposition of Hexamethyldisiloxane and benzene in floating electrode dielectric barrier discharge (FE-DBD) jet adhesion to dental ceramic

1.4.1 Experimental set-up

The experimental pencil-type plasma torch was designed as a FE-DBD jet, in which a hot electrode was connected to the ceramic plasma torch (4 mm inner diameter) and a ground electrode was connected to the specimen stand (Tsai and Staack, 2011). As the parameters to generate plasma in this study, the applied power was 2 KV at 15 kHz, the amount of precursor monomers was 60 sccm, the flow rate of Helium (He) as carrier gas was 2 L/min, the distance between the ceramic surface and the tip of the FE-DBD torch was fixed at 0.5 cm, and the treatment time was fixed at 30 seconds.

1.4.2 Adhesion test

Pressed ceramic blocks (8 x 10 x 15 mm, VITABlOCS Mark II, 2M2C I10, Vita Zahfabrik) were embedded in acrylic molds with self-curing resin. They were ground on 500 grit silicon carbide abrasive papers under running water using an automatic polishing machine. The polished ceramic surfaces were cleaned with 10% citric acid for 10 seconds, rinsed with distilled water twice, and then ultrasonically cleaned for 5 minutes to remove surface contamination and smear layer. They were then dried in a vacuum jar overnight.

The prepared ceramic blocks were randomly divided into five groups (n = 20, Table 10): a negative control group (Group 1), and four experimental groups treated with PECVD of H_2O (Group 2), HMDSO (Group 3), benzene (Group 4), and benzene after HMDSO (Group 5). In the control group, the adhesive of Adper Scotchbond Multi-Purpose adhesive system (SBMP adhesive, 3M ESPE) was applied to the prepared ceramic surface without any treatment. The adhesive was light-cured for 20 seconds using a halogen light source (VIP, Bisco Inc., light intensity 600 mW/cm^2). In the experimental groups, the specimen was exposed to the plasma jet carrying a mixture of the assigned monomer and helium gas for 30 seconds. The SBMP adhesive was immediately applied to the PECVD deposited ceramic surface and light-cured for 20 seconds.

A Teflon-coated coin-shaped stainless steel iris with a concentric hole (3 mm in diameter) in the center was placed on the treated ceramic surface, and composite resin (Filtek Z-250, A3 shade, 3M ESPE) was filled into the hole. The specimen was then light-cured for 40 seconds. All specimens were stored in a humid chamber at room temperature for 24 hours prior to testing. SBS was measured at a crosshead speed of 1.0 mm/min using a universal testing machine (UTM, LF Plus; Lloyd

Instruments Ltd.).

1.4.3 Fracture analysis

After SBS tests, both sides of the fractured surfaces were observed under a stereomicroscope (SZ40, Olympus Corp.) and, for selected cases, a field-emission SEM (FE-SEM, S-4700, HITACHI High Technologies Co.). The fracture modes were classified as adhesive fracture (A), mixed fracture (M), or cohesive fracture (C): A, fracture between the prepared ceramic surface and the cured adhesive layer; M, fracture meandering from the adhesive interface to the ceramic surface; C, an oblique fracture of the ceramic adherend (Table 10)

1.4.4 Surface characterization

The hydrophilicity of the treated ceramic surfaces were evaluated using a contact angle meter (Phoenix 150, Surface Electro Optics). By gently dropping a droplet of deionized water onto the treated surface using the sessile drop method at room temperature, the static contact angle values were obtained by a goniometric method (n = 5). Work of adhesion (*Wa*) was calculated from the Young-Dupré Equation,[39]

$Wa = \gamma_L (1 + \cos \theta)$

where γ_L and θ represent the known surface tension of the test liquid (water, 7.28 x 10^{-2} N/m) and the measured contact angle between the solid and water, respectively. Values of *Wa* for different substrate surfaces indicate their hydrophilicity.[39,40]

The chemical compositions of the PECVD deposited onto ceramic surfaces were characterized by XPS (Sigma Probe, Thermo VG Scientific) with a monochromatized Al Kα X-ray source and FT-IR (Nicolet 6700, Thermo Nicolet) in an ATR mode. Due to nanometer-scale deposition, the PECVD specimens for the FTIR-ATR measurements were deposited for extremely long deposition time of

15 minutes, compared to that of 30 seconds used in the adhesion test. They were obtained in a transmission mode from 32 scans at a resolution of 4 cm^{-1}.

1.4.5 Microscopic observation of bonded interface

In order to observe the bonded interfaces, 2 mm thick flat specimens were additionally prepared for each group. The SBMP adhesive and 1 mm thick composite resin was applied and light-cured sequentially with the same method for all the specimens. They were fractured at a compression mode and the fractured interfaces were observed from the lateral side using the previously described UTM and FE-SEM, respectively.

1.4.6 Statistical Analysis

Data obtained from the SBS test and failure mode evaluation were statistically analyzed using the one-way ANOVA and Chi-square test, respectively. *Post hoc* multiple comparison tests were conducted with the Duncan test. Both analyses were performed at a 5% level of significance.

1.5 Promotion of resin bonding to dental zirconia ceramic using plasma deposition of tetramethylsilane and benzene

1.5.1 Specimen Preparation

A partially sintered zirconia block (Cercon base, DeguDent, Hanau, Germany) was sectioned into square-shaped specimens (10 mm × 10 mm × 3 mm) and the surface for adhesion were sequentially polished with up to 1200-grit silicon carbide paper. After final sintering according to the manufacturer's instructions, a total of 70 specimens were randomly divided into five groups according to surface treatments prior to applying a dental adhesive as follows (n = 14):

Group 1 (control): no previous treatment;

Group 2 (TMS): plasma deposition with tetramethylsilane (TMS);

Group 3 (benzene): plasma deposition with benzene;

Group 4 (TMS/benzene): plasma deposition with TMS and benzene, consecutively;

Group 5 (Z-Prime Plus): applying a commercial zirconia primer (Z-Prime Plus, Bisco)

1.5.2 Experimental set-up

Plasma treatment was performed in a custom-made plasma reactor supplied with a 13.56 MHz RF source. Before a plasma polymer deposition step, a zirconia specimen was subjected to a plasma pre-treatment using a mixture of Ar and H_2 in a ratio of 4:1. The power applied to the plasma was 100 W and the pressure of the chamber was maintained at about 0.9×10^{-2} mbar during the pre-treatment. The plasma pre-treatment was performed to remove organic contaminants from the zirconia surface and activate the surface. Following this pre-treatment, vaporized TMS or benzene was mixed with Ar gas in a ratio of 4:1 and introduced into the chamber maintaining its pressure about 0.7×10^{-1} mbar. In the TMS/benzene group, the plasma deposition was performed sequentially with TMS and benzene. The duration of the deposition process was 5 minutes for each monomer.

1.5.3 Adhesion test

A dental adhesive (Scotchbond Multi-Purpose adhesive, 3M ESPE) was applied to the zirconia surfaces and light-cured for 10 seconds using an LED curing unit (Elipar FreeLight 2, 3M ESPE). A Teflon-coated mold (3 mm in inner diameter and 1.5 mm in height) was place the zirconia surface. The mold was filled with the Filtek Z250 (3M ESPE) resin composite, which was then light-cured for 20 seconds. The bonded specimens were embedded in acrylic resin blocks for a shear bond strength test and stored in a humid chamber at room temperature for 24 hours

before testing. Shear bond strengths were measured using a universal testing machine (LF Plus, Lloyd Instruments) at a crosshead speed of 1.0 mm/min.

1.5.4 Surface characterization

XPS analysis was used to compare surface chemical compositions between non-treated zirconia and plasma-treated zirconia with TMS. Measurements were carried out using a monochromatized Al Kα X-ray source (1486.6 eV) under the conditions of 15 kV and 100 W. The base pressure of the analysis chamber was maintained at about 2×10^{-9} mbar. XPS spectra were collected in high resolution mode with pass energy of 20 eV and an energy step size of 0.1 eV. The energy scale was calibrated using the C 1s level of 284.5 eV.

To visualize plasma-polymerized layers and determine the composition of the layers, a cross-sectioned specimen coated with plasma-polymerized TMS and benzene was prepared by FIB (Nova 200 Nanolab, FEI Company) for TEM (JEOL 3000F, JEOL Ltd.) observation. The specimen was prepared with a Ga liquid-metal ion source at a beam energy of 30 kV after Pt film deposition to protect the specimen surface, and was observed using the TEM at 200 kV equipped with an EDS.

1.5.5 Statistical Analysis

The bond strength data were analyzed using statistical software (SPSS 18.0, SPSS Inc.). One-way ANOVA, followed by the Tukey HSD test for post-hoc pairwise comparisons, was performed at a significance level of $\alpha=0.05$.

2) ADHESION TO TOOTH

2.1 Effect of plasma deposition using low-power/non-thermal atmospheric pressure plasma on promoting adhesion of composite resin to enamel

2.1.1 Equipment Set-up

As a pencil-type plasma torch, a FE-DBD jet with a 4 mm inner diameter was used in the same conditions as plasma coating of ceramic. For intraoral use of plasma, the applied a.f. power was controlled at 5W, the lowest possible level, which was obtained by transforming from an input voltage of 15 V at 60 Hz AC to an output voltage of 2.0 kV in V_{rms} and an output current of 2.5 mA in I_{rms} at 15 kHz. The flow rate of helium (He) as carrier gas was 2 L/min, and the distance between the enamel surface and the torch tip was fixed at 0.5 cm. Part of He gas (80 sccm) was detoured to pass through a glass bubbler containing liquid benzene (BZ) and to carry BZ vapor for plasma polymerization. Gaseous 1,3-butadiene (BD) was pushed into the torch and deposited with He gas simultaneously by connecting to the tube delivering He gas. As precursor monomers, the amounts of benzene (BZ) and 1,3-butadiene (BD) were 12.75 and 2.5 sccm, respectively. The treatment times were fixed at 30 and 10 seconds for BZ and BD, respectively. When no monomer was used, plasma treatment was performed with He gas at a flow rate of 2 L for 30 seconds under 5 W applied power.

2.1.2 Adhesion Test

With permission of the Institutional Review Board of Seoul National University Dental Hospital (IRB076M07-12), extracted single-rooted human premolars were stored in a 0.5% aqueous Chloramine T solution for 2 hours to prevent surface infection. After removing soft tissue, the teeth were stored in isotonic saline solution until use. The teeth were embedded in acrylic molds with self-curing resin, and their mesial or distal surfaces were exposed. They were polished with 600 grit silicon carbide abrasive papers under running water. The specimens were randomly divided into four groups, including a negative control group, a plasma-treated

group without any monomer, and two plasma polymer grafting groups with either BD or BZ. Each group was divided again into two subgroups, in which the MSBS was measured 24 hours after bonding (n = 21) and after 24 hours of storage and 5,000 cycles of TC (n = 22, Table 12). In the negative control group (Group 1), the enamel surface was etched with 37 wt% phosphoric acid (SBMP etchant, 3M ESPE) for 15 seconds, rinsed with copious amounts of water for 15 seconds, and dried completely with compressed air. The adhesive of Adper Scotchbond Multi-Purpose adhesive system (SBMP adhesive, Lot No. 9RL; 3M ESPE) was immediately applied to the etched enamel. The adhesive was light-cured for 10 seconds using a light-emitting diode (LED) light source (Elipar Freelight 2, 3M ESPE, light intensity, 800 mW/cm^2). In the experimental groups, the enamel specimen that was etched with the same phosphoric acid and rinsed was then placed on a stand 0.5 cm below the tip of the plasma torch, and exposed to non-thermal FE-DBD plasma carrying assigned monomer vapor in helium gas for the assigned duration: Group 2, with no monomer; Group 3, with BZ; Group 4, with BD. Immediately after removal from the stand, the SBMP adhesive was applied to the plasma polymer-deposited enamel surface and light-cured for 10 seconds.

A piece of Tygon tubing (0.8 mm in diameter and 1.0 mm in height) was placed on the cured adhesive layer of the enamel specimen.[84] The tubing was filled with composite resin (Filtek Z-250, A3 shade, 3M ESPE) and light-cured for 20 seconds. For each tooth specimen, two composite cylinders were bonded on the adhesive-applied surface of a tooth specimen. After removing the tubing with a scalpel, the specimen was stored in a water bath at 37°C for 24 hours prior to testing. MSBS was measured with a wire loop method at a crosshead speed of 0.5 mm/min using a universal testing machine (UTM, LF Plus; Lloyd Instruments Ltd.).[85] To measure

the MSBS after TC, the specimens stored for 24 hours in the water bath were additionally subjected to 5,000 thermal cycles between a 5°C water bath and a 55°C water bath with a dwell time of 24 seconds and a transferring time of 6 seconds between the two baths.

2.1.3 Fracture Analysis

After the MSBS test, the fractures at the debonded surface of enamel were observed using a stereomicroscope (x 40, SZ40, Olympus Corp.). The fractured surfaces and cross-sections of selected debonded specimens were evaluated using a field-emission scanning electron microscope (FE-SEM, S-4700, HITACHI high technologies Co.) operated at 15 kV.

2.1.4 Contact Angle Measurement

In order to compare the hydrophilicity of the treated enamel surfaces, the contact angles of the surfaces were evaluated using a contact angle meter (Phoenix 150, Surface Electro Optics). By gently placing a droplet of deionized water onto the treated surface using the sessile drop method at room temperature, the static contact angle values were obtained by a goniometric method (n = 5).

2.1.5 Surface Characterization

The chemical composition of the plasma-deposited enamel surfaces were characterized by XPS (Sigma Probe, Thermo VG Scientific) using a monochromatized Al Kα X-ray source at 15 kV and 100 W. The changes in carbon and oxygen levels after plasma polymer deposition were evaluated from the areas of the C1s and O1s peaks. The peaks were obtained in high resolution mode with 20 eV pass energy and 0.1 eV step size. All of the binding energies were calibrated to carbon (C1s) at 284.5 eV. The measurements were carried out in a vacuum at approximately 2 x 10^{-7} Pa. FT-IR was used in this study for two purposes. First, in

order to confirm the change of C=C double bonds in the C1 peak to C-C bonds, chemical changes of the plasma-deposited ceramic surfaces were compared using FT-IR (Nicolet 6700, Thermo Nicolet). Second, in order to interpret the changes of MSBS after TC, the degree of conversion (DC) of the plasma-polymerized layers between two potassium bromide (KBr) pellets were also evaluated using FT-IR. Due to the nanometer-scale of the plasma deposition, each precursor monomer was deposited on a KBr pellet for an extremely long deposition time of 15 minutes for FT-IR detection. The spectra were obtained as uncured, cured, or matured after TC. The uncured spectrum was obtained from a special accessory in which a gas mixture of He and the assigned monomer was filled without plasma. The cured one was obtained from a KBr pellet on which the gas mixture was deposited with activated plasma, and the matured one from a KBr pellet matured in a dark container at 55°C for seven days in order to simulate thermal aging. The spectra were obtained in a transmission mode from 32 scans at a resolution of 4 cm^{-1}. The DC of BZ and BD were calculated from the peak height of the aliphatic C=C double bond at 1635 cm^{-1} corrected with those of the aromatic C=C double bond at 1608 cm^{-1} and the C=O carbonyl group at 1720 cm^{-1}, respectively.

2.1.6 Statistical Analysis

Using two-way ANOVA, statistical analysis of the data obtained from the MSBS test was performed to investigate the main effect of the variables of treatment and measurement time, and their interaction effect. To interpret the main effects, *post hoc* multiple comparison tests with the Scheffe test and t-test were conducted within each variable. Bond strength data were analyzed using statistical software (SPSS 18.0, SPSS Inc.) at a 5% level of significance.

Because of the brittle nature of the adhesion, the MSBS results were once again

analyzed using the Weibull statistics. The Weibull parameters such as the Weibull modulus (m) and the characteristic strength (σ_θ) for each test group were also obtained to compare the distribution of the failure probability of each group among the four surface treatments and between the two measurement times. Linear regression analysis for Weibull statistics was performed with the least-squares method.

2.2 Effects of non-thermal atmospheric pressure pulsed plasma on the adhesion and durability of resin composite to dentin

2.2.1 Generation of non-thermal atmospheric pressure plasma jet

A FE-DBD jet was designed as a pencil-type torch with a 4 mm inner diameter. Helium, as a process gas, was delivered into the tube at a flow rate of 2 L/min. For intra-oral use, the plasma plume was generated by two different audiofrequency power sources in order to control the applied plasma energy as low as possible and, as a result, to reduce patient discomfort. A continuous sinusoidal power source was used under the conditions of 2.4 kV, 2.5 mA, and 8.0 kHz in order to generate a conventional plasma plume with a low-applied energy of 21.6 kW·h. A pulsed power source with a frequency of 0.4 kHz, in which each pulse had five voltage peaks (Hz) and lasted for 500 ns at 12.5 ms intervals, was used to generate a pulsed plasma plume with an applied energy of 1.1 kW·h (Figure 19).

2.2.2 Dentin specimen preparation and adhesion procedure

Sound, caries-free human third molars were used in this study with the permission of the Institutional Review Board of Seoul National University Dental Hospital (IRB No. ERI12003). After removing soft tissue debris, the molars were immersed in a 0.5% chloramine-T solution for one week, then stored in distilled water at 4°C until use. The teeth were embedded in acrylic molds with self-curing resin.

Occlusal enamel was removed perpendicular to the long axis of the tooth using a low-speed diamond saw (Isomet, Buehler). The exposed dentin surface was polished with 600-grit silicon carbide abrasive papers under water-cooling. The teeth were randomly assigned to three groups according to the plasma treatment: no plasma treatment (negative control); pulsed plasma treatment; conventional plasma treatment (Figure 20 and Table 16). Figure 2 summarizes the adhesion procedures. A three-step etch-and-rinse system (Scotchbond Multi-Purpose Plus adhesive system, 3M ESPE) was used, strictly following the manufacturer's instructions. In the control group, after acid-etching, the primer was applied using a blot-dry technique with a moistened Kimwipes tissue (Kimberly-Clark, Roswell, GA, USA). In the plasma treatment groups, after specimens were blot-dried with a moistened Kimwipes tissue, the etched dentin surface was exposed to the assigned plasma jet for 30 seconds at a distance of 5 mm from the nozzle. After plasma treatment, the dried dentin surface was re-wetted with a moistened Kimwipes tissue before application of the primer. The applied primer was dried with compressed air for 10 seconds to obtain a completely dried surface by the naked eye. Then, a coat of the adhesive was applied and light-polymerized for 10 seconds using an LED curing unit (Elipar FreeLight 2, 3M ESPE). The light intensity of 800 mW/cm^2 was frequently monitored with a radiometer (Demetron 100, Demetron Research Co., Danbury, CT, USA). Finally, resin composite (Filtek Z-250, A3 shade, 3M ESPE) was incrementally built up on the dentin surface, and each increment was light-polymerized for 20 seconds.

2.2.3 Micro-tensile bond strength testing

After storage in a humid chamber at 37°C for 24 h, each specimen was trimmed into an hourglass shape and sectioned into slabs in which the area of the adhesive

interfaces were approximately 0.8 mm x 0.8 mm. The specimens of each group were further divided into two subgroups according to the MTBS testing time: one subgroup was immediately submitted to the MTBS (n = 20) test, while the other subgroup was submitted to artificial aging with thermocycling for 5,000 cycles between 5 and 55°C with a 24 seconds dwell time and a 6 seconds transferring time before being tested (n = 14). After measuring the dimensions of the adhesive interface using a digital caliper, each specimen was attached to a testing jig and loaded at a crosshead speed of 0.5 mm/min in a universal testing machine (LF Plus, Lloyd Instruments) until failure occurred.

2.2.4 Examining the adhesive interface and fracture mode using scanning electron microscopy

In order to obtain the exact bond strength value of the adhesion, the MTBS data obtained from the specimens that showed cohesive fractures within the dentin or the resin composite under a stereomicroscope were discarded. Therefore, in this study, after MTBS testing, the fracture of the specimens were all adhesive. For selected specimens, the microscopic images of the fractured surfaces were collected using a scanning electron microscope (SEM, JSM-840A, JEOL Ltd.).

In order to compare the quality of the adhesion after the treatments, the bonded interface of a selected slab from each tooth was also examined using the same SEM. The mineral and organic components of the dentin substrate were removed with sequential dipping into beakers containing 6N HCl and 5% NaOCl for 3 seconds and for 4 minutes, respectively. The samples were examined after overnight desiccation in a vacuum jar and being sputter-coated with gold.

2.2.5 Statistical analysis

The MTBS data were analyzed using statistical software (SPSS 12.0KO, IBM

Corp., Armonk, NY, USA). Two-factor repeated measures ANOVA was used to assess the effects of the plasma treatments, measuring time (artificial aging) and treatment-time interaction. The *t*-test and Scheffe test were used for *post hoc* pairwise comparisons of the MTBS within the factors of treatment and measuring time, respectively. The analyses were performed at a significance level of $\alpha = 0.05$. In addition, the MTBS data were also analyzed using the Weibull statistics. The Weibull parameters, namely the Weibull modulus (*m*) and the characteristic strength (σ_θ), were obtained to compare the changes caused by artificial aging in the distribution of the failure probabilities of the test groups.

2.3 Promotion of Adhesive Penetration and Resin Bond Strength to Dentin using Non-thermal Atmospheric Pressure Plasma

2.3.1 Dentin Specimen Preparation

Sound, caries-free human third molars were collected according to protocols approved by the Institutional Review Board of Seoul National University Dental Hospital (IRB No. ERI12003) and were stored in a solution of 0.5% chloramine T at 4°C until use. The teeth were cut using a low-speed diamond saw (Isomet, Buehler) at the occlusal enamel to expose the dentin surfaces. The exposed dentin surface was polished with 600-grit silicon carbide abrasive papers under water cooling. The teeth were randomly assigned to four groups according to the adhesion procedure: a wet bonding group (positive control), a plasma-drying group, a plasma-drying/rewetting group, and a dry bonding group (negative control).

2.3.2 Adhesion Procedure and Plasma Treatment

The dentin surface was demineralized for 15 seconds with 35% phosphoric acid (Scotchbond Etchant, 3M ESPE) and then rinsed thoroughly with water. In the wet bonding group, the demineralized dentin surface was blot-dried with a moistened

Kimwipes tissue (Kimberly-Clark) before applying a two-step etch-and-rinse adhesive (Adper Single Bond 2, 3M ESPE). Adper Single Bond 2 adhesive contains BisGMA, HEMA, dimethacrylates, ethanol, water, photoinitiators, and silica nanofillers. In the plasma-drying group, the demineralized dentin surface was exposed to a plasma plume for 20 seconds at a distance of 5 mm from the nozzle. The plasma plume was generated at a pulsed power of 0.3 W using the pencil-type plasma torch. Helium as working gas was delivered at a flow rate of 2 L/min. The plasma-dried dentin surface was immediately coated with the adhesive. In the plasma-drying/rewetting group, the demineralized dentin surface was treated with the plasma torch in the same manner as for the plasma-drying group, but the plasma-dried dentin surface was rewetted with a moistened Kimwipes tissue before applying the adhesive. In the dry bonding group, the demineralized dentin surface was dried with oil/water-free compressed air for 20 seconds before applying the adhesive. In all test groups, the applied adhesive was gently dried with oil/water-free compressed air to evaporate solvents, and light-cured for 10 seconds using a light-emitting diode curing unit (Elipar FreeLight 2, 3M ESPE). A resin composite (Filtek Z-250, 3M ESPE) was incrementally built on the dentin surface and each increment was light-cured for 20 seconds. The bonded specimens were stored in a humid chamber at 37°C for 24 hours before being tested.

2.3.3 Microtensile Bond Strength Test

The bonded specimens were trimmed into an hourglass shape and then sectioned into slabs with a cross-sectional bonded area of approximately 0.8 × 0.8 mm^2. Twenty-four specimens were obtained from each group for the microtensile bond test (n = 24). The specimens were attached to a testing jig and loaded at a crosshead speed of 0.5 mm/min in a universal testing machine (LF Plus, Lloyd

Instruments) until failure. The dimension of the adhesion interface was measured for each specimen using a digital caliper to determine the MTBS value.

2.3.4 Micro-Raman Spectroscopy

Micro-Raman spectral analysis was performed in order to evaluate the penetration of the adhesive monomers, especially BisGMA, into the demineralized dentin, as well as to evaluate the polymerization efficacy of the adhesive at the adhesive/dentin interface. A Renishaw In Via Raman microscope (Renishaw) was used with a 785 nm diode laser at 125 mW and focused through an 100× Leica lens to an approximately 1 μm beam diameter. Raman spectra were acquired across the adhesive/dentin interface at 0.5 μm intervals from the dentin to the adhesive layer. The penetration of the adhesive monomers were compared by measuring the penetration of BisGMA into the demineralized dentin and the relative content of BisGMA in the adhesive, which were determined based on the respective band ratio of 1113 cm^{-1} (phenyl C-O-C of BisGMA)/1667 cm^{-1} (amide I of collagen) and 1113 cm^{-1}/1454 cm^{-1} (CH_2 of all adhesive monomers).[21,22] The band ratio of 1640 cm^{-1} (aliphatic C=C)/1609 cm^{-1} (aromatic C=C) was also determined in order to compare the polymerization efficacy of the adhesive between the test groups. Band ratios were calculated by the spectral subtraction technique.[133,134]

2.3.5 Scanning Electron Microscopy

The micromorphological characteristics of the adhesive/dentin interface were observed using a SEM (JSM-840A, JEOL). Selected specimens from each group were sequentially soaked in 6N HCl for 3 seconds and in 5% NaOCl for 4 minutes, followed by washing twice with water. The prepared specimens were desiccated overnight in a vacuum jar and sputter-coated with gold.

2.3.6 Statistical analysis

One-way ANOVA was performed to compare the MTBS data using a statistical software (SPSS 12.0, IBM). The Tukey's HSD test was used for *post-hoc* pairwise comparisons at a significance level of $\alpha = 0.05$. In addition, the MTBS data were also analyzed using the Weibull statistics to obtain the Weibull modulus (m) and the characteristic strength (σ_θ).

3. RESULT

1) ADHESION TO CERAMIC

1.1 The effect of plasma polymer coating using non-thermal atmospheric pressure plasma (NT-APP) jet on the shear bond strength of composite resin to ceramic

Table 3 shows the SBSs of composite resin to variously treated surfaces of feldspathic porcelain blocks. Compared to the SBS of the adhesive of SBMP to untreated ceramic surfaces (group 1), the SBS value of the adhesive to the ceramic surface exposed to NT-APP jet carrying vaporized TEGDMA (group 2) increased slightly, but the difference was not statistically significant. However, when the plasma polymer coating with vaporized TEGDMA was performed after pre-treatment of the adherent surface with plasma carrying vaporized DW (group 3), the SBS of the adhesive was significantly higher than both those to the untreated surface (group 1) and to the surface coated only with TEGDMA (group 2, $p < 0.05$). The SBS value was still lower than the bond strength to the ceramic surface etched with HF acid and consecutively coated with silane coupling agent (group 5, $p < 0.05$), a routine bonding procedure for feldspathic porcelain in dental clinics. Sequential plasma polymer coatings with HMDSO and TEGDMA after plasma

cleaning with water (group 4) also failed to obtain significantly different SBS values from those of the untreated control group (group 1). In group 1, the fractures caused by shear loading mostly occurred at the interface between the polished ceramic surface and the cured adhesive layer (adhesive fractures, Figure 2a and Table 3). With plasma polymer coating (group 2), small cohesively fractured fragments of ceramic were observed on the adhesively fractured flat adhesive surface after shear fracture (mixed fractures, Figure 2b). When plasma surface cleaning with vaporized DW was performed additionally before plasma polymer coating with TEGDMA (group 3), the incidence of mixed fractures increased significantly (Chi-square test, $p < 0.05$). The small fragments observed on the adhesive surface at the bottom of the iris were found to be ceramic after line scanning with EDS (Figure 3). In group 4, all of the fractures that occurred were adhesive. In group 5, all specimens showed cohesive fractures of the ceramic at the opposite side of the loading plunger (Figure 2c). From the EDS line scanning of fragments on the adhesively fractured flat adhesive surface at the bottom of an iris from group 3 (Figure 3), the composing elements of ceramic such as Si and Al were detected (asterisk), although they were not detected on the flat smooth surface.

The contact angle measurement of the ceramic specimens was 12.1 ± 1.7 ° when the surface was tested in an initial polished state. When the polished surface was altered through water plasma cleaning or TEGDMA plasma coating, the contact angle decreased to less than 10 °. However, when the plasma polymer coating was performed with hydrophobic HMDSO, the contact angle increased to 85.3 ± 8.5 °, even though it was applied on the hydrophilic surface obtained via water plasma cleaning. Once the surface was coated with HMDSO and when hydrophilic TEGDMA was applied to the hydrophobic surface obtained through HMDSO

treatment, the contact angle decreased (30.8 ± 2.6 °) but could not be lowered to the value of the TEGDMA-coated surface. Compared to the contact angle of the water droplet on the uncured oxygen-inhibited layer of the adhesive (45.2 ± 3.5 °), the polished surface or the various plasma-treated surfaces used in this study were more hydrophilic, except for the HMDSO plasma-treated surface.

1.2 The effect of the applied power of non-thermal atmospheric pressure plasma (NT-APP) jet on the adhesion of composite resin to dental ceramic

The current and voltage profiles of the applied a.f. power had a smooth sinusoidal form with a frequency of 15 kHz. The applied a.f. plasma power was amplified from an input voltage of 9 ~ 18 V at 60 Hz AC to an output voltage of 1.13 ~ 1.98 kV in V_{rms} and an output current of 7.07 ~ 14.14 mA in I_{rms} (Table 4).

The experimental groups with deposited plasma polymer of TEGDMA had a significantly greater mean SBS of the composite resin to ceramic surface than the negative control group (Table 4, $p < 0.05$). Although the mean SBSs of plasma treated groups were not significantly different, only the mean SBS obtained at a highest output voltage of 1.98 kV was statistically not different from that obtained by the conventional clinical protocol of HF etching and silane coupling agent coating. As the applied a.f. power increased, the number of adhesive fractures decreased and the number of mixed and cohesive fractures increased (Table 4 and Figure 4).

The contact angle between deionized water and the ground ceramic surface and the calculated work of adhesion from the measured contact angle were used as reference values for the ceramic substrate itself. HF etching and silane coating increased the contact angle value and made the surface slightly more hydrophobic than ceramic itself (Table 5). Regardless of the applied a.f. power, deposition of

plasma polymer decreased the contact angle values below the limit of measurement of the goniometric method, that is, less than 10 °, which indicated that plasma deposition made the ceramic surface extremely hydrophilic. Because the work of adhesion was calculated with the limit value of 10 °, the actual values of the adhesion work of all the plasma polymer deposited groups were in reality higher than the presented value of 144.5 mN/m.

Figure 5 shows a set of the C1s and O1s spectra of the ceramic specimens after plasma polymer deposition. The concentration of each chemical component was calculated from the C1s and O1s spectra by deconvolution using Gaussian fitting (Tables 6 and 7). As shown in Figure 5a, the C1s spectrum of the treated ceramic surface could be decomposed into three components: 1) C1, a component with a binding energy of 284.5 eV due to C-C bonds; 2) C2, a component with a binding energy of 286.1 eV due to C-O-C bonds; 3) C3, a component with a binding energy of 288.2 eV due to O=C-O bonds. The O1s spectrum of a treated ceramic surface could also be decomposed into two components: 1) O1, a component with a binding energy of 532.4 eV due to O=C-O bonds; 2) O2, a component with a binding energy of 531.3 eV due to a mixed peak of C=O in carboxyl group, -OH and C-O-C bonds (Figure 5b). The changes in the C1s and O1s spectra reflected chemical changes due to the various treatments. After the treatments, the atomic concentration (%) of the C1 peak decreased, while the atomic concentrations of both the C2 and C3 peaks increased (Table 7 and Figure 6). Compared to the C2 peak, the C3 peak showed a relatively prominent chemical shift after plasma polymer deposition (Figure 6c and Table 6). The atomic concentration (%) of the O1 peak increased, while the atomic concentration of the O2 peak decreased (Table 7 and Figure 7). The O1 and O2 peaks did not show chemical shifts, except for the

O2 peak of the silane-coated specimen. For the groups with deposited plasma polymer, the relative concentration of the C3 and O1 peaks increased as the applied power increased. The n(O1s)/n(C1s) ratios of the ceramic surfaces with plasma polymer deposition were higher than that of the untreated polished ceramic surface (Table 7).

1.3 1,3-Butadiene as adhesion promoter between composite resin and dental ceramic in a floating electrode dielectric barrier discharge (FE-DBD) jet

The current and voltage profiles of the experimental FE-DBD jet showed uniformly smooth sinusoidal curves (Figure 9). At a flow rate of more than 2.0 sccm of 1,3-butadiene gas, the mean SBS of the composite resin to ceramic exhibited a plateau and was significantly higher than those of the control group and the experimental group at a flow rate of 0.5 sccm (One-way ANOVA, $p < 0.05$, Table 8). At a flow rate of 3.0 sccm, the incidence of cohesive fracture were significantly different from that of the control group, in which all the specimens were adhesively fractured (Kruskal-Wallis non-parametric test, $p < 0.05$, Table 8).

The atomic concentration of carbon increased from 25.5% of untreated ceramic surface to 86.4% of the plasma-treated surface with a flow rate of 3.0 sccm, while the oxygen concentration decreased from 49.7% to 12.5%, respectively (Table 9). The atomic concentrations of the exposed silicon also decreased from 24.8% to 1.1%. With the plasma-deposition of 1,3-butadiene, the n(O1s)/n(C1s) ratio dropped from 1.96 to 0.15. This indicated a relative increase of carbon atomic concentration of the ceramic surface through plasma-deposition of the hydrocarbon gas.

As shown in Figures 11a and 11c, the C1s spectrum of the treated ceramic surface could be deconvoluted into three components: 1) C1, a component with a binding

energy of 284.5 eV due to C-C and C=C bonds; 2) C2, a component with a binding energy of 285.9 eV due to the singly bonded oxygen to carbon C-O-C bonds; 3) C3, a component with a binding energy of 287.6 eV due to the additionally doubly bonded oxygen to carbon O=C-O bonds. The O1s spectrum could also be deconvoluted into two components: 1) O1, a component with a binding energy of 532.2 eV due to -OH group; 2) O2, a component with a binding energy of 531.4 eV due to O-Si bonds of SiO_2 crystals (Figures 11b and 11d). With increasing flow rates of precursor monomer gas, the C1s peaks increased more than three times compared to the peaks of untreated ceramic surface, but the O1s and Si2p peaks and n(O1s)/n(C1s) ratio decreased (Table 9 and Figures 11c and 11d). The O2 peak disappeared completely from the spectra.

Compared to the FTIR spectra obtained from the ground ceramic surface, the FTIR peaks of the various functional groups were apparently observed after plasma deposition (Figure 12). The heights of these peaks related to the carbon atoms such as those of the C=C bonds and C-H stretches showed an increasing tendency with the increase of the monomer flow rate. The increase in the peak height of C=C bonds observed from the FTIR results supported the fact that the increase in the C1s peak partially resulted from the increase of C=C bonds, in addition to the increase of C-C bonds. When the ceramic sample was prepared with an FIB and observed under a TEM, the PECVD polymer layer was approximately 500 nm thick (Point 2 in Figure 10). The PECVD layer was observed between the sputter-coated Pt layer (Point 1) and the underlying ceramic substrate (Point 3), which was confirmed with EDS.

1.4 Sequential deposition of Hexamethyldisiloxane and benzene in floating electrode dielectric barrier discharge (FE-DBD) jet adhesion to dental

ceramic

When the ceramic surface was deposited with PECVD of H_2O, the SBS was significantly higher than that of the negative control group ($p < 0.05$, Table 10). In the case of H_2O, even though the *Wa* became higher than 144.5 x 10^{-2} N/m, the adaptation of the adhesive into the irregularities and the gap at the interface looked similar to those of the negative control group (Figures 13a and 13b). However, when HMDSO was deposited on the ceramic surface, the surface showed superhydrophobicity, and as a result, a wide gap was apparently observed at the interface and the SBS was the lowest (Table 10 and Figure 13c). In the case of benzene, in spite of the lower *Wa* than the negative control group and H_2O Group 2, the adaptation of the adhesive looked better (Figure 13d). The SBS was also significantly higher than that of the negative control group, but it was not superior to that of the water-treated group. When the ceramic surface was plasma-deposited with benzene after HMDSO deposition, it showed a higher *Wa* value than the HMDSO deposited surface. The adhesive adaptation was quite different from the HMDSO-deposited group and looked similar to the other groups (Figure 13e). The SBS was significantly higher than those of the water plasma treated group and the group plasma-treated with benzene only ($p < 0.05$, Table 10). All the fractures in Group 3, which showed superhydrophobicity by HMDSO deposition and had the lowest bond strength, were adhesive ones. Although the negative control group had a very high *Wa* value, the adaptation of the adhesive was not good and the SBS was low, and as a result, all fractures were also adhesive. However, in the groups treated with water, benzene, and HMDSO/benzene, and showing higher SBS, the incidence of cohesive and mixed fractures significantly increased (Chi-square test, $p < 0.05$, Table 10).

After PECVD of benzene with or without HMDSO, C1 peak was increased more than two times compared to the negative control group (Table 11). The increase of C1 peak was attributed to the increase of C=C double bonds rather than C-C bonds, that can be referred to the aromatic C=C double bonds at 1600 cm^{-1} in the FTIR-ATR spectra of the ceramic surfaces plasma-deposited with benzene or HMDSO/benzene (Figure 14). In the case of HMDSO deposition, with the increase of C1 peak, the peaks corresponding to methyl groups ($C-H_3$) in $Si-CH_3$ at 1255 cm^{-1} was also increased prominently in both groups 3 and 5 (Figure 14). In the groups that were treated with water and benzene and showed high bond strengths, oxygen-containing ether and carbonyl groups (C2 and C3 peaks, C-O and C=O, respectively) increased about ten times and ester group (C4 peak, O-C=O) also increased about three times (Table 11). HMDSO deposition increased siloxane networks (Si2, O-Si-O) by the reaction between HMDSO and silicon dioxide. However, subsequent deposition of benzene masked the siloxane networks, but left Si1 (Si-O-C) peak on the surface (Table 11). Along with the aromatic C=C bonds in the FTIR spectra (Figure 14), deposition of HMDSO or benzene completely masked or at least decreased the O1 (Si-OH) peak and O2 (O-Si-O) peak that related with the silicon dioxide of the ceramic component (Table 11).

1.5 Promotion of resin bonding to dental zirconia ceramic using plasma deposition of tetramethylsilane and benzene

Figure 15 shows the comparison of mean shear bond strength values for all groups. Plasma deposition and the use of the zirconia primer significantly improved bond strengths compared with the control group (4.5 ± 2.6 MPa) ($P < 0.05$). The TMS (10.3 ± 2.8 MPa) and benzene (10.1± 4.1 MPa) groups exhibited similar bond strengths to that of the zirconia primer (10.3 ± 3.2 MPa). Consecutive

plasma deposition with TMS and benzene (22.7 ± 3.7 MPa) showed the highest bond strength among all groups ($P < 0.05$).

Figure 16 shows the O1s and Zr3d spectra of a specimen after plasma deposition with TMS compared with those of a non-treated zirconia specimen. The O1s spectrum of the non-treated zirconia was able to be deconvoluted into thee peaks centered at 529.7, 531.4, and 532.5 eV. The peak at 529.7 eV, which appeared most strongly, was assigned to O–Zr bonds of zirconium oxides, while the peaks at 531.4 and 532.5 eV were assigned to O=C and O=C–O groups. The Zr3d spectrum of the non-treated zirconia showed characteristic doublet peaks of zirconium oxides centered at 181.6 and 184.0 eV. After plasma deposition with TMS, the O1s spectrum was detected only at 532.3 eV, which can be ascribed to Si–O–Zr bonds. The doublet peaks of Zr3d spectrum were not detected after plasma deposition with TMS.

A representative TEM image of a cross-sectioned specimen, which was plasma-deposited sequentially with TMS and benzene, showed two distinct layers on the zirconia surface (Figure 17). The plasma-polymerized layers were intimately adhered to the zirconia surface. There were no flaw and discontinuity within the layers. The thickness of each layer was approximately 50 nm. EDS analysis clearly showed the differences in composition between the two deposited layers: the first Si-rich layer resulting from the plasma deposition with TMS and the second C-rich layer resulting from the plasma deposition with benzene.

2) ADHESION TO TOOTH

2.1 Effect of plasma deposition using low-power/non-thermal atmospheric pressure plasma on promoting adhesion of composite resin to enamel

In 1,3 butadiene plasma coating study, the plasma deposition was extremely thin

(less than 10 nanometers), so that it could not be observed easily even under highly magnified SEMs. Therefore, before preparing specimens for MSBS tests, the deposition of plasma polymer was verified by measuring the increase in the contact angle. The static contact angle values obtained by a goniometric method are shown in Table 13. The hydrophilic characteristics of the etched enamel surface was preserved after He plasma treatment when no monomer was used. However, the plasma polymer deposition of BD and BZ caused the etched enamel surface to become hydrophobic. The contact angle values were well adapted to the plasma polymer-deposited surfaces with contact angles of approximately 60 degrees. Using XPS, deposition of plasma polymer was also confirmed by the changes in the chemical composition between the etched enamel surface and the plasma polymer-deposited surfaces. After plasma deposition of BD or BZ, the C1s peaks increased, but the O1s peaks and n(O1s)/n(C1s) ratio decreased (Table 14). These changes indicated deposition of carbon-containing plasma polymers.

Surface treatments and TC significantly affected the MSBS of composite resin to enamel surface (2-way ANOVA, $p < 0.05$, Table 12). When the etched enamel surface was deposited with plasma polymer of BD or BZ using the low-power, non-thermal atmospheric pressure plasma jet, the initial MSBS of composite resin to enamel increased significantly (Scheffe's test, $p < 0.05$). The increase in the initial MSBS might be ascribed partly to the moderate hydrophobicity of approximately 60^{o} in contact angle measurements, and as a result, to the improved wettability and adaptation of the adhesive to the hydrophobic plasma-treated enamel surface. In addition to the wettability, the increase in the MSBS might have been mediated partly by the chemical reactions between the C=C double bonds remaining in the plasma-deposited polymer and those in the adhesive monomers.

From the XPS results, the C1s peaks at the plasma polymer-deposited enamel surface increased compared to the untreated enamel surface (Table 14). Because the C1 peak at a binding energy of 284.5 eV was a mixed peak of -C-C-, -C=C-, and -CH bonds, it was not clear whether there was -C=C- in the plasma polymer deposition and whether there was a chemical reaction between -C=C- of the plasma polymer deposition and the adhesive. However, according to the FT-IR spectra, aliphatic C=C double bonds appeared at 1635 cm^{-1} after plasma polymer deposition of BZ or BD, unlike the spectra of BZ monomer and BD gas (Figure 18a, 18a). In the spectrum of plasma deposition of BZ, the peak for aliphatic C=C double bonds at 1635 cm^{-1} disappeared after aging in a dark room at 55^{o}C for 7 days, which simulated the thermal aging of TC (Figure 18b). The peak in the spectrum of plasma-deposited BD also decreased slightly (Figure 19b).

2.2 Effects of non-thermal atmospheric pressure pulsed plasma on the adhesion and durability of resin composite to dentin

Table 16 shows the mean and standard deviation of MTBS for all test groups. The two-factor repeated measures ANOVA revealed that the plasma treatment ($F = 50.928$, $p = 0.000$) had a significant effect on the bond strength, but the effect of artificial aging ($F = 0.736$, $p = 0.397$) and the interaction effect ($F = 2.815$, $p = 0.067$) were not significant. The plasma treatment groups showed significantly higher bond strength than the control group, both at 24 hours and after thermocycling (Scheffe test, $p < 0.05$). However, there were no significant differences between plasma treatment groups at either measurement time. After artificial aging, the mean bond strength of the control group and the conventional plasma group did not significantly decrease from the initial mean bond strength, but that of the pulsed plasma group increased significantly ($p < 0.05$).

The Weibull moduli and the characteristic strengths with their corresponding confidence intervals are summarized in Table 17, and the Weibull cumulative probability plots are shown in Figure 24. The Weibull moduli and the characteristic strengths of the plasma treatment groups were higher than those of the control group. Thermocycling increased the Weibull moduli of the plasma treatment groups, particularly in the pulsed plasma group.

In this study, because the bond strength data obtained from the specimens that showed cohesive fractures within dentin or resin composite were discarded in order to obtain the exact value of the adhesion, the fractures of all the specimens after MTBS testing were adhesive (Figure 25). Therefore, the fractured surfaces of the MTBS specimens showed shiny surfaces that resulted from fracture at the interface of the hybrid layer and the adhesive layer (white arrows) that were evaluated as the adhesive fractures. In addition, the shiny surfaces of the adhesive fractures showed adhesive resin remnants that were fractured cohesively within the adhesive layer (asterisks); these were categorized as mixed fractures.

The bonded interface of the sliced specimens selected from each group showed high-quality adhesion as a result of the treatments (Figure 26). Intimate contact was observed between the resin composite and the adhesive layer and between the adhesive layer and the hybrid layer, i.e., there was no gap at the interface. Abundant resin tags were also observed in the specimens of all three groups. However, resin tags on the dentin surface treated with plasma, particularly those in the conventional plasma group, were more abundant, longer, and more tortuous with lateral projections compared to those on the control surfaces (Figure 26c).

2.3 Promotion of Adhesive Penetration and Resin Bond Strength to Dentin using Non-thermal Atmospheric Pressure Plasma

One-way ANOVA indicated that there were significant differences in the MTBS between the groups (Table 18, $P < 0.001$). The plasma-drying group presented the highest mean MTBS value of 61.2 ± 14.3 MPa, followed by the plasma-drying/rewetting group (58.6 ± 14.6 MPa) and wet bonding group (52.2 ± 16.8 MPa). The bond strength of the plasma-drying group significantly improved as compared to the wet bonding group ($P < 0.05$). The dry bonding group presented the lowest mean MTBS value of 28.9 ± 9.5 MPa ($P < 0.05$). According to the Weibull statistics, the plasma-drying group possessed a higher Weibull modulus (m = 4.93) and characteristic strength (σ_θ = 66.8 MPa) than the plasma-drying/rewetting (m = 4.50, σ_θ = 64.3 MPa) and wet bonding (m = 3.45, σ_θ = 58.1 MPa) groups (Table 18). The dry bonding group possessed the lowest Weibull modulus (m = 3.39) and characteristic strength (σ_θ = 32.3 MPa).

Representative micro-Raman mapping spectra acquired across the adhesive/dentin interface for a specimen selected from the wet bonding group is shown in Figure 27. The intensities of the Raman bands associated with the adhesive monomer (1113, 1454, and 1609 cm^{-1}) decreased gradually from the adhesive layer to the dentin. Figure 2 shows the band ratios of 1113 cm^{-1}/1667 cm^{-1}, 1113 cm^{-1}/1454 cm^{-1}, and 1640 cm^{-1}/1609 cm^{-1} as a function of the position across the hybrid layer, from the bottom part to the upper part of the hybrid layer. The band ratio of 1113 cm^{-1}/1667 cm^{-1}, which indicated BisGMA penetration, gradually decreased when approaching the bottom part of the hybrid layer in all the test groups (Figure 28A). However, in the upper part of the hybrid layer, the plasma-drying group possessed a higher 1113 cm^{-1}/1667 cm^{-1} ratio than those of the wet bonding and plasma-drying/rewetting groups. The band ratio of 1113 cm^{-1}/1454 cm^{-1} indicated the relative content of BisGMA in the penetrating adhesive (Figure 28B). The plasma-drying and dry

bonding groups were similar in the 1113 cm^{-1}/1454 cm^{-1} ratio, except at the bottom part of the hybrid layer. The ratio of the plasma-drying group was apparently greater than those of the wet bonding and plasma-drying/rewetting groups across the hybrid layer. The band ratio of 1640 cm^{-1}/1609 cm^{-1} was inversely proportional to the degree of conversion of the adhesive (Figure 28C). The dry bonding group presented the lowest ratio, which indicated the highest polymerization efficacy. The plasma-drying group possessed a lower 1640 cm^{-1}/1609 cm^{-1} ratio than those of the wet bonding and plasma-drying/rewetting groups.

Representative SEM images of the adhesive/dentin interface are shown in Figure 29. The wet bonding, plasma-drying, and plasma-drying/rewetting groups presented intimate contact between the adhesive layer and hybrid layer with well-developed resin tags, whereas the dry bonding group presented distinct gaps in the interfacial region. The plasma-drying group presented a more uniform and homogeneous adhesive/dentin interface than the wet bonding and plasma-drying/rewetting groups. Furthermore, in the plasma-drying group, lateral branches of resin tags, which projected into dentinal canaliculi, were abundant and clearly observed throughout the entire length of the resin tags.

4. DISCUSSION

1) ADHESION TO CERAMIC

1.1 The effect of plasma polymer coating using non-thermal atmospheric pressure plasma (NT-APP) jet on the shear bond strength of composite resin to ceramic

We applied new innovative NT-APP jet equipment to ceramic bonding. In the

clinic, feldspathic porcelain restorations are bonded according to a routine protocol using hydrofluoric acid etching and silane coupling agent coating such as ceramic primer.[41] In this study, the plasma polymer coating was evaluated as a chemical mediator for ceramic bonding and as an effective substitute for HF etching and silane coupling agent coating. In the SBS test, although the bond strength obtained after plasma polymer coating with only TEGDMA (group 2) failed to show a statistical difference from the bond strength obtained from the polished surface (group 1, negative control group), the bond strength obtained after sequential plasma surface cleaning with DW and plasma polymer coating with TEGDMA (group 3) was significantly greater than that of the negative control group (group 1). The results showed that the NT-APP jet polymer coating technique could contribute to the enhancement of ceramic bonding with conventional dental adhesives. Additional surface treatment with water plasma seemed to have the effect of surface activation due to the ionized –OH radicals or at least the effect of cleaning, which was similar to the effect of the oxygen plasma used to increase the hydrophilicity under vacuum conditions.[2,8,17,42] It was assumed that the –OH radicals created a very hydrophilic surface. The values of groups 2, 3, and 4 were comparable to the results obtained by Derand et al. (15.2 ± 2.6 MPa in SBS) in a reactor using plasma deposition consisting of the activation of substrate surfaces with oxygen, RF plasma deposition with HMDSO and additional activation of the polymer with oxygen[17]. Polar liquids, such as ethanol or methanol, can also be good candidates for surface modification to graft hydroxyl group (–OH)[43]. Further study using ethanol or methanol plasma is needed to modify the hydrophilicity of the substrate surface.

This study also evaluated the effect of HMDSO deposition on ceramics because,

in many studies on plasma adhesion performed in a vacuum chamber, HMDSO was used as a precursor monomer to coat a thin film onto substrates.[17,44] Plasma polymer coating with HMDSO has been proven to be an effective primer coating for adhesion promotion because –Si–O– bonds are known to form covalent bonds with metal and ceramic, and oxygen has been widely used as a carrier gas in plasma surface treatment[17,42,44]. Radicals like Si–O, Si–C, Si–O–Si, or Si–CH(x) (x can be 2, 3, or 4), dissociated from HMDSO molecules by high energy electrons, can react with surface metal, metal oxide, or metal hydrate to form metallic-silane, metallic-siloxane, organo-metallic-silane, or organo-metallic- siloxane. M–Si or M–O–Si is known to create very stable chemical bonds.[13,45] However, an additional HMDSO plasma polymer coating (group 4) applied before TEGDMA plasma coating failed to show a significant difference in SBS from that of the negative control (group 1). Although radicals like Si–O, Si–C, Si–O–Si, or Si–CH(x) (x can be 2, 3, or 4) that dissociated from the HMDSO molecule were expected to promote the adhesion between the ceramic primed by the monomer and the overlying adhesive, all of the specimens in group 4 showed adhesive fractures (Table 3). It seemed that hydrophilic adhesive failed to adequately wet the hydrophobic surface of the plasma polymer of HMDSO. Group 5, which consisted of specimens bonded with HF etching and silane coupling agent coating, showed significantly higher bond strength than the other groups, and all specimens exhibited cohesive fractures in the ceramic (Figure 2c). Among the groups in which specimens were treated with plasma polymer coating, only group 3 showed a significantly higher bond strength (Kruskal–Wallis test, $p < 0.05$) and significantly more mixed fractures (Chisquare test, $p < 0.05$, Table 3 and Figures 2b, Figure 3) than did the negative control group. At the fractured bottom surface

of the composite resin in the iris, the specimens showing mixed fractures had small fragments of ceramic on the flat adhesive layer that resulted from the adhesive fracture between the polished surface of the ceramic and the adhesive layer (Figure 3). These fragments demonstrated that there was an island of cohesively fractured ceramic fragments on the flat cured adhesive layer and that the element Si, included in the composite resin as filler, was masked by the adhesive layer.

Although it was not clear whether the plasma-coated polymer was on the polished ceramic surface or on the composite resin side due to its extremely thin thickness, the adhesive layer must have been attached to the composite resin side. The small fragments observed especially at the point at which the plasma flame was directly applied were confirmed as ceramic according to an EDS scan. Even though the effective area of the flame was small, the fragment of ceramic cohesive fracture showed that the NT-APP jet polymer coating technique could contribute to enhance the ceramic bonding of conventional dental adhesives.

The water contact angle of the HMDSO plasma polymer coating (85.3 ± 8.5 °) was higher than that of the TEGDMA plasma polymer coating (less than 10 °). During the pilot study, it was also found that, because the adhesive (SBMP adhesive) aggregated on the HMDSO plasma coated surface, the surface could not be coated and failed to obtain good bond strength due to the poor wetting. In the other conditions of contact angle measurement, the values of the substrate surfaces were lower than those of the adhesive (45.2 ± 3.5 °, Table 2).

Although the exact level of fracture could not be differentiated, the relatively low bond strength and high number of adhesive fractures in group 4 were assumed to be attributed to the large difference in the hydrophobicity between HMDSO and TEGDMA. Therefore, the hydrophilicity of the plasma polymer-coated substrate

surface was necessary to facilitate the wetting of the adhesive. In this study, we chose TEGDMA as the precursor monomer, a constituent of dental adhesives which is more hydrophilic than other adhesive ingredients such as Bis-GMA and which can be vaporized due to its high volatility. In this study, helium gas was used as the carrier gas because of its inertness and ability to stabilize a glow discharge outside of a vacuum chamber.[8] Although plasma treatments of oxygen, air, nitrogen, and argon gases increased wettability,[46] oxygen is an electron-negative gas that requires a much higher breakdown voltage to generate plasma. Argon also requires high breakdown voltage. As a result, the plasma temperature was elevated to the level at which the plasma could not be applied to vital dental ceramic. Moreover, because oxygen can also be involved in co-polymerization with monomer gas, it was difficult to prepare a stable NT-APP jet and to create a plasma polymer with proper characteristics.

1.2 The effect of the applied power of non-thermal atmospheric pressure plasma (NT-APP) jet on the adhesion of composite resin to dental ceramic

The properties of a plasma polymer are influenced by the electrode configuration, gas flow rate, gas type, applied power, and distance between the plasma applicator nozzle and the substrate surface.[9, 31] NT-APP jet are more homogeneous and thus less physically aggressive to the polymer surface, while corona treatment is known to be inhomogeneous and to increase surface roughness.[21,37] Within the range of the applied powers used in this study, the waveforms of the applied voltage and discharge current had homogeneous characteristics of glow discharge (Figure 1). An increase in the treatment time and applied power of homogeneous plasma discharge can induce an increase in the number of hydrophilic polar groups on a surface.[33] In this study, because the mean SBSs of plasma polymer deposited

groups were statistically not different, we could not reject the null hypothesis that there were no differences in adhesion strength according to changes in the applied a.f. power. However, only the adhesive strength of the group with the highest output power (transformed from an input power of 18 V to an output power of 1.98 kV in V_{rms}) was statistically not different from that of the positive control group treated with a conventional clinical protocol of HF etching and silane coupling agent coating. This result still suggested the possibility that by increasing the applied power, the adhesive strength might also increase. The fracture mode also changed from mostly adhesive to mostly mixed or cohesive, that is, the number of adhesive fractures decreased and the number of mixed and cohesive fractures increased.

Contact angle studies were conducted to compare the hydrophilicity of the treated ceramic surfaces. The values of the work of adhesion calculated from the contact angles of deionized water to variously treated ceramic surfaces indicate the hydrophilicity of each surface.[39] A low contact angle, that is, the high adhesion work indicates high hydrophilicity. The contact angle of the ground ceramic surface was relatively low because of its surface roughness. Regardless of the applied power, the plasma polymer of TEGDMA decreased the contact angle value drastically to below the limit of measurement of the goniometric method, i.e., less than 10^{o}. In addition to the roughness of the ground ceramic surface, the deposited plasma polymer improved the hydrophilicity of the dental ceramic surface substantially. Because we used a contact angle of 10^{o} to calculate the adhesion work using Equation 1, the work of adhesion, i.e., hydrophilicity of the plasma treated surfaces was higher than the presented value (144.5 mN/m) in Table 5. However, because the contact angle values of three plasma treated groups were all

below the limit of measurement of the goniometric method, we were not able to detect the differences in the hydrophilicity of deposition among these groups. This may explain why the mean SBS values of these samples were not significantly different.

The application of silane as well as hydrophobic adhesives made the ceramic surface hydrophobic. However, during application of NT-APP jet, TEGDMA can be decomposed randomly at various positions according to the applied power, flow rate, and residence time in the reactor, etc.[19] NT-APP jet deposited a great number of oxygen-containing polar functional groups derived from decomposed TEGDMA monomers on the ceramic surface, which made the ceramic surface hydrophilic. The observation that the application of NT-APP jet decreased the contact angle values of water from 15.9 ± 3.8° (untreated polished surface) to less than 10° (treated surface) strongly indicated that chemical deposition occurred.

XPS analysis was performed to investigate the chemical functional groups deposited on the ceramic surface by the application of NT-APP jet. For the XPS analysis, the specimens were prepared without adhesive coating because an extremely thin plasma-deposited layer (nanometer scale) cannot be discerned from a thick adhesive layer. Just after a cleaning procedure of etching with 10% citric acid, rinsing with distilled water and then cleaning ultrasonically for 5 minutes, the cleaned ceramic surfaces of all the specimens were inevitably contaminated by environmental hydrocarbons before the assigned surface treatments.[5,47] The circumstances would be the same in a clinical situation. We assumed that, before treatment, the chemical composition of the ceramic surfaces of all the samples were the same by contamination of environmental hydrocarbons. Therefore, we interpreted the changes in the C1s spectra of ceramic surfaces as the chemical

changes resulting from the assigned surface treatments.

XPS results also showed that the improvement of the hydrophilicity of the treated ceramic surfaces could be attributed to the introduction of oxygen-containing polar groups from random decomposition of the precursor monomer TEGDMA on the ceramic surfaces. After application of NT-APP jet, the changes in the atomic concentrations (%) of the C1, C2, and C3 peaks and the chemical shift of the C3 peak suggested that a number of oxygen-containing polar groups were deposited onto the ceramic surface. After plasma treatment, the content of C-C bonds decreased, while the content of oxygen-containing hydrophilic polar groups, such as C-O-C and O=C-O bonds, increased. According to the simple additivity rule, the binding energy shift caused by carbon doubly bonded to oxygen is ~2.6 eV, and the binding energy shift from a carbonyl to a carboxyl group because of the additional oxygen singly bonded to carbon is ~1.4 eV, giving a total of ~4.0 eV.[5,48] C2 corresponds to a simple ether bond (C-O-C) and C3 corresponds to a carboxyl group (O=C-O) rather than a simple carbonyl bond (C=O). It has been reported that for simple carbonyls, alcohols, and ethers, the binding energies for the O1s levels are essentially the same, while the O1s peak corresponding to the singly bonded oxygen in the carboxyl group is substantially shifted (~1.5 eV).[48] For O1s spectra, the atomic concentration of the O2 peak corresponding to a mixed peak of C=O, -OH, and C-O bonds decreased, while the O1 peak corresponding to the singly bonded oxygen in the carboxyl group increased. For the plasma polymer-deposited samples, a chemical shift and increase in the relative concentration of C3 were observed as the input power increased. These results suggested that the concentration of polar carboxyl groups deposited onto the ceramic surface increased with increasing input power, resulting in an increase in adhesive strength.

This finding is consistent with that of a previous report of surface treatment of polyethylene terephthalate (PET) using DBD.[33]

Although there were no significant differences in the mean SBS values among the plasma polymer-deposited groups at different input powers, only the mean SBS of the group treated with the highest input power of 18 V was not statistically different from that of the silane coated group. Compared to the other plasma polymer-deposited groups with input powers of 9 and 15 V, the atomic concentrations of C3 (O=C-O) and O1 (O=C-O) increased and those of C2 (C-O-C) and O2 (a mixed peak of C=O in carboxyl group, -OH and C-O-C) decreased in the group at 2.0 kV input power. After silane coating, the n(O1s)/n(C1s) ratio decreased. The plasma treatments increased the ratio of n(O1s)/n(C1s), but the ratio of n(O1s)/n(C1s) obtained at an input power of 18 V was lower than the ratios obtained at the lower input powers. These observations suggested that silane coating and plasma polymer deposition at a higher input voltage induce more carboxyl groups (C3 and O1) on the ceramic surface than simple C2 ether groups (C-O-C) or O2 a mixed peak of C=O, -OH, and C-O bonds. The adhesive applied on the silane-coated ceramic surface formed a strong covalent bond even at a low n(O1s)/n(C1s) ratio and, as a result, caused typical cohesive fractures. (Table 7.) However, studies have indicated that the mechanism of plasma polymerization is dominantly free radical polymerization.[5,29] Therefore, to enhance adhesion using NT-APP jet, it would be required to induce more polar carboxyl groups compared to simple ether groups and C-C linkages by regulating parameters such as increasing applied power. Increasing the applied power results in more intensive discharge and results in the formation of a higher amount of active species, which in turn interact with the substrate surface and induce the formation of more radicals

on the surface.

1.3 1,3-Butadiene as adhesion promoter between composite resin and dental ceramic in a floating electrode dielectric barrier discharge (FE-DBD) jet

The 'PECVD' technique using the equipment and TEGDMA precursor monomer was comparable in the adhesion effectiveness to the currently-used ceramic surface treatment with hydrofluoric acid and silane coupling agent. However, it was difficult to prevent from heat and streamer generation with the pencil-type plasma torch design, in which a rod electrode was passing through a dielectric ceramic tube and a hot electrode wrapped the tube. In order to use the equipment in dental ceramic, the plasma should be generated in ambient air, in low power, and with low temperature. It should be very stable, so that it should not generate high-current filamentous discharges.[18,19] FE-DBD jet can be generated with low energy consumption, so that it has several advantages.[34,35] It is non-thermal and silent. It generates uniform glow discharges in low power and it can be sustained for many hours. The FE-DBD as a direct plasma method is also known to be very effective to transfer excited species and charged species with homogeneous and high-rate deposition.

The plasma jet used in this study showed the characteristics of homogeneous DBD during plasma deposition of 1,3-butadiene gas (Figure 8a). The light emission image had no randomly distributed bright filaments. Corresponding waveforms of the applied voltage and discharge current were uniformly repeating and oscillating bipolar form (Figure 8b). Each current pulse appeared in each applied voltage pulse and their amplitudes were constant. These features are apparently different from those of filamentary discharges, in which a number of current pulses with nanoseconds duration time appears in each applied voltage

pulse and a number of randomly distributed bright filaments were observed in the emission images.[33]

When TEGDMA was used as a precursor monomer, NT-APP jet enhanced the adhesion of composite resin to ceramic surface by inducing carboxyl groups on the surface and by improving surface hydrophilicity. The improvement of the hydrophilicity of the ceramic surfaces was attributed to the oxygen-containing polar groups from randomly decomposed TEGDMA on the ceramic surfaces with XPS analysis. However, TEGDMA can be decomposed randomly at various positions according to various conditions such as the applied power, flow rate, and residence time in the reactor, etc.[29] Even with simple hydrocarbons, the complexity of chemical reaction in the PECVD made the system unstable and limited their clinical usage[18]. Therefore, the precursor monomer used in a plasma polymer deposition system needs to be simple and relatively low molecular weight hydrocarbons. We selected 1,3-butadiene among simple hydrocarbons. Despite the relatively low molecular weight, 1,3-butadiene has two aliphatic C=C double bonds that may be broken easily to active radicals with plasma energy. It can evaporate easily because it is in a gas state at a room temperature. A large amount of activated species can be transferred to the substrate surface with a low flow rate of the gas.

By virtue of the advantages of the FE-DBD equipment design and 1,3-butadiene precursor monomer, a stable and equivalent adhesion-promoting effect of PECVD was obtained with very low applied energy of 5.15 W and low flow rate of 2.0 sccm of precursor monomer, respectively. The fractures of the specimens treated with the FE-DBD and 1,3-butadiene (40 – 70%) showed relatively higher proportions of cohesive fracture than those with the NT-APP jet and TEGDMA (30

– 35%). The SBS and the incidence of cohesive fracture of the ceramic specimens increased with the increase of flow rate of 1,3-butadiene. However, when the flow rate of the monomer exceeds 2.0 sccm, the SBS and the incidence of cohesive fracture showed a plateau. Therefore, the hypothesis was partly accepted.

The chemical composition of ground ceramic surface showed a great amount of silicon (Si2p), and oxygen (O1) and hydroxyl group (O2) bound to silicon of the ceramic surface (Group 1 in Table 9).[23] Although there was no oxygen in 1,3-butadiene, a great deal of ether (C2) and ester (C3) bonds were also detected in the XPS and FTIR-ATR analyses. The unexpected carbon atoms might come from the environmental carbon dioxide. By the plasma-deposition with increasing amount of 1,3-butadiene, the total atomic concentration of C1s increased up to 86.4%, while those of the components Si2p, O1 and O2 existing on the ground ceramic surface decreased to 12.5%, 0.0% and 1.1%, respectively (Groups 3, 4 and 5 in Table 9). As a result, the ratio of n(O1s)/n(C1s) decreased from 1.96 of ground ceramic surface to 0.15 of PECVD-deposited ceramic surface. It means that the carbon atoms originated from the breaking 1,3-butadiene coated the ceramic surface.

The increase of C1 peak in the plasma-treated ceramic surface was the most prominent change. However, the C1 peak includes both C-C and C=C bonds. It is not discernable how much is the proportion of each bonds in the C1 peak with the XPS result. In this study, the increase of aliphatic C=C double bond was confirmed by the FTIR spectra in an ATR mode. Because the deposition by PECVD had a thickness of nanometer scale, it is too difficult to detect the composition using FTIR. In order to increase the thickness of the deposition, PECVD were performed for 15 minutes with different flow rates of 1,3-butadiene. Although 15 minutes of plasma deposition was too long and thus clinically not practical, the increase in the

flow rate of 1,3-butadiene resulted in the proportional increase of the aliphatic C=C bond at 1635 cm^{-1} (Figure 12). The effect of the PECVD with 1,3-butadiene was also confirmed visually with the apparent polymer layer in the transmission electron microscopic image (Figure 10).

When the monomer was carried into the reactor by helium gas, it was broken down by plasma energy. The excited monomer species were carried onto the ceramic surface by helium gas. In this study, the plasma deposition of 1,3-butadiene with FE-DBD effectively coated the ground ceramic surface with carbon atoms (C1s) originating from the monomers broken-down by plasma energy. Silicon and oxygen and hydroxyl groups bound to silicon (Si2p and O1s, respectively) were covered with the carbon atoms from the plasma deposition. Because the atomic concentrations of C1, C2 and C3 peaks showed a similar increasing trend with a flow rate of more than 2.0 sccm of 1,3-butadiene and there was no apparent change in the binding energy of each peak of the XPS spectra by plasma deposition, the oxygen consisting the C2 and C3 peaks must have come from the environmental oxygen. After the plasma was turned off, the highly reactive excited species on the ceramic surface might also react with the oxygen in the air. The carboxyl groups suggested in the previous report were found in a little fraction. The fragmented C=C double bonds of 1,3-butadiene molecules were suggested to cover the ceramic surface with simple deposition and, in a very small part, with chemical bonds (O1) to ceramic surface. Therefore, among the increased C1 peak observed by XPS, the fragmented aliphatic C=C double bond that was confirmed with FTIR was the most active species on the ceramic surface. The increase in the C=C double bonds on the plasma-treated ceramic surface was attributed to the increase of the SBS in case of PECVD using FE-DBD equipment

with no oxygen-containing 1,3-butadiene precursor monomer gas, the increase in the C=C double bonds on the plasma-treated ceramic surface was attributed to the increase of the SBS.

1.4 Sequential deposition of Hexamethyldisiloxane and benzene in floating electrode dielectric barrier discharge (FE-DBD) jet adhesion to dental ceramic

In industries, HMDSO was used to establish a stable siloxane network on substrate surfaces for adhesion promotion.[28,49] In this study, we observed the increase of the Si2 and C1 peaks in Group 3, in which bifunctional HMDSO was deposited by FE-DBD jet (Table 11). However, the SBS of this group was significantly lower than those of the other groups ($p < 0.05$). The increase of the C1 peak observed in the XPS spectrum was well agreed with the increase of the Si-CH_3 peak at 1255 cm^{-1} and the aliphatic C-H vibration peak at 2927 cm^{-1} in the FTIR-ATR spectra.[49,50] The increase in the hydrophobic Si-CH_3 group and lack of the hydrophilic carbonyl and ester groups of the HMDSO deposited surface lead to the superhydrophobicity of the surface,[51] which in turn, resulted in a wide gap between the treated ceramic surface and the adhesive and low bond strength.

In contrast to HMDSO, plasma-deposited benzene in a nano-meter scale made the ceramic surface moderately hydrophobic. However, because the plasma polymer was aged in ambient air before the application of the adhesive, the hydrophilic groups seeded by ambient air (C2, C3, and C4 peaks) improved the adaptation of the adhesive into the irregularity on the ceramic surface,[49] like O_2 treatment of plasma polymerized HMDSO coatings.[28,51] In the case of water plasma, the C1 peak decreased but the hydrophilic C2, C3, and C4 peaks increased about three times compared to the negative control group. The increase of the oxygen-

containing hydrophilic groups was coincident with the decrease of the contact angle measurement, improved wettability of the surface, and lead to the good adaptation. The cleaning effect of water plasma was confirmed by the decrease of environmental carbon (C1 peak) on the negative control ceramic surface and might also contribute to the increase of bond strength.[5]

PECVD of benzene increased the C1 peak, which corresponded to the aromatic C=C double bond at 1600 cm^{-1} of the FTIR-ATR spectrum (Figure 14). The decrease of n(O1s)/n(C1s) ratio in benzene treated groups showed that benzene had a masking effect onto the silica (O1, Si-OH) of the ceramic substrate itself and the siloxane networks (Si2, O-Si-O) formed by HMDSO. The benzene-deposited ceramic surface was moderately hydrophobic. However, the adhesive showed good adaptation to the surface due to the hydrophilic groups (C1, C2 and C3 peaks) implemented after exposure to ambient air. Additionally, the benzene coating itself improved the adhesion by the chemical reaction of the aromatic C=C double bonds (C1 peak) to bind with the overlying adhesive. Although benzene might induce Si1 (Si-O-C) peak with direct interaction with the silica of the ceramic surface, underlying deposition of HMDSO before benzene increased siloxane network (Si2 peak) by the fragmentation and deposition of the HMDSO. Additional deposition of HMDSO lead to an additional increase of the bond strength obtained by the benzene deposition (Table 11). Therefore, the hypothesis was accepted.

From the fact that mixed fractures increased in the experimental groups showing high bond strength values, high wettability and good adaptation into the irregularity of the ceramic surface must be a prerequisite for good adhesion of composite resin to dental ceramic. PECVD of water, benzene, and HMDSO/benzene increased the adhesion of composite resin to dental ceramic by improving wettability, adaptation

and chemical bond with active species, such as aromatic C=C double bonds, silanol groups, and hydrophilic ether, carbonyl and ester groups. Even with the siloxane network obtained, single PECVD of HMDSO failed to obtain good bond due to the superhydrophobicity and resultant poor wetting of the deposited surface.

1.5 Promotion of resin bonding to dental zirconia ceramic using plasma deposition of tetramethylsilane and benzene

A strong resin bonding relies on micromechanical interlocking and chemical bonding to substrates. With regard to silica-based ceramic, surface roughening (for micromechanical interlocking) and functionalization (for chemical bonding) are effectively obtained by the hydrofluoric acid etching and silane coupling agents.[62] However, traditional adhesive strategies are ineffective on zirconia ceramics due to their high mechanical and chemical stability.[55-57] Although the use of airborne-particle abrasion and phosphoric acid primers has been shown to improve bond strengths to zirconia ceramics, bond strength values reported in the literature were generally lower than those reported for silane-bonded traditional ceramics.[55,57,59,63,80] Airborne-particle abrasion has contributory effect on the bond strength through increasing the surface roughness, but a degree of surface roughness does not positively correlate with the bond strength between resin cements and zirconia.[61,64] Furthermore, there is some concern that airborne-particle abrasion with Al_2O_3 particles could produce microcracks that would cause premature, catastrophic failure.[65] Thus, a non-destructive method for functionalizing zirconia surfaces would be very useful. The present study did not include airborne-particle abrasion process in order to focus on the chemical aspects of the resin-zirconia bonding. The plasma deposition processes with functional monomers tested significantly improved the resin bond strength to zirconia

compared with the control group.

Silane chemistry is well adapted for improving adhesion between organic resin-based materials and metal or ceramic in the dental field.[66] Accordingly, there have been several approaches to facilitate a siloxane bond between resin composites and zirconia surfaces.[55,57,67,80] Derand *et al.*[80] reported that fusion of glass pearls on a zirconia surface follow by a silane coupling agent significantly improved the resin bond strength to the zirconia. However, this technique requires an additional fusing process, which can interfere with a veneering process. Furthermore, the thickness of the glass pearls layer can disrupt complete seating of a restoration. Another method to form silica-like layer on zirconia is a vapor-phase deposition technique using chloro-silane.[57] A chloro-silane pretreatment allowed for conventional silanation with a silane coupling agent and presented higher bond strength than a tribochemical silica-coating technique. These previous studies[57,80] showed that chemical functionalization of zirconia surfaces allowed for the use of conventional silane coupling agent and adhesives, which are very affordable and familiar to most dental practitioners. However, organosilanes which are applied from aqueous solutions usually produce fairly thick coatings which have a low strength and are vulnerable to hydrolytic degradation.[66] Therefore, alternative strategies for forming a strong and highly crosslinked interface have been of interest not only in industry applications but also dental fields.

Recently, there has been a growing interest in plasma-enhanced deposition processes which are versatile techniques for forming films with functional properties suitable for a wide range of modern applications.[28,68] Plasma-polymerized coatings have excellent physical and chemical properties, and can highly coherent and adherent to a variety of substrates. HMDSO and TMS have

been widely used as organosilane monomer precursors due to their volatility and good reactivity in plasma.[68,69] Silica-like films deposited from HMDSO and TMS have been widely used as anti-scratch coatings, corrosion protection layers, and biocompatible films. In addition, due to the electron sharing ability of silicon, these silica-like films can act as coupling agents which promote adhesion between inorganic substrates and the polymer matrix.[28,36,83] In the dental field, Derand *et al.*[80] reported that plasma deposition with HMDSO significantly improved the resin bond strength to a zirconia ceramic compared with an untreated control group. Because they did not involve a group of practically used methods, e.g. air-borne particle abrasion and primers, it was not possible to assess the usefulness of the plasma treatment. Nevertheless, the bond strength with the plasma deposition (mean 3.5–5.3 MPa) was lower than values reported in literature. In our 1,3 butadiene plasma coating study, plasma treatment with HMDSO alone did not effectively improve the resin bond strength to a silica-based ceramic. The results were ascribed to the fact that the hydrophobicity of the coated layer interfered a subsequent adhesive resin from wetting adequately. In order to improve wettability of the HMDSO-coated surface and induce polymerizable functional group, benzene (a pure hydrocarbon) was subsequently coated over the plasma-polymerized HMDSO layer. The sequential deposition of HMDSO and benzene improved the bond strength as high as that obtained with the hydrofluoric acid-etching/silane treatment. The results from the previous study provided a theoretical base for the design of the present study. This study, though, was different from the previous study in that a higher power was used to activate the zirconia surface which has higher chemical inertness than conventional dental ceramics. In accordance with the results of the previous study, the TMS/benzene group showed the highest bond

strength, which was about twice as high as that of the Z-Prime Plus group.

The plasma deposition with TMS or benzene alone was not as effective as the sequential deposition with TMS and benzene, but the resultant bond strengths were similar to that for the commercially available primer (Z-Prime Plus). The plasma treatment could have the effects of surface cleaning, removing organic contaminants and passive oxide layers, which in turn have a contributory effect on chemical bond formation between zirconia and resin adhesives.[28] On the other hand, Z-Prime Plus contains 10-methacryloyloxydecyl dihydrogen phosphate (MDP) monomer, which is well-known as the most effective monomer for improving the bond strength between resin-based materials and zirconia.[55,61,63,70] The bonding mechanism has been speculated to be based on the reaction between a phosphate moiety of MDP and passive oxide layers of zirconia.[67] However, such condensation reaction could be vulnerable to hydrolysis, and thus there has been a concern about the bonding durability.[59,67,71] In contrast to the use of aqueous functional monomers, the plasma-enhanced deposition could provide additional covalent bonds, such zirconium silicide (Zr–Si), by cleaving chemical bonds and inducing new chemically reactive sites. Although the bond strength values were similar for plasma deposition with either TMS or benzene and for Z-Prime Plus, the interfacial bonding characteristics could differently affect the durability of the interfaces. Future studies should further investigate the nature of bonding at the zirconia-resin interface and the its durability, comparing plasma deposition and commercially available primers.

Zirconia surfaces are easily covered with passive oxide layers like as metal. The XPS results showed that non-treated zirconia was covered with organic contaminants as shown by the peaks at 532.5 eV (a binding energy of O=C–O

groups). The O1s spectra also clearly showed the presence of O–Zr bonds by the peak at 529.7 eV. The Zr3d spectra of non-treated zirconia showed typical doublet peaks corresponding to $Zr3d_{5/2}$ and $Zr3d_{3/2}$ centered at 181.6 eV and 184.0 eV, respectively.[72] The relatively lower binding energy for the $Zr3d_{5/2}$ compared to 182.1 eV for pure zirconia was attributed to lower oxidation state resulting from incorporating cubic oxides, such as yttria, in order to stabilize the polymorphic structure of zirconia ceramics. After the plasma deposition with TMS, the O1s spectrum appeared only at 532.3 eV which was ascribed to Si–O–Zr bonds.[73] The disappearance of Zr3d spectra also indicated that the plasma treatment formed a coating of good quality which had a siloxane-like network on the zirconia surface. In accordance with the XPS results, the TEM image of a cross-sectioned specimen, which was treated sequentially with TMS and benzene, showed two distinctive defect-free coating layers (Figure 17). The coating layers were in intimate contact and their thickness was approximately 50 nm for each. The EDS results confirmed the formation of silica-like layer by plasma deposition with TMS and the abundant presence of carbon in the plasma-polymerized benzene layer. The improved bond strength was attributed to interfacial chemical reactions in which the first silica-like layer established covalent bonds with zirconia surface and the subsequent layer polymerized with benzene was able to copolymerized with the organic resin matrix.

A limitation of the present study was that the plasma deposition process requires laboratory equipment including a RF power source, reactor equipped with a vacuum pump, and control of working gases. To improve the clinical usability of the plasma-enhanced adhesion to zirconia surfaces, treatment time and thicknesses of plasma-polymerized layers should be optimized to enhance the stability of the bonded interface and to maximize bond strength. However, future studies to

evaluate solubility of the plasma-deposited polymers will be necessary in the point of toxicity.

2) ADHESION TO TOOTH

2.1 Effect of plasma deposition using low-power/non-thermal atmospheric pressure plasma on promoting adhesion of composite resin to enamel

The photoinitiators in dental adhesives, mostly camphorquinone, can initiate the radical formation from monomers by curing light, which in turn can react with surface double bonds. The photoinitiators can also create radicals from the surface double bonds as an active site for surface graft polymerization. The same radical polymerization occurs between the light-cured adhesive and overlying composite resin by light-curing.[86,87] Therefore, from the XPS results and FT-IR spectra, the increase in the MSBS could be attributed partly to the chemical reactions between C=C double bonds of the plasma-deposited polymer and the adhesive. However, how much the C=C double bonds in the plasma-deposited polymer remain after plasma deposition and how much the chemical reaction between the C=C double bonds in the plasma-deposited polymer and those in the adhesive monomer need to be investigated in the future studies.

After TC, the MSBS decreased significantly in Groups 1, 3, and 4 (t-test, $p < 0.05$, Table 12). The MSBS did not decrease significantly in Group 2 only, in which the He plasma was applied with no monomer. Only the MSBS of Group 2 was significantly higher than that of the control group (Scheffe's test, $p < 0.05$). A significant interaction effect was observed between plasma treatment method and measurement time (2-way ANOVA, $p < 0.05$). The mean MSBS of the plasma polymer-deposited groups decreased significantly and showed no difference from that of the control group, which suggested that there might be no benefit to plasma

deposition with respect to durability. Therefore, the first and the second null hypotheses were rejected. The plasma polymer depositions increased the bond strengths of composite resin to enamel, but their durability failed to be confirmed in terms of the mean bond strength values.

However, considering a logarithmic loss of bond strength beyond 100 cycles,[88] the decrease of MSBS after 5,000 cycles of TC in the groups except Group 2 can be regarded as relatively small. Generally, the overall dentin bond strength of the adhesives have been reported to decrease after TC, [89-94] the negative effect of TC was attribute to the accelerated hydrolysis of collagen and incompletely-cured resin monomers and the mechanical stresses from repetitive expansion and contraction of polymeric materials at the interface.[95] In other studies, the effect of TC on the enamel bond strength differed according to the adhesives and the etching and drying procedures used.[89,91,93,94,96,97] The increase in DC after TC has also been reported in self-etching adhesives.[98,99] Göhring *et al*. suggested a higher DC due to higher polymerization temperature during TC as a reason for no decrease in flexural strength.[100] In order to understand these controversial results, the DC of the adhesive joint need to be evaluated in a dry condition with the same temperature with that of TC. In this study, assuming that the DC and the strength of the adhesive layer were the same in all groups, the similar MSBSs after TC must have resulted from the use of the same adhesive in all the groups (Table 12). Due to the extremely thin plasma polymer layer, the DC of the intermediated layers were evaluated indirectly from the measurements of a thick plasma polymer layer deposited on KBr pellets for 15 minutes. The DC of the simulated plasma polymer layers were different depending on the monomers used (Table 15). The effect of the high temperature (55^{o}C) used during TC on the DC was simulated by storing the

material in a dark container at 55°C for 7 days. From the elevated DC, it was deduced that the properties of the plasma polymer layer were improved by the thermal aging effect of TC (Table 15). Therefore, it can be suggested that the durability of the enamel adhesion in the complex having two layers of the plasma polymer and the adhesive is determined by the adhesive layer, not by the plasma-deposited polymer layer.

In contrast to the decrease in the mean MSBS of Groups 3 and 4 after TC, when the data were analyzed using the Weibull statistics, the Weibull modulus, *m*, increased in all the tested groups after TC, especially in Group 3 using BZ as a precursor monomer (Figure 20). It is well-known that the adhesive layer is brittle after polymerization due to crystallization.[101,102] The Weibull statistics shows that the cumulative failure probability resulted from the flaw distribution within the brittle materials. [103] In this study, in addition to the comparisons between means and standard deviations of the experimental groups, the reliability and durability of the adhesion were investigated by comparing the changes in the Weibull parameters, due to the brittle nature of the adhesion.[91,104] According to the definition of characteristic strengths (σ_θ), the distribution of the σ_θ at a 63.2% cumulative failure probability was similar to that of the mean values of the experimental groups. However, while the *m*'s of Groups 3 and 4 became prominently high after TC (Figure 20b), the *m* of Group 4 using BD was already very high at 24 hours (Figure 20a). Especially in Group 3, the *m* of the bond mediated by the plasma polymerization of BZ increased by more than two times after TC, compared to the initial *m* at 24 hours. As was mentioned earlier, because the condition of the etched surface and the properties of the adhesive layer were assumed to be the same among all the groups, the difference in the *m* values must

have come from the plasma polymer layer.

The higher was the shape parameter, *m*, the lower was the scatter of the failure stresses.[103] The *m* values increased with the plasma treatments. After TC, the *m* values also increased in all the groups, especially in the plasma polymer-deposited Groups 3 and 4. This finding indicates that the plasma treatment and TC narrowed the range of the failure stresses of the enamel adhesion. Plasma treatment might have contributed to the adhesion by improving wettability and chemical interactions within the adhesion complex, which in turn decreased the flaw probability at the enamel surface. The durability of Group 2 might be attributed to the sophisticated drying effect of the He plasma.[26] However, when the plasma polymer was deposited, although it must have suffered from repeated contraction/expansion and water attack, the applied temperature of 55°C during TC improved the DC of the plasma-polymerized layer (Table 15) as well as of the overlying adhesive layer. These effects occurred continuously, like dark-cure occurring in most polymerizing materials.[105] Although the improvement in the DC of the extremely thin plasma-polymerized layer within the adhesion complex failed to increase the mean MSBS, the increase of *m* was suggested to improve the wettability and the mechanical property of the adhesive complex and finally to result in the low scatter of the failure stresses. Moreover, the presence of the plasma-deposited layer could not be observed under SEM. In this study, the intimate contact between the plasma-deposited polymer layer and the enamel surface was suggested by high *m* values.

As a result, it was also difficult to discriminate the remnants of plasma polymer on the enamel surface for classification of fracture modes. Therefore, a fracture mode was classified as cohesive when a chipping or cohesive fracture (C) of

enamel was observed under a stereomicroscope. The specimens showing a smooth surface were classified as adhesive fracture (A), irrespective of whether the location of the fracture was within the plasma polymer, within the adhesive layers, or between the adhesive and enamel (Figure 21). According to the classification, only four specimens demonstrated enamel cohesive fracture (Table 12). This finding suggested that the wire loop method of the MSBS test used in this study prevented stress propagation from deviating into the enamel, the adherend, irrespective of the MSBS value.[38] The MSBS test used in this study induced cohesive fracture of the adhesive and allowed for measurement of the inherent strength of the adhesive.

Considering the low DC of the plasma-deposited layer and subsequent increase after thermal aging (Table 15), the applied power for the plasma polymerization used in this study was too low to result in dense cross-linkage of the polymer layer.[83] As a result, the deposited polymer layer might still have suffered hydrolysis and failed to contribute to the durability of the enamel adhesion.[90] Regarding plasma adhesion, future studies using high applied powers are needed to investigate the best combination of two opposing aspects, which are the physical property of the intermediate layer of variously cross-linked plasma polymer, and the chemical interaction of the overlying adhesive with the double bonds of the less cross-linked plasma-deposited polymer.

2.2 Effects of non-thermal atmospheric pressure pulsed plasma on the adhesion and durability of resin composite to dentin

As the plasma reactor comes out from a vacuum chamber and cold plasma has been rapidly developed, the plasma equipment can be applied directly to vital tissues.[117] Dielectric barrier discharge is one of the low-temperature plasmas that

has been attempted in medical and dental applications.[34] This plasma equipment was designed with a pencil-type torch for versatile usage, but the applied power still needs to be reduced in order to decrease patient discomfort or injury from the electric current.[114] For intra-oral use and especially for direct exposure to sound dentin, which is very sensitive to irritants, both the applied energy and frequency have to be kept as low as possible.[114] For that purpose, the present study used a pulsed power source with a frequency of 0.4 kHz, in which each pulse had five voltage peaks and lasted for 500 ns at 12.5 ms intervals, resulting in a minimal applied energy of 1.1 kW·h, without compromising the adhesion promotion effect of the conventional plasma (Table 16). The decrease in the frequency by applying a pulse power source reduced the applied energy and, as a result, relieved possible patient discomfort.

The results of this study show that plasma treatment using a low-power NT-APP has a significant effect on the adhesion of resin composite to dentin. However, there was no significant difference between the groups treated with pulsed plasma or conventional plasma. This indicates the possibility of applying pulsed plasma, with a minimal applied energy of 1.1 kW·h, in order to promote dentin adhesion. After thermocycling, the mean bond strength did not change significantly from the initial mean bond strength in either the control group or the conventional plasma group. Moreover, the bond strength in the pulsed plasma group increased significantly after thermocycling (*t*-test, $p < 0.05$). Because bond strength generally decreases after thermocycling[93], the effect of the plasma treatment on the durability of dentin adhesion is still uncertain. However, Göhring *et al*.[100] suggested the higher temperature during thermocycling as the reason for the maintained strength. The positive effect of helium (He) plasma on the durability of dentin adhesion was

consistent with the results of Göhring *et al*.. and those of our previous study on the durability of enamel adhesion.[100] In our enamel plasma coating study, the increase in the initial mean bond strength by plasma treatment and the improvement in the durability by thermocycling were attributed to the increase in wettability and to the thermal effect (55°C) of thermocycling and persistent dark cure of the adhesive complex, respectively.

With respect to the durability, the Weibull parameters showed more definite changes than the mean bond strength. According to the definitions of the Weibull parameters, considering crack distribution within the brittle adhesion complex, the increase in characteristic strength indicates an increase in failure strength at a critical cumulative failure probability of 63.2% in the Weibull distribution and reflects the increase in failure resistance.[101,104] The Weibull modulus better represents the effect of plasma treatment than does the characteristic strength.[101,104] The shape parameter *m* indicates the spread in the data distribution, similar to the magnitude of standard deviation. The present increase in *m* clearly represents the consistent distribution of data. In addition to the increase or lack of change in the characteristic strength, the increased *m* shows matured adhesion in the plasma-treated groups exposed to artificial aging, especially in the pulse plasma-treated group (Table 17 and Figure 24).

During the pilot study, we compared the contact angle measurements among the acid-etched dentin and various plasma-treated dentin surfaces. The acid-etched dentin surface had already become too hydrophilic, and the changes in contact angle value by successive He plasma spraying were too low to be measured using a goniometer (data not presented, less than 10 degrees). In our ceramic and enamel studies, plasma treatment with inert He gas improved the hydrophilicity of ceramic

and enamel surfaces. Grafting active species, such as carboxyl and carbonyl groups, onto the surfaces was suggested to contribute to the wetting and chemical interaction of the adhesive monomers.[118] In the present study, the monomers included in the primer also adapted well to the etched and subsequently plasma-treated dentin surface. The adaptation might have been facilitated through the hydrophilic groups grafted onto the plasma-treated dentin surface, as suggested by DONG *et al*.[118] According to the SEM images, this was confirmed by the intimate contact at the interfaces of the layers of the adhesion complex (Figure 26).

The SEM images show that the plasma-treated experimental groups had more abundant and longer resin tags than the control group (Figure 26). Especially in the conventional plasma treatment group, the resin tags looked more tortuous with lateral projections. The well-developed resin tags of the plasma-treated groups can be attributed to the grafting effect of active species during the plasma treatment procedure. Due to the grafted species, the inner walls of dentinal tubules can sustain hydrophilicity for penetration and adaptation of the primer. As a result, the drying procedure of the dentin surface with the plasma jet caused the exposed dentin surface and inner surfaces of dentinal tubules to become hydrophilic and facilitated the penetration of the primer and subsequent adhesive deep into the tubules. Although the contribution of resin tags to the bond strength is known to be limited in self-etching adhesives,[119] the improved resin tag formation facilitated by the plasma treatment in this study might have contributed to the increase in initial MTBS.[118] According to the SEM images of the fractured surfaces (Figures 25b, 25c), the fracture modes of the plasma-treated surfaces were adhesive or mixed ones. The observation is also well-coincident with the increased resin tag formation.

With respect to the durability of dentin adhesion, the monomers in the primer can

infiltrate into the interfibrillar spaces within the collagen mesh exposed by acid etching. In order to minimize the exposed hydrophilic domains within the adhesion complex and to improve the penetration of the hydrophilic monomers of the primer, the uninfiltrated demineralized dentin zone should be minimized by improving the hydrophilicity of the collagen fibrils.[90] Although Ritts *et al*.[26] and Dong *et al*. [118] reported that argon plasma treatment of the dentin surface increased its hydrophilicity by increasing carbonyl groups, they did not specify whether the collagen mesh maintained its interfibrillar spaces. However, the plasma spraying must have dried the dentin surface, so that the collagen mesh structure should be collapsed and the hydrophilic carbonyl groups should be present on the dentin surface. Because this situation should exist in both the study by Dong *et al*.[118] and the present study, rewetting of the dentin surface dried by plasma spraying was performed in both studies. The effect of thermocycling on the bond strength was the same in all the groups, such that their values did not decrease after thermocycling. The increase in the Weibull moduli in the plasma-treated groups might be attributed to the increased resin tag formation and their maturation.[100] Within the limitations of this study, it is inappropriate to suggest that the plasma treatment grafts the active species on the collagen fibrils and makes each fibril hydrophilic. As a result, it is also not clear whether the plasma treatment stiffens the collagen mesh structure, as is the case in ethanol wet bonding.[120] Whether well-developed resin tags seal the hydrophilic domains within the adhesive complex and whether the plasma treatment maintains the interfibrillar spaces of the collagen mesh for monomer penetration need to be investigated in future studies.

When the pulse was on, the continuous character of the alternating current changed to an intermittent activation, in which each pulse had five voltage peaks

(Hz) and lasted 500 ns at 12.5 ms intervals (Figure 1). Using pulsed plasma, although the energy applied to the dentin surface was greatly reduced, the mean MTBS values at 24 h and after thermocycling were the same as those obtained with conventional plasma. This suggests that the amount of active species delivered into the dentinal tubules by the pulsed plasma might be sufficient to cause the inner surface of the dentinal tubules to become hydrophilic. However, the penetration of monomers into the tubules and the resultant resin tag formation appeared to be less than that of the continuous plasma quantitatively (Figures 26b, 26c). In this study, the Weibull modulus of the pulsed plasma group was higher than that of the continuous plasma. Further study is required to determine the optimal conditions of applied energy and pulse frequency for maximal bond strength and durability.

2.3 Promotion of Adhesive Penetration and Resin Bond Strength to Dentin using Non-thermal Atmospheric Pressure Plasma

NT-APPs include a large amount of charged species, radicals, and energetic photons, which can enhances the surface energy of a substrate, making it better for molecular interactions.[129] NT-APP treatment of demineralized dentin surfaces is a promising approach to improve the adhesive penetration and resin bond strength to dentin.[26,120,132] Conversely, a rewetting procedure is necessary after plasma treatment in accordance with the wet bonding philosophy.[26,120] In the present study, the bond strength for the plasma-drying group was significantly greater than that of the wet bonding group and it was two times greater than that of the dry bonding group (Table 18). The structural integrity of the collagen network may be maintained despite the loss of water by the plasma-drying, allowing adequate penetration of adhesive monomers. A possible mechanism for the effect of plasma-drying is that many energetic and chemically reactive species in plasma lead

structural changes of the exposed collagen fibers by breaking intrafibrillar bonds, such as hydrogen bond, thereby preventing collapse of the collagen network even under dry conditions.[26,125]

The results of the micro-Raman spectroscopy analysis indicated that the plasma-drying group presented a higher degree of BisGMA penetration than the wet bonding and plasma-drying/rewetting groups, although the differences between the groups in the BisGMA penetration decreased when approaching to the bottom part of the hybrid layer (Figure 28A). In addition, the relative content of BisGMA in the infiltrating adhesive was greater in the plasma-drying group than in the wet bonding and plasma-drying/rewetting groups (Figure 28B). Although the effect of the plasma treatment on the adhesive penetration was more prominent in the upper part of the hybrid layer, the plasma treatment generally improved the penetration of BisGMA into the demineralized dentin. The band ratios of 1113 cm^{-1}/1667 cm^{-1} (the relative content of BisGMA to dentin collagen) and 1113 cm^{-1}/1454 cm^{-1} (the relative content of BisGMA in the penetrating adhesive) showed the highest values for the dry bonding group; however, this could not be interpreted as that BisGMA effectively penetrated into the demineralized dentin surface. The dry bonding group produced the lowest bond strength and poorer quality of the hybrid layer than the other groups (Table 18 and Figure 29). It was assumed that the collapsed collagen fibrils in the dry bonding group were not hybridized but instead covered with adhesive and, as a result, the separate adhesive layer over the dentin surface was responsible for a higher spectral intensity of BisGMA. Interestingly, the penetration degree and relative content of BisGMA for the plasma-drying group were comparable to that of the dry-bonding group in the upper part of the hybrid layer. In contrast to the dry-bonding group, the plasma-drying group presented a uniform

adhesive/dentin interface with good integrity (Figure 29C, 29D). Therefore, the highest bond strength for the plasma-drying group can be explained by the high BisGMA content in the hybrid layer. BisGMA has better mechanical properties than monomethacrylates such as HEMA, but does not adequately infiltrate the wet dentin surface due to its hydrophobicity and large molecular size.[136] The plasma-drying would displace excess water from interfibrillar space without collapse of the collagen network, resulting in improved BisGMA penetration and bond strength.

A previous study using an argon plasma brush[132] showed that plasma treatment improved the adhesive penetration into the demineralized dentin surface and the polymerization efficacy of a model adhesive. However, in contrast to the current results, the improvement of the adhesive penetration was ascribed mainly to hydrophilic HEMA. The different results may be attributed to the differing composition of adhesives and characteristics of the plasmas. The previous study[132] used a model adhesive with a higher concentration of HEMA (a mass ratio of BisGMA to HEMA of 0.43) than the currently used adhesive (a mass ratio of BisGMA to HEMA of approximately 1.5). In addition, argon plasma makes a polymer surface more hydrophilic than helium plasma does.[137,138] When compared with He plasma, Ar plasma generates larger amounts of reactive species such as hydroxyl group and is more effective at inducing chain scission, etching, and cleaning through ion bombardment.[137-139] The improved hydrophilicity of dentin surface in conjunction with the more hydrophilic adhesive may markedly enhance HEMA penetration. However, the high contents of HEMA in the adhesive/dentin interface adversely influence mechanical properties and make the interface prone to hydrolytic degradation.[140] Enhancing the infiltration of hydrophobic monomers, like BisGMA, is desired for achieving high bond strength and durable adhesion to

dentin, and thus the plasma treatment demonstrated in the present study seems promising.

A lower band ratio of 1640 cm^{-1}/1609 cm^{-1} indicated higher polymerization efficacy in the interfacial region (Figure 28C). The dry bonding group showed a lower 1640 cm^{-1}/1609 cm^{-1} ratio throughout the examined region than the other groups, but this did not imply that a high-quality hybrid layer was formed. In the dry bonding group, the adhesive could simply cover the collapsed collagen structure instead of infiltrating. The low 1640 cm^{-1}/1609 cm^{-1} ratio for the dry bonding group can be explained by the least amount of residual water, as well as poor hybridization between the adhesive and collapsed collagen matrix.[141-143] On the other hand, it is noteworthy that the polymerization efficacy for the plasma-drying group was comparable to that of the dry-bonding group. Excess residual water causes phase separation between the hydrophobic and hydrophilic components and compromise the polymerization efficacy of the adhesive monomers.[141,144] Plasma treatment effectively removed residual water from the dentin surface without causing collapse of the demineralized collagen matrix. In addition, energetic and chemically reactive species included in the plasma can induce polymerization of the adhesive monomers and enhance interaction between the dentin substrate and the infiltrating adhesive.

SEM observations demonstrated that the plasma-drying group had abundant and well-developed lateral branches of resin tags, which anastomosed with adjacent dentinal tubules (Figure 29C, 29D). Hydrophobic monomers, such as BisGMA, do not adequately infiltrate the demineralized dentin where there is excess residual water. However, complete removal and/or replacement of water from the interfibrillar space is practically unattainable.[145,146] Plasma-drying may effectively

remove residual water from the interfibrillar space, allowing for an effective penetration of the adhesive monomers. In addition to the high BisGMA content in the hybrid layer, well-developed resin tags could contribute to improving the bond strength for the plasma-drying group.

The Weibull statistics was used for the interpretation of the bond strength data in a view point of fracture analysis, which can be explained with crack distribution. The MTBS data fitted the Weibull distribution well, as shown by the correlation coefficient values being greater than 0.9 for all the test groups (Table 18). Most studies on the strength of brittle materials, such as ceramics and resin composites, have used means and standard deviation, which, however, do not provide information about unpredictable brittle failure due to the presence of critical flaws.[101,103,147] The overall performances of adhesives bonded to dentin can be better evaluated by predicting the likelihood of failure at specific stress levels. The Weibull parameters provide insights about the reliability (Weibull modulus *m*) and the probability of failure for a given stress level.[101,103,104,147,148] A higher *m* indicated a narrow spread of data and a high reliability of the characteristic strength (σ_θ) which represents the stress responsible for 63.2% of the sample failures. Adhesion procedure with a high Weibull moduli is considered to be reliable and less technique-sensitive. The plasma treatment groups (plasma-drying and plasma-drying/rewetting) showed higher Weibull moduli *m* than the wet bonding group. Plasma-drying improved the reliability of dentin adhesion by making adhesion procedures less dependent on the moisture condition of demineralized dentin. When adhesion procedures are clinically performed, plasma treatment will expand the window of opportunity in which optimal intertubular and intratubular dentin infiltration are simultaneously achieved and reduce the technique sensitivity of

etch-and-rinse adhesive systems.

5. CONCLUSION

5.1 ADHESION TO CERAMIC

We found that the Plasma polymer coating technique could contribute to enhance the ceramic and zirconia bonding of conventional dental adhesives. PECVD with 1,3-butadiene gas enhanced the adhesion of composite resin to ceramic surfaces through the simple deposition of fragmented aliphatic C=C double bonds. When HMDSO and benzene were plasma-polymerized sequentially on the ceramic surface, siloxane networks were formed on the ceramic surface by HMDSO and enhanced the adhesion of benzene to the ceramic surface. The plasma polymerized benzene containing increased amount of aromatic C=C double bonds attributed to the ceramic adhesion of the adhesive by chemical interaction between the double bonds of the plasma polymerized benzene and the adhesive. The plasma deposition of TMS and benzene on zirconia surface successfully increased the bond strength to resin composite. TMS formed a siloxane-like network on zirconia surface and benzene provided reactive functional groups which were able to copolymerize with the resin matrix.

The plasma polymer coating technique was found to have a potential promoting adhesion to dental materials. In addition, Plasma treatment is a promising method to overcome the limitation of zirconia restorations with respect to bonding efficacy.

5.2 ADHESION TO TOOTH

The plasma polymer deposition of benzene and 1,3-butadiene using a low-power, plasma coating improved the adhesion of resin composite to enamel. However, the

mean values of the MSBS of the plasma polymer-deposited groups decreased after TC. Plasma polymer deposition failed to improve the durability of the enamel bond.

The Plasma treatment using a low-power, plasma coating improved the adhesion of resin composite to dentin. And plasma treatment after acid etching enhanced the penetration of adhesive, especially hydrophobic BisGMA, and as a result, improved the bond strength of resin composite to dentin. Moreover, omitting the rewetting procedure after plasma treatment enhanced the effect of plasma treatment in improving dentin adhesion. The plasma-drying will be a reliable method to control moisture of demineralized dentin surfaces in adhesion procedures. By adopting a pulsed energy source, the energy delivered to the dentin, a vital tissue in the oral cavity, was effectively reduced, without compromising the bond strength or durability.

6. REFERENCE

1. Moffa JP. Porcelain materials. Adv Dent Res. 1988;2:3–6

2. Brentel AS, Özcan M, Valandro LF, Alarça LG, Amaral R, Bottino MA. Microtensile bond strength of a resin cement to feldspathic ceramic after different etching and silanization regimens in dry and aged conditions. Dent Mater 2007;23:1323-1331

3. Stangel I, Nathanson D, Hsu CS. Shear strength of the composite bond to etched porcelain. J Dent Res 1987;66:1460-1465.

4. Choi YH, Kim JH, Paek KH, Ju WT, Hwang YS. Characteristics of atmospheric pressure N_2 cold plasma torch using 60-Hz AC power and its application to polymer surface modification. Surf Coat Technol 2005;193:319-324.

5. Clark DT, Thomas HR. Applications of ESCA to polymer chemistry. X. Core and valence energy levels of a series of polyacrylates. J Polym Sci Polym Chem Ed 1976;14:1671-1700

6. Yen TW, Blackman RB, Baez FJ. Effect of acid etching on the flexure strength of a feldspathic porcelain and a castable glass ceramic. J Prosthec Dent. 1993;70:224-33.

7. Leloup G, D'Hoore W, Bouter D, Degrange M, Vreven J. Meta-analytical review of factors involved in dentin adherence. J Dent Res 2001;80:1605-1614

8. Tendero C, Tixier C, Tristant P, Desmaison J, Leprince P. Atmospheric pressure plasma: A review. Spectrochimica Acta Part B 2006;61:2-30

9. Yasuda H. Plasma Polymerization. New York: Academic Press. 1985

10. Chan C, Ko T, Hiraoka H. Polymer surface modifications by plasmas and photons. Surf Sci Rep 1996;24:1-54

11. Mandracci P, Mussano F, Ricciardi C, Ceruti P, Pirri F, Carossa S. Low temperature growth of thin film coatings for the surface modification of dental prostheses. Surf Coat Technol 2008;202:2477-2481
12. Ono T, Nemoto T. Two forms of apatite deposited during mineralization of the hen tendon. Matrix Biol 2005;24:239-244
13. Hayakawa T, Yoshinari M, Nemoto K. Characterization and protein-adsorption behavior of deposited organic thin film onto titanium by plasma polymerization with hexamethyldisiloxane. Biomaterials 2004;25:119-127
14. Puleo D, Kissling R, Sheu M. A technique to immobilize bioactive proteins, including bone morphogenetic protein-4, on titanium alloy. Biomaterials 2002;23:2079-2087
15. Cokeliler D, Erkut S, Zemek J, Biederman H, Mutlu M. Modification of glass fibers to improve reinforcement: a plasma polymersization technique. Dent Mater 2007;23:335-342
16. Yavirach P, Chaijareenont P, Boonyawan D, Pattamapun K, Tunma S, Takahashi H, Arksornnukit M. Effects of plasma treatment on the shear bond strength between fiber-reinforced composite posts and resin composite for core build-up. Dent Mater J 2009;28:686-692
17. Derand T, Molin M, Kvam K. Bond strength of a composite luting agent to alumina ceramic surfaces. Acta Odontol Scand 2006;64:227-230
18. Chirokov A, Gutsol A, Fridman A. Atmospheric pressure plasma of dielectric barrier discharges. Pure Appl. Chem 2005; 77:487-495.
19. Laroussi M, Akan T. Arc-free atmospheric pressure cold plasma jets: a review. Plasma Process. Polym. 2007;4:777-788

20. Kogelschatz U. Filamentary, patterned, and diffuse barrier discharges. IEEE Trans Plasma Sci 2002;30:1400-1408.
21. Lee S, Kim YK. Adhesion improvement of polyimide/metal interface by $He/O_2/NF_3$ atmospheric pressure plasma. Plasma Process Polym 2009;6:S525-S529.
22. Kong MG, Kroesen G, Morfill G, Nosenko T, Shimizu T, van Dijk J, Zimmermann JL. Plasma midicine: an introductory review. New J Physics 2009;11:115012
23. Gonzalez E, Barankin MD, Guschl PC, Hicks RF. Remote atmospheric-pressure plasma activation of the surfaces of polyethylene terephthalate and polyethylene naphthalate. Langmuir 2008;24:12636-12643
24. Grace JM, Gerenser LJ. Plasma treatment of polymers. J Dispers Sci Technol 2003;24:305-341
25. Liston EM, Martinu L, Wertheimer MR. Plasma surface modification of polymers for improved adhesion: A critical review. J Adhes Sci Technol 1993;**7**:1091-1127
26. Ritts AC, Li H, Yu Q, Xu C, Yao X, Hong L, Wang Y. Dentin surface treatment using a non-thermal argon plasma brush for interfacial bonding improvement in composite restoration. Eur J Oral Science 2010;118:510-516
27. Nishigawa G, Maruo Y, Oka M, Oki K, Minagi S, Okamoto M. Plasma treatment increased shear bond strength between heat cured acrylic resin and self-curing acrylic resin. J Oral Rehabil 2003;30:1081-1084
28. Pihan SA, Tsukruk T, Förch R. Plasma polymerized hexamethyl disiloxane in adhesion applications. Surf Coat Technol 2009;203:1856-1862.

29. Sharma AK, Millich F, Hellmuth EW. Adhesion and hydrophilicity of glow-discharge-polymerized propylene coatings. J Appl Phys 1978;49:5055-5059.
30. Xi M, Li YL, Shang SY, Li DH, Yin YX, Dai XY. Surface modification of aramid fiber by air DBD plasma at atmospheric pressure with continuous on-line processing. Surf Coat Technol 2008;202:6029-6033.
31. Nwankire CE, Law VJ, Nindrayog A, Twomey B, Niemi K, Milosavljević V, Graham WG, Dowling DP. Electrical, thermal and optical diagnostics of an atmospheric plasma jet system. Plasma Chem Plasma Process 2010;30:537-552.
32. Donmez N, Belli S, Pashley D, Tay F. Ultrastructural correlates of in vivo/in vitro bond degradation in self-etch adhesives. J Dent Res 2005;84:355-359
33. Fang Z, Yang H, Qiu Y. Surface treatment of polyethylene terephthalate films using a microsecond pulse homogeneous dielectric barrier discharges in atmospheric air. IEEE Trans Plasma Sci 2010;38:1615-1623.
34. Tsai TC, Staack D. Low-temperature polymer deposition in ambient air using a floating-electrode dielectric barrier discharge jet. Plasma Process Polym 2011;8:523-534.
35. Walsh JL, Shi JJ, Kong MG. Contrasting characteristics of pulsed and sinusoidal cold atmospheric plasma jets. Appl Phys Lett 2006;88:171501
36. Bringmann P, Rohr O, Gammel FJ, Jansen I. Atmospheric pressure plasma deposition of adhesion promotion layers on aluminium. Plasma Process Polym 2009;6(Supplement):S496-S502.
37. Leroux F, Campagne C, Perwuelz A, Gengembre L. Polypropylene film chemical and physical modifications by dielectric barrier discharge plasma treatment at atmospheric pressure. J Colloid Interface Sci 2008;328:412-420.

38. Dickens S, Milos M. Relationship of dentin shear bond strengths to different laboratory test designs. Am J Dent 2002;15:185-192

39. Kim JH, Kim CK. Ultrafiltration membranes prepared from blends of polyethersulfone and poly(1-vinylpyrrolidone-co-styrene) copolymers. J Membr Sci 2005;262:60-68.

40. Awaja F, Gilbert M, Kelly G, Fox B, Pigram PJ. Adhesion of polymers. Prog Polym Sci 2009;34:948-968.

41. Sladek R, Stoffels E, Walraven R, Tielbeek P, Koolhoven R. Plasma treatment of dental cavities: a feasibility study. IEEE Trans Plasma Sci 2004;32:1540-1543

42. Wei J, Yoshinari M, Takemoto S, Hattori M, Kawada E, Liu B, Oda Y. Adhesion of mouse fibroblasts on hexamethyldisiloxane surfaces with wide range of wettability. J Biomed Mater Res B Appl Biomater 2007;81:66-75

43. Kopczynska A, Ehrenstein GW. Polymeric surfaces and their true surface tension in solids and melts. J Mater Educ 2007;29:325-340

44. Turner R, Segall I, Boerio F, Davis G. Effect of Plasma Polymerized Primers on the Durability of Aluminum/Epoxy Adhesive Bonds. J Adhes 1997;62:1-4

45. Lin T, Chun B, Yasuda H, Yang D, Antonelli J. Plasma polymerized organosilanes as interfacial modifiers in polymer-metal systems. J Adhes Sci Technol 1991;5:893-904

46. Bismarck A, Brostow W, Chiu R, Hagg Lobland HE, Ho KKC. Effects of surface plasma treatment on tribology of thermoplastic polymers. Polym Eng Sci 2008;48:1971-1976

47. Tang S, Kwon OJ, Lu N, Choi HS. Surface characteristics of AISI 304L stainless steel after an atmospheric pressure plasma treatment. Surf Coat Technol 2005;195:298-306.

48. Clark DT, Thomas HR. Applications of ESCA to polymer chemistry. XVII. Systematic investigation of the core levels of simple homopolymers. J Polym Sci Polym Chem Ed 1978;16:791-820.

49. Saulou C, Despax B, Raynaud P, Zanna S, Marcus P, Mercier-Bonin M. Plasma deposition of organosilicon polymer thin films with embedded nanosilver for prevention of microbial adhesion. Appl Surf Sci 2009;256S:S35-S39

50. Retzko I, Friedrich JF, Lippitz A, Unger WES. Chemical analysis of plasma-polymerized films: The application of X-ray photoelectron spectroscopy (XPS), X-ray absorption spectroscopy (NEXAFS) and fourier transform infrared spectroscopy (FTIR). J Electron Spectrosc 2001;121:111-129.

51. Yoshinari M, Hayakawa T, Matsuzaka K, Inoue T, Oda Y, Shimono M, Ide T, Tanaka T. Oxygen plasma surface modification enhances immobilization of simvastatin acid. Biomed Res 2006;27:29-36.

52. Manicone PF, Rossi iommetti P, Raffaelli L. An overview of zirconia ceramics: basic properties and clinical applications. J Dent 2007; 35: 819-826.

53. Miyazaki T, Hotta Y, Kunii J, Juriyama S, Tamaki Y. A review of dental CAD/CAM: current status and future perspectives from 20 years of experience. Dent Mater J 2009; 28: 44-56.

54. Burke FJ, Fleming GJ, Nathanson D, Marquis PM. Are adhesive technologies needed to support ceramics? An assessment of the current evidence. J Adhes Dent 2002; 4: 7-22.

55. Kern M, Wegner SM. Bonding to zirconia ceramic: adhesion methods and their durability. Dent Mater 1998; 14: 64-71.

56. Blatz MB, Sandan A, Arch JR, Lang BR. In vitro evaluation of long-term bonding of Procera AllCeram alumina restorations with a modified resin luting agent. J Prosthet Dent 2003; 89: 381-387.

57. Plascik JR, Swift EJ, Thompson JY, Gergo S, Stoner BR. Surface modification for enhanced silanation of zirconia ceramics. Dent Mater 2009; 25: 1116-1121.

58. Aboushelib MN, Kleverlaan CJ, Fellzer AJ. Selective infiltration-etching technique for a strong and durable bond of resin cements to zirconia-based materials. J Prosthet Dent 2007; 98: 379-388.

59. Wegner SM, Kern M. Long-term resin bond strength to zirconia ceramic. J Adhes Dent 2000; 2: 139-147.

60. Blatz MB, Sadan A, Martin J, Lang B. In vitro evaluation of shear bond strengths of resin to densely-sintered high-purity zirconium-oxide ceramic after long-term storage and thermal cycling. J Prosthet Dent 2004; 91: 356-362.

61. Tsuo Y, Yoshida K, Atsuta M. Effects of alumina-blasting and adhesive primers on bonding between resin luting agent and zirconia ceramics. Dent Mater J 2006; 25: 669-674.

62. Blatz MB, Sadan A, Kern M. Resin-ceramic bonding: a review of the literature. J Prosthet Dent 2003; 89: 268-274.

63. Yun JY, Ha SR, Lee JB, Kim SH. Effect of sandblasting and various metal primers on the shear bond strength of resin cement to Y-TZP ceramic. Dent Mater 2010; 26: 650-658.

64. Lohbauer U, Zipperle M, Rischka K, Petschelt A, Muller FA. Hydroxylation of dental zirconia surfaces: characterization and bonding potential. J Biomed Mater Res B Appl Biomater 2008; 87: 461-467.

65. Ozcan M, Melo RM, Souza RO, Machado JP, Felipe Valandro L, Bottino MA. Effect of air-particle abrasion protocols on the biaxial flexural strength, surface characteristics and phase transformation of zirconia after cyclic loading. J Mech Behav Biomed Mater 2013; 20: 19-28.

66. Lung CY, Matinlinna JP, Lung CY. Aspects of silane coupling agents and surface conditioning in dentistry: an overview. Dent Mater 2012; 28: 467-477.

67. Yoshida K, Tsuo Y, Atsuta M. Bonding of dual-cured resin cement to zirconia ceramic using phosphate acid ester monomer and zirconate coupler. J Biomed Mater Res B Appl Biomater 2006; 77: 28-33.

68. Benitez F, Martinez E, Esteve J. Improvement of hardness in plasma polymerized hexamethyldisiloxane coatings by silica-like surface modification. Thin Solid Films 2000; 377: 109-114.

69. Marchand DJ, Dilworth ZR, Stauffer RJ, Hsiao E, Kim J-H, Kang J-G, Kim SH. Atmospheric rf plasma deposition of superhydrophobic coatings using tetramethylsilane precursor. Surf Coat Technol 2013; 234: 14-20.

70. Margne P, Paranhos MP, Burnett LH Jr. New zirconia primer improves bond strength of resin-based cements. Dent Mater 2010; 26: 345-352.

71. Blatz MB, Chiche G, Holst S, Sadan A. Influence of surface treatment and simulated aging on bond strengths of luting agents to zirconia. Quintessence Int 2007; 38: 745-753.

72. Suchorski Y, Wrobel R, Becker S, Opalinska A, Narkiewicz U, Podsiadly M, Weiss H. Surface chemistry of zirconia nanopowders doped with Pr_2O_3: an XPS study. Acta Physica Polonica A 2008; 114: S125-S134.

73. Ahn H, Chen H-W, Landheer D, Wu X, Chou L, Chao T-S. Characterization of interfacial layer of ultrathin Zr silicate on Si (100) using spectroscopic ellipsometry and HRTEM. Thin Solid Films 2004; 455: 318-322.

74. Pashley DH, Tay FR, Breschi L, Tjaderhane L, Carvalho RM, Carrilho M, Tezvergil-Mutluay A. State of the art of etch-and-rinse adhesives. Dent Mater 2011;27:1-16

75. Van Meerbeek B, Yoshihara K, Yoshida Y, Mine A, De Munck J, Van Landuyt KL. State of the art of self-etch adhesives. Dent Mater 2011;27:17-28

76. Valandro LF, Ozcan M, Bottino MC, Bottino MA, Scotti R, Bona AD. Bond strength of a resin cement to high-alumina and zirconia-reinforced ceramics: the effect of surface conditioning. J Adhes Dent 2006;8:175-181

77. Abdalla AI, Feilzer AJ. Four-year water degradation of a total-etch and two self-etching adhesives bonded to dentin. J Dent 2008;36:611-617

78. Abdalla AI, El Zohairy AA, Aboushelib MM, Feilzer AJ. Influence of thermal and mechanical load cycling on the microtensile bond strength of self-etching adhesives. Am J Dent 2007;20:250-254

79. Cardoso MV, de Almeida Neves A, Mine A, Coutinho E, Van Landuyt K, De Munck J, Van Meerbeek B. Current aspects on bonding effectiveness and stability in adhesive dentistry. Aust Dent J 2011;56(Suppl 1):31-44

80. Derand T, Molin M, Kvam K. Bond strength of composite luting cement to zirconia ceramic surfaces. Dent Mater 2005;21:1158-1162

81. Piascik JR, Wolter SD, Stoner BR. Development of a novel surface modification for improved bonding to zirconia. Dent Mater 2011;27:e99-e105
82. Nishigawa G, Maruo Y, Oka M, Okamoto M, Minagi S, Irie M, Suzuki K. Effect of plasma treatment on adhesion of self-curing repair resin to acrylic denture base. Dent Mater J 2004;23:545-549
83. Hegemann D, Brunner H, Oehr C. Plasma treatment of polymers for surface and adhesion improvement. Nucl Instrum Meth B 2003;208:281–286
84. McDonough WG, Antonucci JM, He J, Shimada Y, Chiang MYM, Schumacher GE, Schultheisz CR. A microshear test to measure bond strengths of dentin-polymer interfaces. Biomaterials 2002;23:3603-3608
85. Santos VH, Griza S, Moraes RR, Faria-e-Silva AL. Bond strength of self-adhesive resin cements to composite submitted to different surface pretreatments. Restor Dent Endod 2014;39:12-16
86. Shawkat ES, Shortall AC, Addison O, Palin WM. Oxygen inhibition and incremental layer bond strengths of resin composites. Dent Mater 2009;25:1338-1346
87. Lohbauer U, Pelka M, Belli R, Schmitt J, Mocker E, Jandt KD, Müller FA. Degree of conversion of luting resins around ceramic inlays in natural deep cavities: a micro-Raman spectroscopy analysis. Oper Dent 2010;35:579-586
88. Seto KB, McLaren EA, Caputo AA, White SN. Fatigue Behavior of the Resinous Cement to Zirconia Bond. J Prosthodont 2013;doi: 10.1111/jopr.12053
89. Khoroushi M, Rafiei E. Effect of thermocycling and water storage on bond longevity of two self-etch adhesives. Gen Dent 2013;61:39-44

90. De Munck J, Van Landuyt K, Peumans M, Poitevin A, Lambrechts P, Braem M, Van Meerbeek B. A critical review of the durability of adhesion to tooth tissue: methods and results. J Dent Res 2005;84:118-132

91. Hashimoto M, Ohno H, Sano H, Tay FR, Kaga M, Kudou Y, Oguchi H, Arakai Y, Kubota M. Micromorphological changes in resin-dentin bonds after 1 year of water storage. J Biomed Mater Res 2002;63:306-311

92. De Munck J, Van Meerbeek B, Yoshida Y, Inoue S, Vargas M, Suzuki K, Lambrechts P, Vanherle G. Four-year water degradation of total-etch adhesives bonded to dentin. J Dent Res 2003;82:136-140

93. Hariri I, Shimada Y, Sadr A, Ichinose S, Tagami J. The effects of aging on shear bond strength and nanoleakage expression of an etch-and-rinse adhesive on human enamel and dentin. J Adhes Dent 2012;14:235-243

94. Dos Santos PA, Garcia PP, Palma-Dibb RG. Shear bond strength of adhesive systems to enamel and dentin. Thermocycling influence. J Mater Sci Mater Med 2005;16:727-732

95. Morresi AL, D'Amario M, Capogreco M, Gatto R, Marzo G, D'Arcangelo C, Monaco A. Thermal cycling for restorative materials: does a standardized protocol exist in laboratory testing? A literature review. J Mech Behav Biomed Mater 2014;29:295-308

96. Sheets JL, Wilcox CW, Barkmeier WW, Nunn ME. The effect of phosphoric acid pre-etching and thermocycling on self-etching adhesive enamel bonding. J Prosthet Dent 2012;107:102-108

97. Frankenberger R, Krämer N, Petschelt A. Long-term effect of dentin primers on enamel bond strength and marginal adaptation. Oper Dent 2000;25:11-19

98. Toledano M, Cabello I, Yamauti M, Giannini M, Aguilera FS, Osorio E, Osorio R. Resistance to degradation of resin-dentin bonds produced by one-step self-etch adhesives. Microsc Microanal 2012;18:1480-1493

99. Park JS, Kim JS, Kim MS, Son HH, Kwon HC, Cho BH. Aging effect on the microtensile bond strength of self-etching adhesives. J Korean Acad Conserv Dent 2006;31:415-426

100. Göhring TN[1], Gallo L, Lüthy H. Effect of water storage, thermocycling, the incorporation and site of placementof glass-fibers on the flexural strength of veneering composite. Dent Mater 2005;21:761-772

101. Burrow MF, Thomas D, Swain MV, Tyas MJ. Analysis of tensile bond strengths using Weibull statistics. Biomaterials 2004;25:5031-5035

102. Cho BH, Dickens SH. Effects of the acetone content of single solution dentin bonding agents on the adhesive layer thickness and the microtensile bond strength. Dent Mater 2004;20:107-115

103. McCabe JF, Carrick TE. A statistical approach to the mechanical testing of dental materials. Dent Mater 1986;2:139-142

104. Dickens SH, Cho BH. Interpretation of bond failure through conversion and residual solvent measurements and Weibull analyses of flexural and microtensile bond strengths of bonding agents. Dent Mater 2005;21:354-364

105. Abu-elenain DA, Lewis SH, Stansbury JW. Property evolution during vitrification of dimethacrylate photopolymer networks. Dent Mater 2013;29:1173-1181

106. Soderholm KJ. Dental adhesives .... how it all started and later evolved. J Adhes Dent 2007; 9: 227-230.

107. Armstrong SR, Vargas MA, Chung I, Pashley DH, Campbell JA, Laffoon JE, Qian F. resin-dentin interfacial ultrastructure and microtensile dentin bond strength after five-year water storage. oper dent 2004; 29: 705-712.

108. Fridman G, Gutsol A, Shekhter AB, Vasilets VN, Fridman A. Applied plasma medicine. Plasma Process Polym 2008; 5: 503-533.

109. Kim J-H, Lee M-A, Han G-J, Cho B-H. Plasma in dentistry: A review of basic concepts and applications in dentistry. Acta Odontol Scand 2014; 72: 1-12.

110. Chen FF, Lieberman MA. Introduction to plasma physics and controlled fusion. New York: Plenum Press, 1984.

111. Lieberman MA, Lichtenberg AJ. Principles of plasma discharges and materials processing. 2nd ed. Hoboken, New Jersey: John Wiley & Sons, Inc., 2005.

112. Çökeliler D, Erkut S, Zemek J, Biederman H, Mutlu M. Modification of glass fibers to improve reinforcement: A plasma polymerization technique. Dent Mater 2007; 23: 335-342.

113. Costa dantas MC, Do prado M, Costa VS, Gaiotte MG, Simão RA, Bastian FL. Comparison between the effect of plasma and chemical treatments on fiber post surface. J Endod 2012; 38: 215-218.

114. Jiang C, Chen MT, Schaudinn C, Gorur A, Vernier PT, Costerton JW, Jaramillo DE, Sedghizadeh PP, Gundersen MA. Pulsed atmospheric-pressure cold plasma for endodontic disinfection. IEEE Trans Plasma Sci 2009; 37: 1190-1195.

115. Lu X, Cao Y, Yang P, Xiong Q, Xiong Z, Xian Y, Pan Y. An RC. plasma device for sterilization of root canal of teeth. IEEE Trans Plasma Sci 2009; 37: 668-673.

116. Lee HW, Kim GJ, Kim JM, Park JK, Lee JK, Kim GC. Tooth bleaching with nonthermal atmospheric pressure plasma. J Endod 2009; 35: 587-591.

117. Lee HW, Park GY, Seo YS, Im YH, Shim SB, Lee HJ. Modelling of atmospheric pressure plasmas for biomedical applications. J Phys D Appl Phys 2011; 44: 053001.

118. Dong X, Ritts AC, Staller C, YU Q, Chen M, Wang Y. Evaluation of plasma treatment effects on improving adhesive-dentin bonding by using the same tooth controls and varying cross-sectional surface areas. Eur J Oral Sci 2013; 121: 355–362.

119. Lohbauer U, Nikolaenko SA, Petschelt A, Frankenberger R. Resin tags do not contribute to dentin adhesion in self-etching adhesives. J Adhes Dent 2008; 10: 97-103.

120. Sadek FT, Braga RR, Muench A, Liu Y, Pashley DH, Tay FR. Ethanol wet-bonding challenges current anti-degradation strategy. J Dent Res 2010; 89: 499-504.

121. Van Meerbeek B, De Munck J, Yoshida Y, Inoue S, Vargas M, Vijay P, Van Landuyt K, Lambrechts P, Vanherle G. Buonocore memorial lecture. Adhesion to enamel and dentin: current status and future challenges. Oper Dent 2003; 28: 215-235.

122. Peumans M, Kanumilli P, De Munck J, Van Landuyt K, Lambrechts P, Van Meerbeek B. Clinical effectiveness of contemporary adhesives: A systematic review of current clinical trials. Dent Mater 2005; 21: 864-881.

123. Pashley DH, Carvalho RM. Dentine permeability and dentine adhesion. J Dent 1997; 25: 355-372.

124. Gwinnett AJ. Moist versus dry dentin: its effect on shear bond strength. *Am J Dent* 1992; **5**: 127-129.

125. Kanca J. Improving bond strength through acid etching of dentin and bonding to wet dentin surfaces. J Am Dent Assoc 1992; 123: 35-43.

126. Nakabayashi N, Kojima K, Masuhara E. The promotion of adhesion by the infiltration of monomers into tooth substrates. J Biomed Mater Res 1982; 16: 265-273.

127. Pasquantonio G, Tay FR, Mazzoni A, Suppa P, Ruggeri A, Jr., Falconi M, Di Lenarda R, Breschi L. Electric device improves bonds of simplified etch-and-rinse adhesives. Dent Mater 2007; 23: 513-518.

128. Fang M, Liu R, Xiao Y, Li F, Wang D, Hou R, Chen J. Biomodification to dentin by a natural crosslinker improved the resin-dentin bonds. J Dent 2012; 40: 458-466.

129. Lieberman MA, Lichtenberg AJ. Principles of plasma discharges and materials processing. MRS Bulletin 1994; 30: 899-901.

130. Kim JH, Lee MA, Han GJ, Cho BH. Plasma in dentistry: A review of basic concepts and applications in dentistry. Acta Odontol Scand 2014; 72: 1-12.

131. Bárdos L, Baránková H. Cold atmospheric plasma: Sources, processes, and applications. Thin Solid Films 2010; 518: 6705-6713.

132. Zhang Y, Yu Q, Wang Y. Non-thermal atmospheric plasmas in dental restoration: improved resin adhesive penetration. J Dent 2014; 42: 1033-1042.

133. Wang Y, Spencer P. Quantifying adhesive penetration in adhesive/dentin interface using confocal Raman microspectroscopy. J Biomed Mater Res 2002; 59: 46-55.

134. Guo X, Spencer P, Wang Y, Ye Q, Yao X, Williams K. Effects of a solubility enhancer on penetration of hydrophobic component in model adhesives into wet demineralized dentin. Dent Mater 2007; 23: 1473-1481.

135. DONG X, CHEN M, WANG Y, YU Q. A mechanistic study of plasma treatment effects on demineralized dentin surfaces for improved adhesive/dentin interface bonding. *Clin Plasma Med* 2014; **2**: 11-16.

136. Pashley DH, Tay FR, Carvalho RM, Rueggeberg FA, Agee KA, Carrilho M, Donnelly A, Garcia-Godoy F. From dry bonding to water-wet bonding to ethanol-wet bonding. A review of the interactions between dentin matrix and solvated resins using a macromodel of the hybrid layer. Am J Dent 2007; 20: 7-21.

137. Chiper A, Rusu G, Vitelaru C, Mihaila I, Popa G. A comparative study of helium and argon DBD plasmas suitable for thermosensitive materials processing. Rom J Phys 2011; 56S: 126-131.

138. Aziz G, Cools P, De Geyter N, Declercq H, Cornelissen R, Morent R. Dielectric barrier discharge plasma treatment of ultrahigh molecular weight polyethylene in different discharge atmospheres at medium pressure: A cell-biomaterial interface study. Biointerphases 2015; 10: 029502.

139. Seo YS, Mohamed A-AH, Woo KC, Lee HW, Lee JK, Kim KT. Comparative studies of atmospheric pressure plasma characteristics between He and Ar working gases for sterilization. IEEE Trans Plasma Sci 2010; 38: 2954-2962.

140. Nishitani Y, Yoshiyama M, Donnelly AM, Agee KA, Sword J, Tay FR, Pashley DH. Effects of resin hydrophilicity on dentin bond strength. J Dent Res 2006; 85: 1016-1021.

141. Jacobsen T, Soderholm KJ. Some effects of water on dentin bonding. Dent Mater 1995; 11: 132-136.

142. Paul SJ, Leach M, Rueggeberg FA, Pashley DH. Effect of water content on the physical properties of model dentine primer and bonding resins. J Dent 1999; 27: 209-214.

143. Wang Y, Spencer P, Yao X, Ye Q. Effect of coinitiator and water on the photoreactivity and photopolymerization of HEMA/camphoquinone-based reactant mixtures. J Biomed Mater Res A 2006; 78: 721-728.

144. Tay FR, Gwinnett JA, Wei SHY. Micromorphological spectrum from overdrying to overwetting acid-conditioned dentin in water-free acetone-based, single-bottle primer/adhesives. Dent Mater 1996; 12: 236-244.

145. Sano H, Takatsu T, Ciucchi B, Horner JA, Matthews WG, Pashley DH. Nanoleakage: leakage within the hybrid layer. Oper Dent 1995; 20: 18-25.

146. Wang Y, Spencer P. Hybridization efficiency of the adhesive/dentin interface with wet bonding. J Dent Res 2003; 82: 141-145.

147. Quinn JB, Quinn GD. A practical and systematic review of Weibull statistics for reporting strengths of dental materials. Dent Mater 2010; 26: 135-147.

148. Robin C, Scherrer SS, Wiskott HWA, de Rijk WG, Belser UC. Weibull parameters of composite resin bond strengths to porcelain and noble alloy using the Rocatec system. Dent Mater 2002; 18: 389-395.

Figures

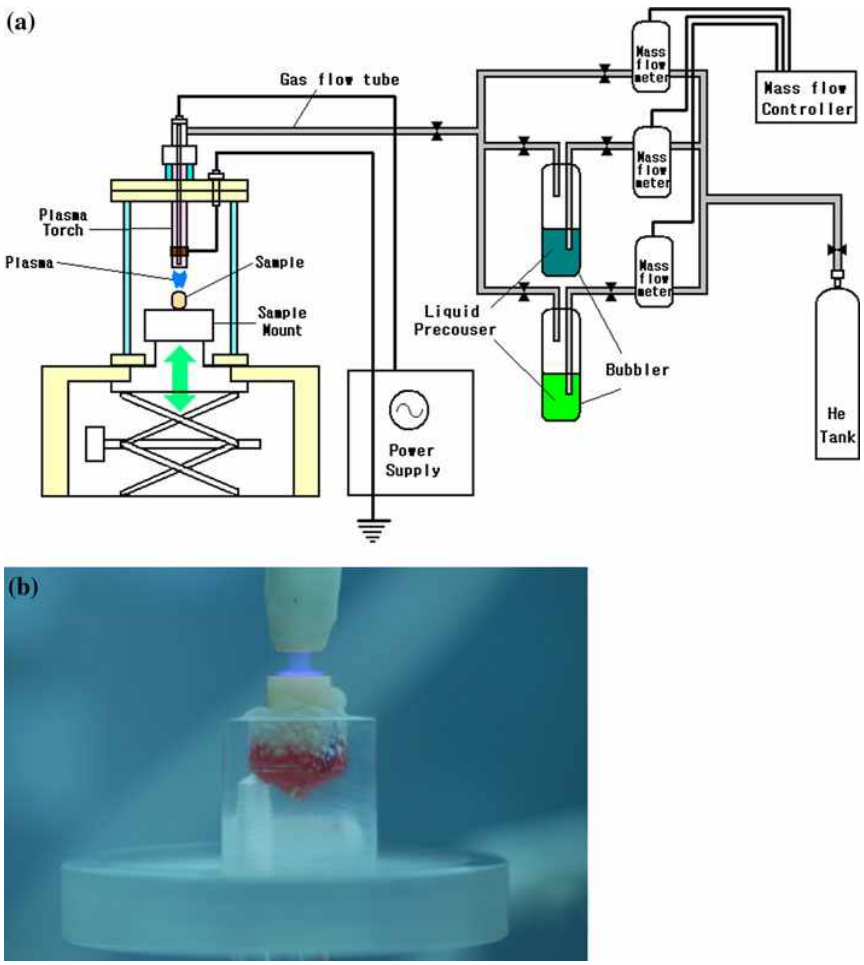

Figure 1. (a) Schematic illustration of the non-thermal atmospheric plasma (NT-APP) jet equipment used in this study; (b) Plasma flame was applied to the sample on a stand through a pencil-type plasma torch which was located 0.5 cm above the sample surface

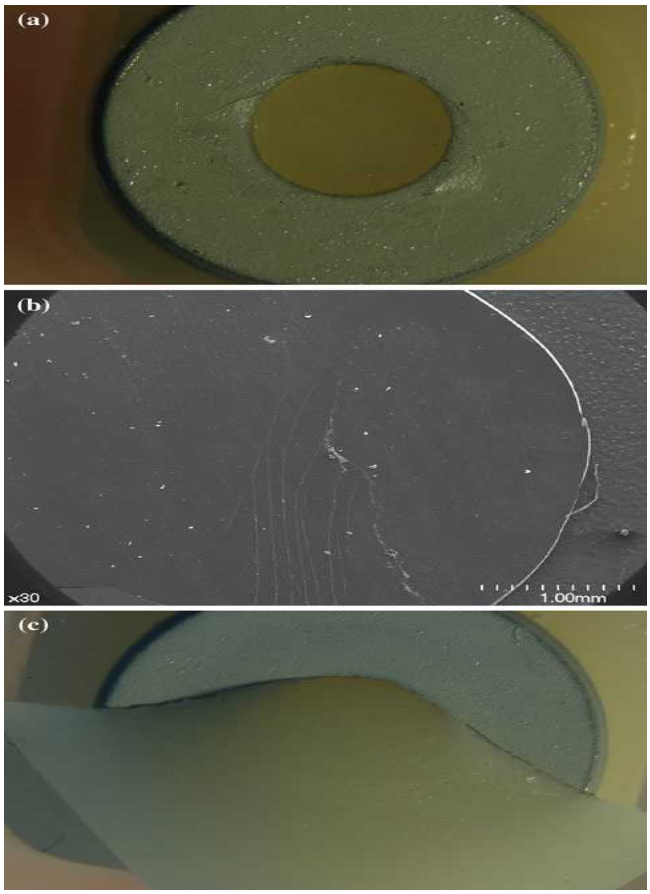

Figure 2. The fractured surfaces obtained after the shear bond strength test. (a) In group 1, the fractured surfaces due to shear loading appeared flat and shiny, like the original polished surfaces of the ceramic blocks. The fracture occurred at the interface between the polished ceramic surface and the cured adhesive layer (Adhesive fracture); (b) In group 2 with the plasma polymer coating, small fragments of ceramic were occasionally observed on the adhesive surface covering the fractured bottom surface of the composite resin in the iris (Mixed fracture). When the plasma surface treatment with DW was additionally performed before plasma polymer coating with TEGDMA (group 3), the incidence of mixed fracture increased; (c) In group 4, cohesive fracture of ceramic was observed at the opposite side of the loading plunger in all specimens

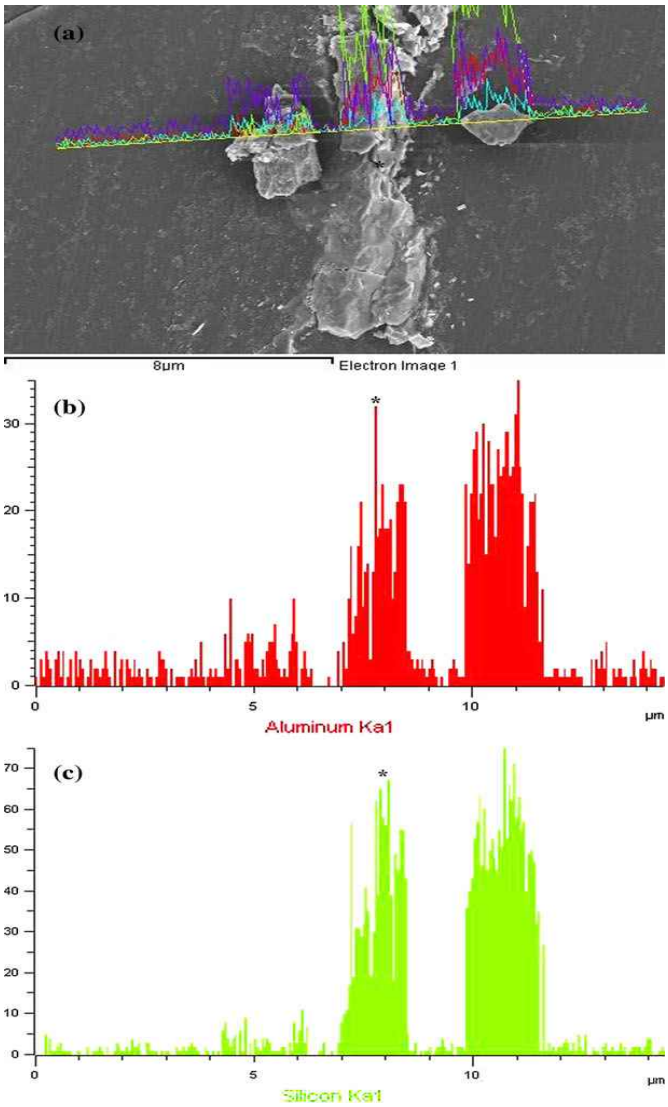

Figure 3. (a) SEM image of the fractured surface at the bottom of the composite resin in the iris after the shear bond strength test. Small fragments (asterisk) observed on the flat fractured surface were confirmed as ceramic according to EDS line scanning; (b) and (c), from EDS line scanning, elements of ceramic, such as Si and Al, were detected in the fragments, but not on the flat smooth surface, demonstrating that there was an island of ceramic on the flat cured bonding layer which masked the underlying composite resin

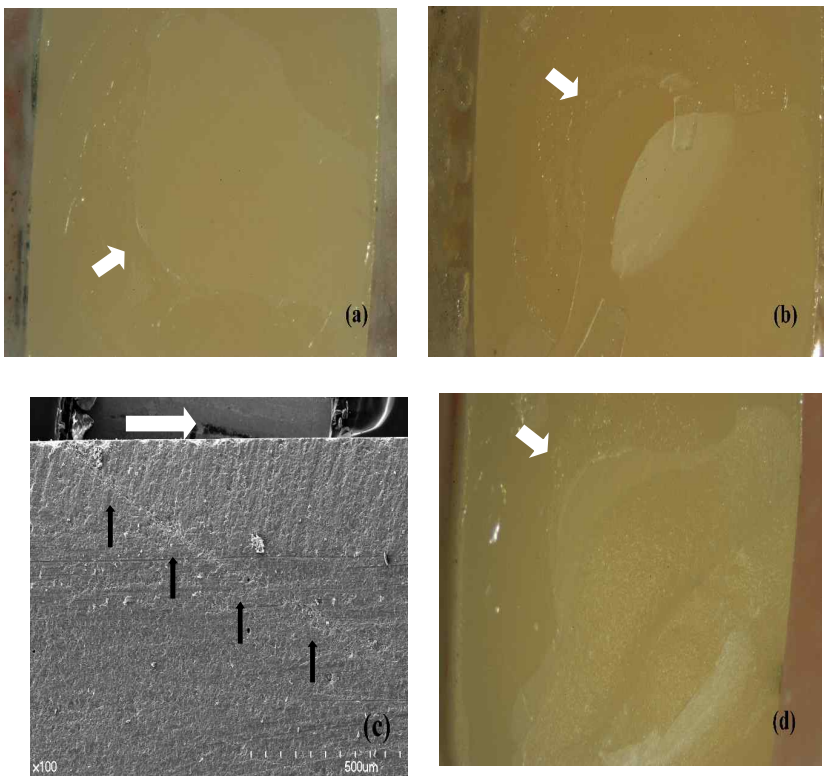

Figure 4. Stereomicroscopic photographs of typical fracture modes and a scanning electron micrograph (SEM) of a cross section of a fractured specimen. (a), Adhesive fracture (A) between the ground ceramic surface and the cured adhesive layer; (b), Mixed fracture (M), in which the crack propagated from the adhesive interface to the ceramic substrate. As a result, an irregularly reflected white opaque area was observed just beneath the adhesively-fractured flat ceramic surface due to subsurface-crack propagation and incomplete fracture (black asterisk); (c), cross-sectional SEM of the white opaque reflected surface of b (black asterisk), showing a subsurface-crack propagation and incomplete fracture (black arrows); (d), Cohesive fracture (C), an oblique fracture of the ceramic adherend (white asterisk). White arrow shows the direction of loading by the plunger.

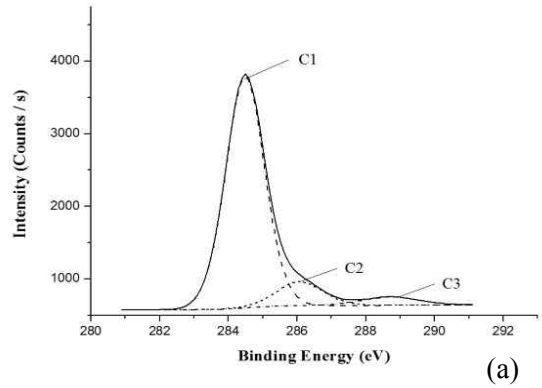

(a)

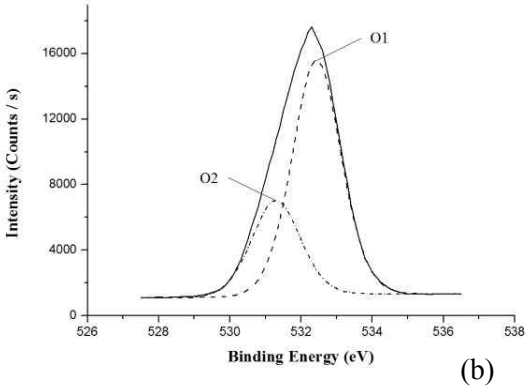

(b)

Figure 5. Deconvolution of the C1s and O1s spectra of the ceramic specimens after plasma polymer deposition at an input power of 15 V. (a), Three components of the C1s spectrum of a treated ceramic surface: C1, a component with a binding energy of 284.5 eV due to C-C bonds; C2, a component with a binding energy of 286.1 eV due to C-O-C bonds; C3, a component with a binding energy of 288.2 eV due to O=C-O bonds. (b), Two components of the O1s spectrum of a treated ceramic surface: O1, a component with a binding energy of 532.4 eV due to O=C-O bonds; O2, a component with a binding energy of 531.3 eV due to a mixed peak of C=O in carboxyl group, -OH and C-O-C bonds.

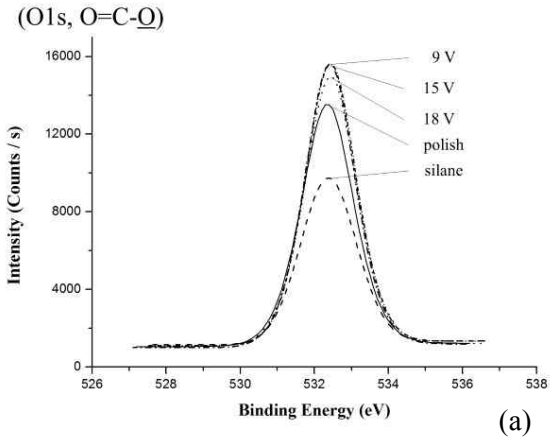

(a)

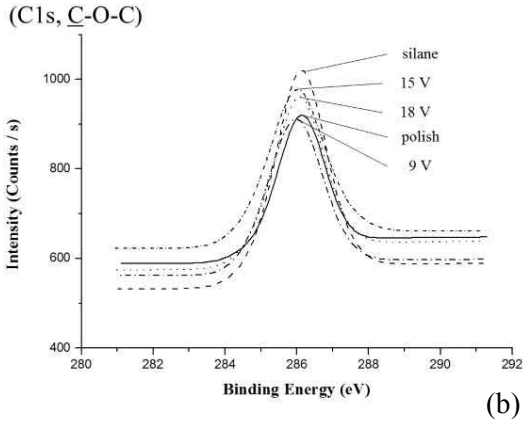

(b)

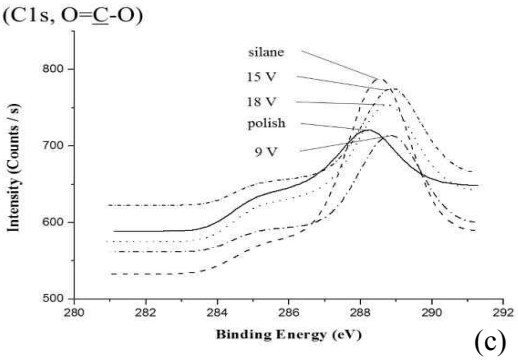

(c)

Figure 6. Changes in the height of each peak deconvoluted from C1s spectra obtained after treatments. The height of each peak was evaluated as the height from the baseline to the peak. After treatment, the peak height of C1 decreased (a), while the peak heights of both C2 and C3 increased (b and c). Compared to the C2 peak, the C3 peak showed a relatively prominent chemical shift after plasma polymer deposition (c).

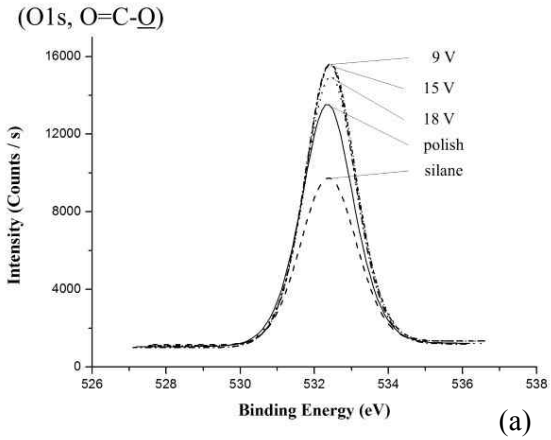

(a)

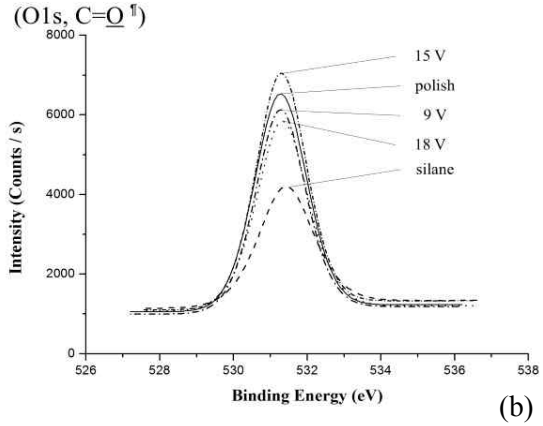

(b)

Figure 7. Changes in the height of each peak deconvoluted from O1s spectra obtained after treatments. After treatments, the peak height of O1 increased (a), while the peak height of O2 decreased (b). The O1 and O2 peaks did not show chemical shifts, except for the O2 peak of the silane-coated specimen. ¶ a mixed peak of C=O, -OH, and C-O

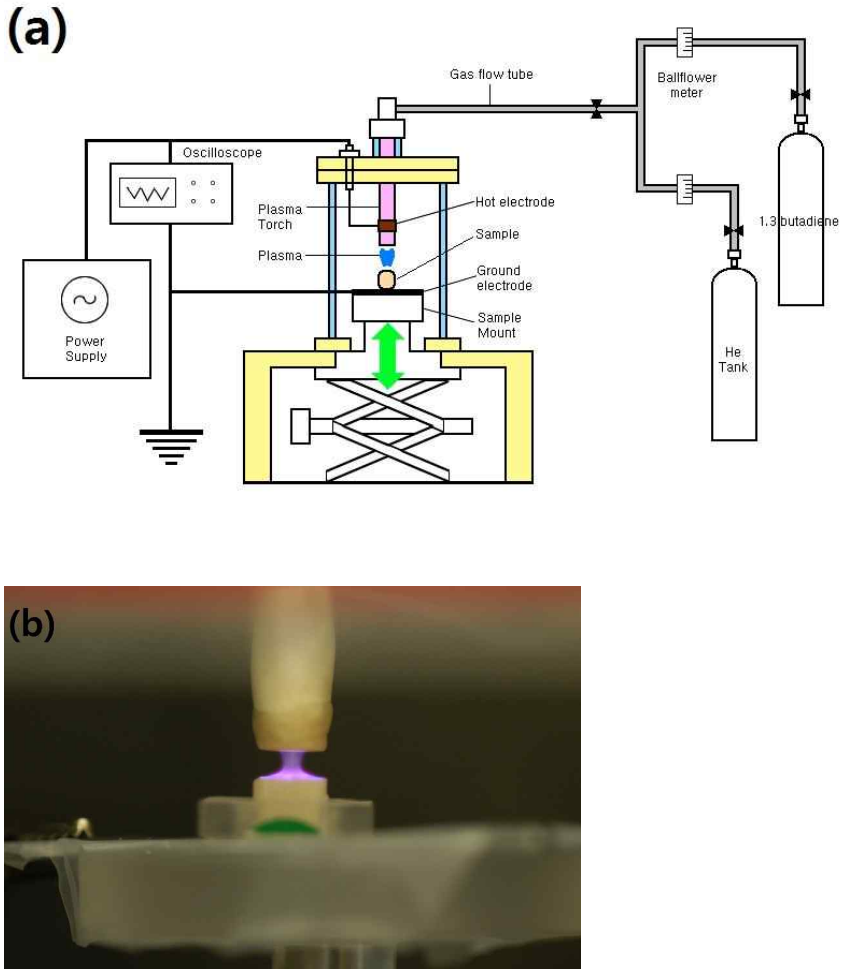

Figure 8. Schematic illustration of the floating-electrode dielectric barrier discharge (FE-DBD) jet used in this study.

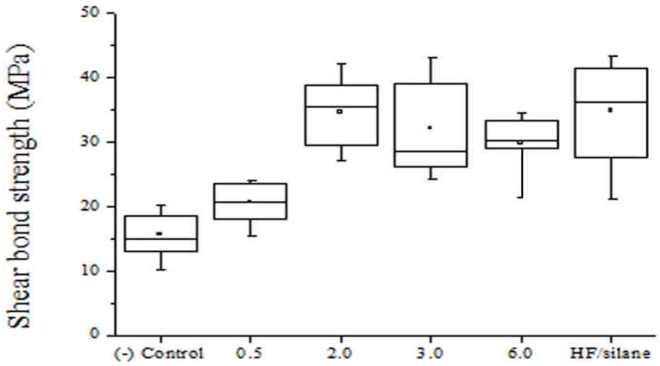

Figure 9. Shear bond strength (SBS) between composite resin and dental ceramic according to various flow rates of 1,3-butadiene (BD) gas as a precursor monomer using an experimental floating electrode dielectric barrier discharge (FE-DBD) jet. Note that the SBS values of the plasma-treated groups with a flow rate of BD more than 2 sccm were not different from that of the group treated with conventional protocol with hydrofluoric acid etching and silane coating.

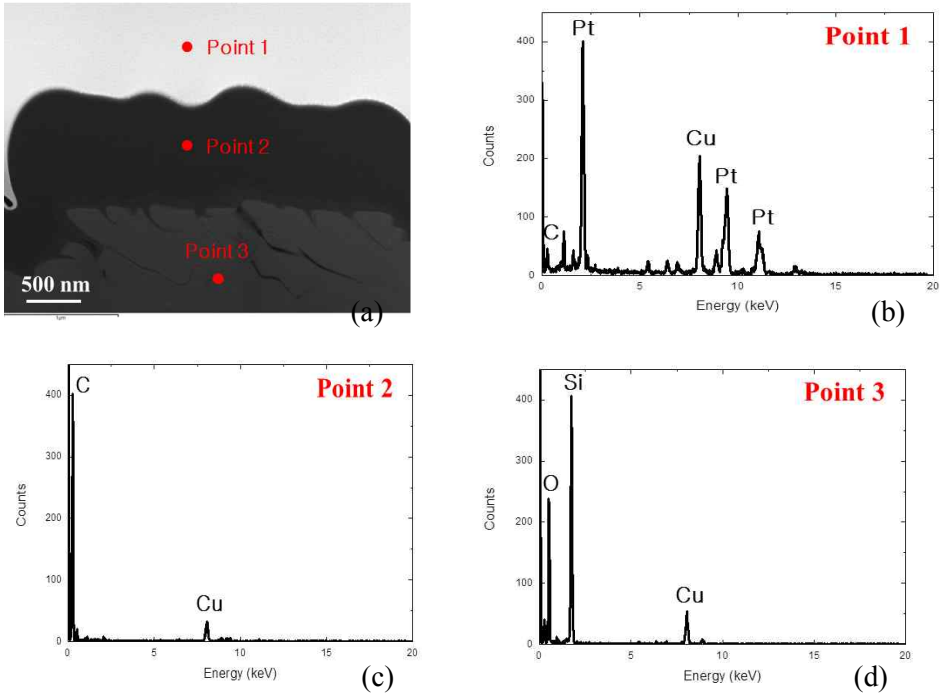

Figure 10. (a), Transmission electron micrographic image of a cross-section of the ceramic sample that was plasma-deposited with 6 sccm of 1,3-butadiene for 15 minutes and prepared with a focused ion beam technique. The plasma-deposited layer was approximately 500 nm thick (Carbon peak from Point 2). (b) – (d), The plasma-deposited layer was characterized with EDS. It (Point 2) was observed between the sputter-coated Pt layer (Point 1) for the protection of the top portion of the sample and the underlying ceramic substrate (Point 3).

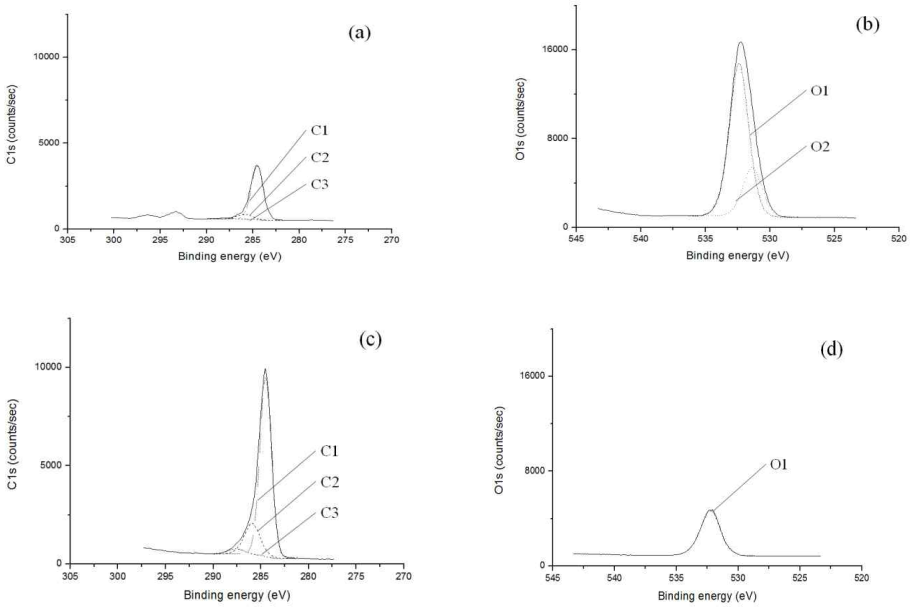

Figure 11. Deconvolution of the C1s and O1s spectra of the ceramic surface of the control group (a and b) and deconvolution of the one after plasma deposition of 1,3-butadiene at a flow rate of 3 sccm (c and d). (a) and (b), the ground ceramic surface of the control group had relatively less carbon atoms and abundant oxygen atoms; (c) and (d), after plasma deposition, the C1s peaks increased more than three times compared to the peaks of untreated ceramic surface, but the O1s peaks decreased. With sufficient levels of monomer gas, a low level of the O1 peak was detected with an abundant level of carbon atoms including C1, C2, and C3 peaks, but the O2 peak disappeared completely from the spectra.

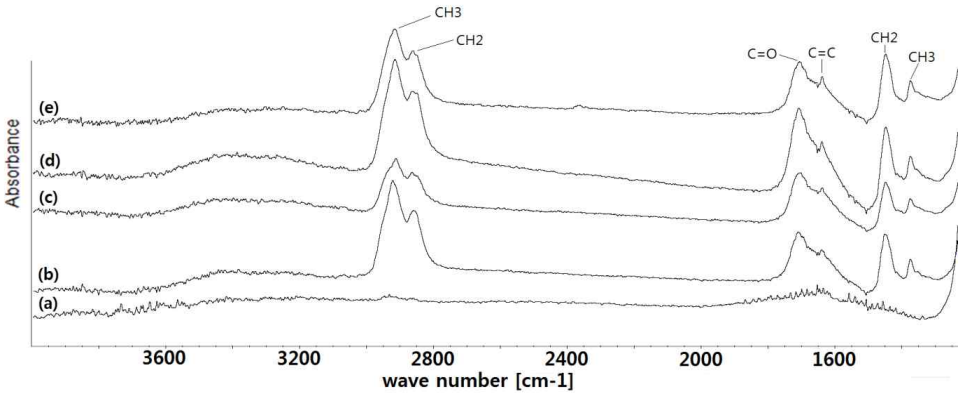

Figure 12. Fourier-transform infrared spectroscopy (FTIR) spectra of the plasma-deposited ceramic surface with different flow rates of 1,3-butadiene precursor monomer gas for 15 minutes. (a), control; (b), with a flow rate of 0.5 sccm; (c), with a flow rate of 2 sccm; (d), with a flow rate of 3 sccm; (e), with a flow rate of 6 sccm. The heights of these peaks showed an increasing tendency with the increase of flow rate of the monomer gas. The increase in the peak height of C=C bonds supported the fact that the increase in the C1s peak resulted from the increase of C=C bonds, in addition to the increase of C-C bonds.

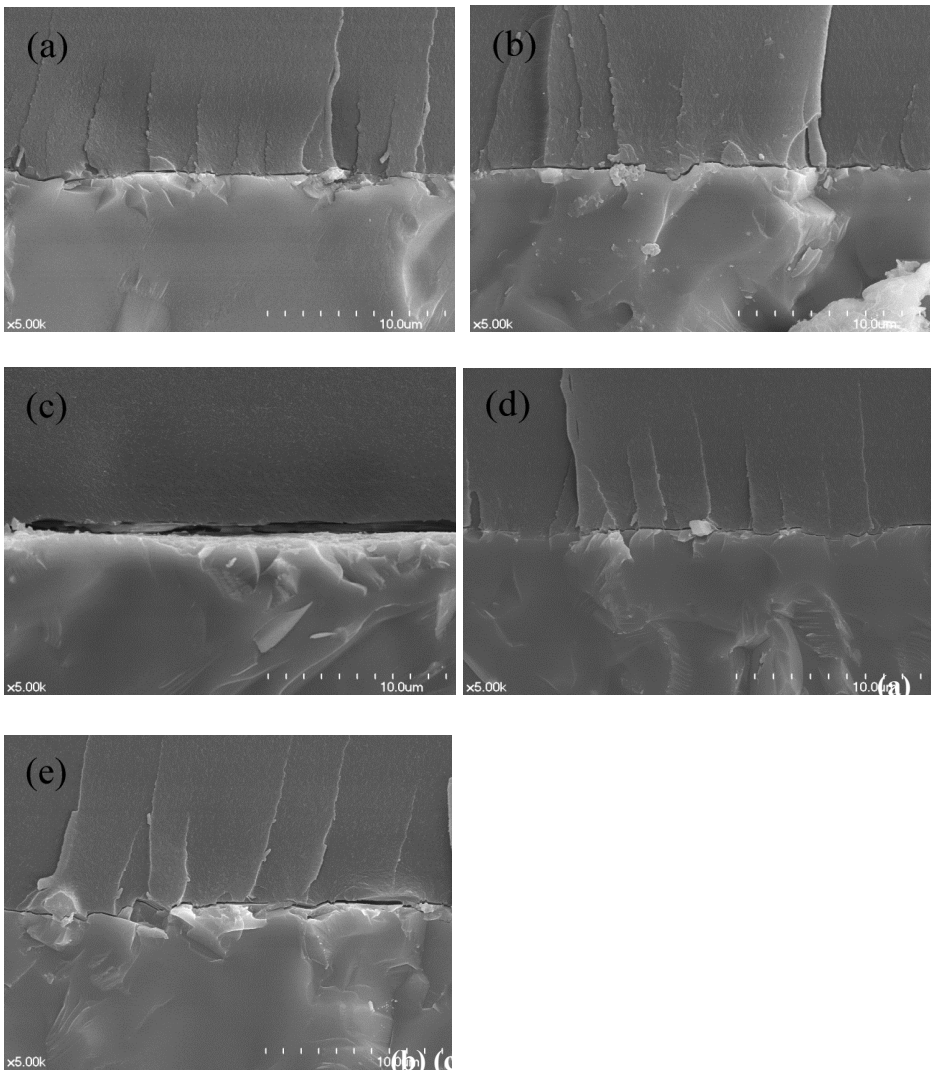

Figure 13. Comparison of the adaptation between the adhesive and the ceramic surfaces treated with plasma-enhanced chemical vapor deposition (PECVD) of the assigned monomers for each group from the flat specimens additionally prepared and fractured at a flexural mode. (a) group 1, negative control; (b) group 2, plasma-enhanced chemical vapor deposition (PECVD) of H_2O; (c) group 3, PECVD of HMDSO; (d) group 4, PECVD of benzene; (e) group 5, PECVD of HMDSO and benzene sequentially. When HMDSO was deposited on the ceramic surface (c), the surface showed superhydrophobicity, a wide gap at the interface, and as a result,

the SBS was the lowest. When the ceramic surface was deposited with PECVD of H_2O (b), even with the highest work of adhesion (*Wa*), the adaptation of the adhesive into the irregularities and the gap at the interface looked similar to those of the control group (a). However, the SBS was significantly higher than that of the negative control group due to increased hydrophilic groups (Group 2 in Table 2). In the case of benzene (d), in spite of the lower *Wa*, the adaptation of the adhesive looked better than the control group (a) and the water-treated group (b) due to increase hydrophilicity and functional groups (Group 4 in Table 2). The SBS was also significantly higher than that of the control group, but it was not superior to that of the water-treated group. When the ceramic surface was plasma-deposited with benzene after HMDSO deposition (e), although it showed a higher *Wa* value than the HMDSO deposited surface, the adaptation was quite different from the HMDSO-deposited group and looked similar to the other groups. The SBS was significantly higher than those of the water plasma treated group and the group plasma-treated with benzene only, that might be attributed to the chemical reaction of siloxane network, aromatic C=C double bonds and increased hydrophilic functional groups.

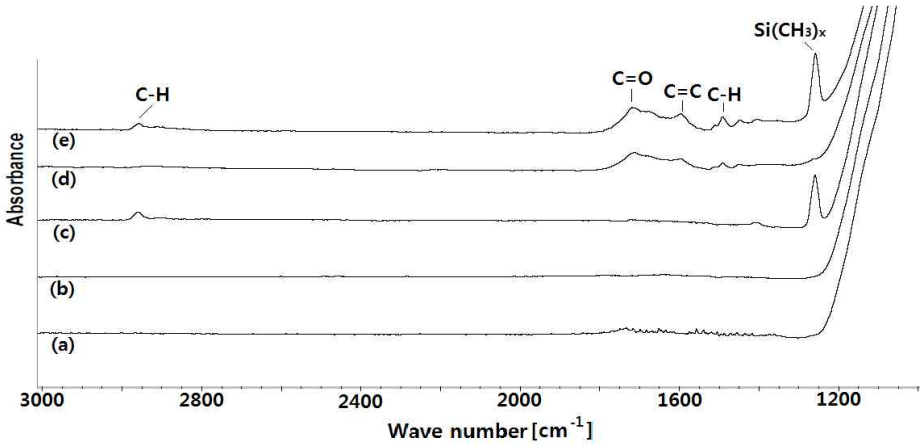

Figure 14. FTIR-ATR spectra of experimental groups, (a) group 1, negative control; (b) group 2, plasma-enhanced chemical vapor deposition (PECVD) of H_2O; (c) group 3, PECVD of HMDSO; (d) group 4, PECVD of benzene; (e) group 5, PECVD of HMDSO and benzene sequentially. After PECVD of HMDSO, the C-H peaks in methyl groups (C-H_3) in Si-CH_3 and the aliphatic C-H vibration peak were detected at 1255 and 2927 cm^{-1}, respectively. After PECVD of benzene, the aromatic C=C double bond and the carbonyl C=O bond were detected at 1600 and 1720 cm^{-1}, respectively. When the ceramic surface was plasma-deposited with HMDSO and then benzene, all the peaks that were detected on the ceramic surface treated with each monomer were detected simultaneously in the FTIR-ATR spectra.

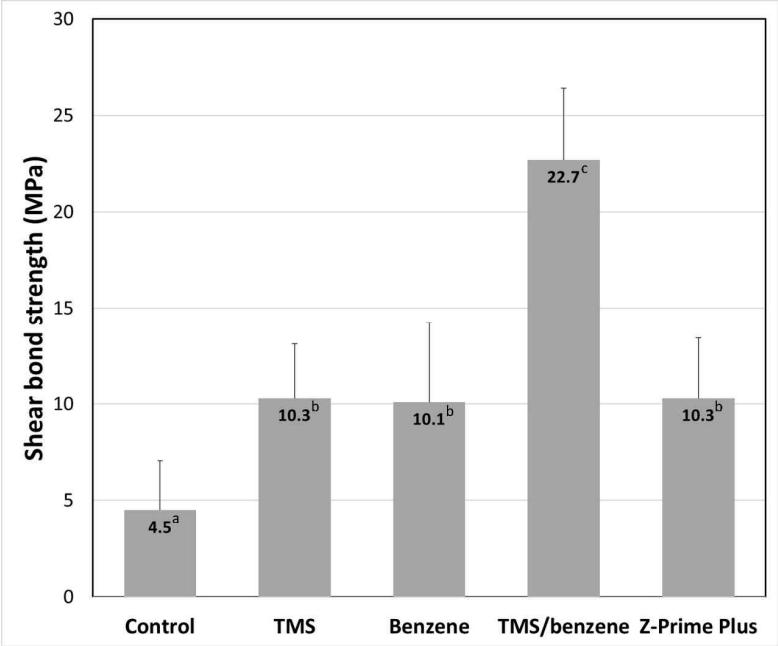

Figure 15. Shear bond strengths of resin composite to zirconia according to surface treatments. The different superscripts of the mean values indicate statistical significances ($P < 0.05$, Tukey HSD test).

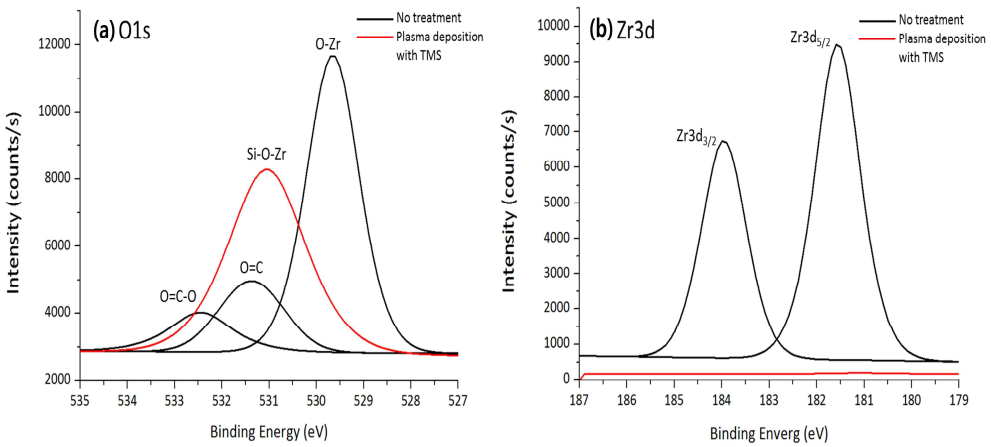

Figure 16. Deconvoluted (a) O1s and (b) Zr3d spectra obtained from a non-treated zirconia specimen (black line) and a specimen after plasma deposition with TMS (red line). The non-treated zirconia showed three peaks of the O1s spectrum at 529.7, 531.4, and 532.5 eV, while the TMS-deposited zirconia showed a peak centered at 532.3 eV. The non-treated zirconia showed two peaks of the Zr3d spectrum at 181.3 and 183.9 eV. The Zr3d spectrum disappeared after plasma deposition with TMS.

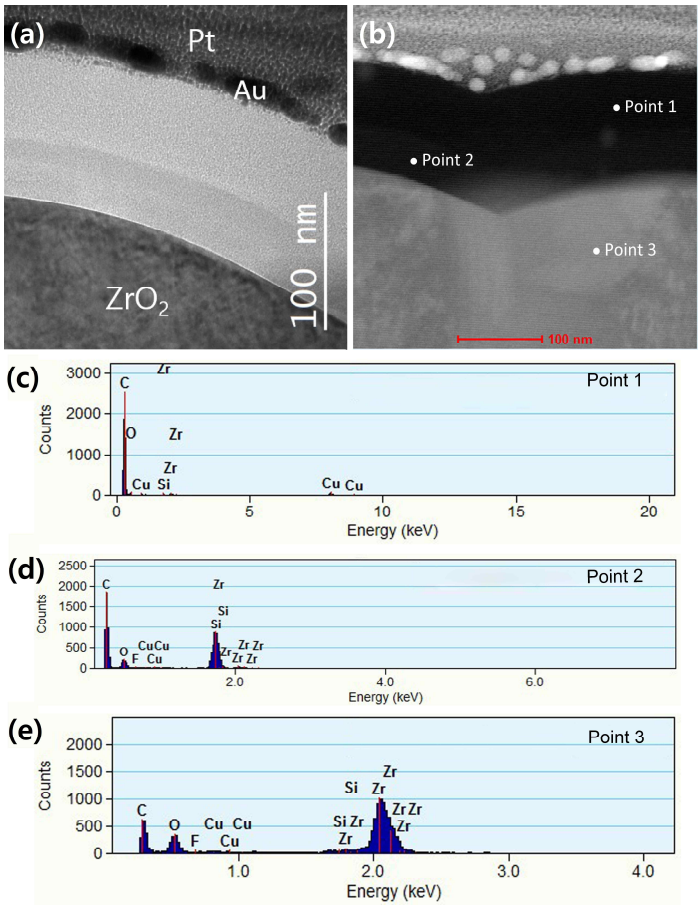

Figure 17. (a) Bright-field TEM image of a cross-sectioned specimen which was plasma-deposited sequentially with TMS and benzene. Two distinct flawless layers were observed between the zirconia surface and the Pt layer for the protection of the sample. (b) FIB-milled cross-sectional image for the EDS analysis. (c-e) EDS spectrum acquired from the point 1, point 2, and point 3. The EDS results showed that the main elements of the benzene-deposited (point 1) and TMS-deposited (point 2) layers were C and Si, respectively. The peaks corresponding to Zr and O were clearly observed in the spectra acquired from the zirconia substrate (point 3)

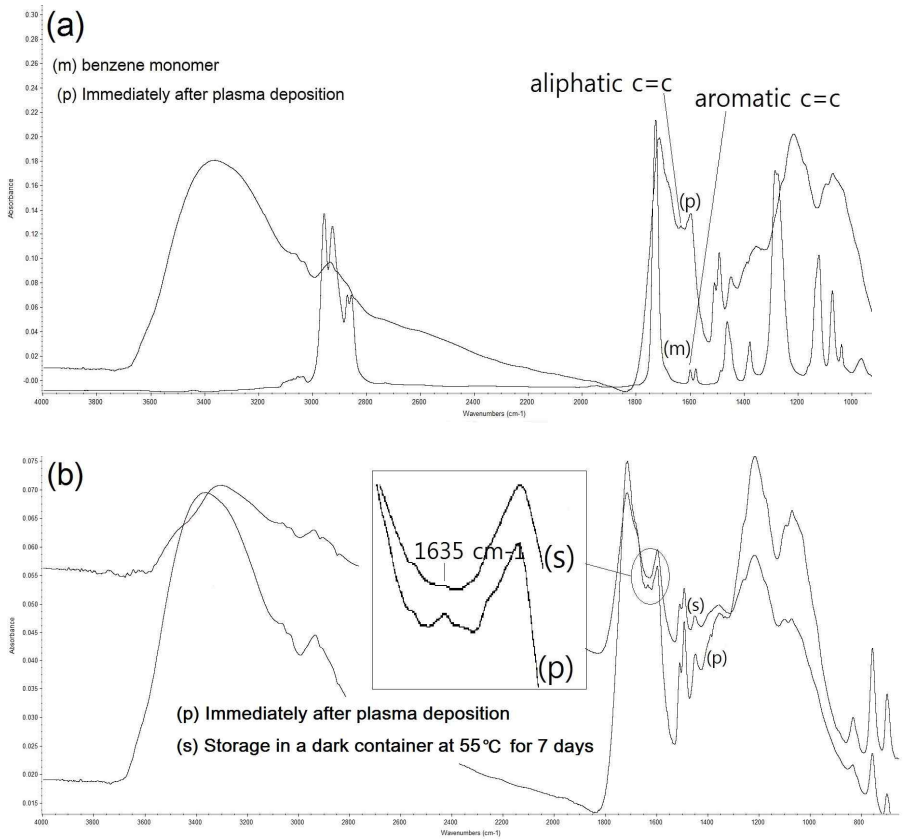

Figure. 18 Fourier-transform infrared spectroscopy (FTIR) spectra of benzene monomer (m), plasma-deposited layer of benzene immediately after deposition (p), and the layer after storage in a dark container at 55°C for 7 days (s). (a) Contrary to the spectrum obtained from monomer (m), the peak of aliphatic C=C double bonds appeared at 1635 cm^{-1} in the spectrum obtained from the plasma-deposited benzene layer (p); (b) the peak height of aliphatic C=C double bonds decreased after storage in a dark container at 55°C for 7 days (s), which showed a progressive dark-cure.

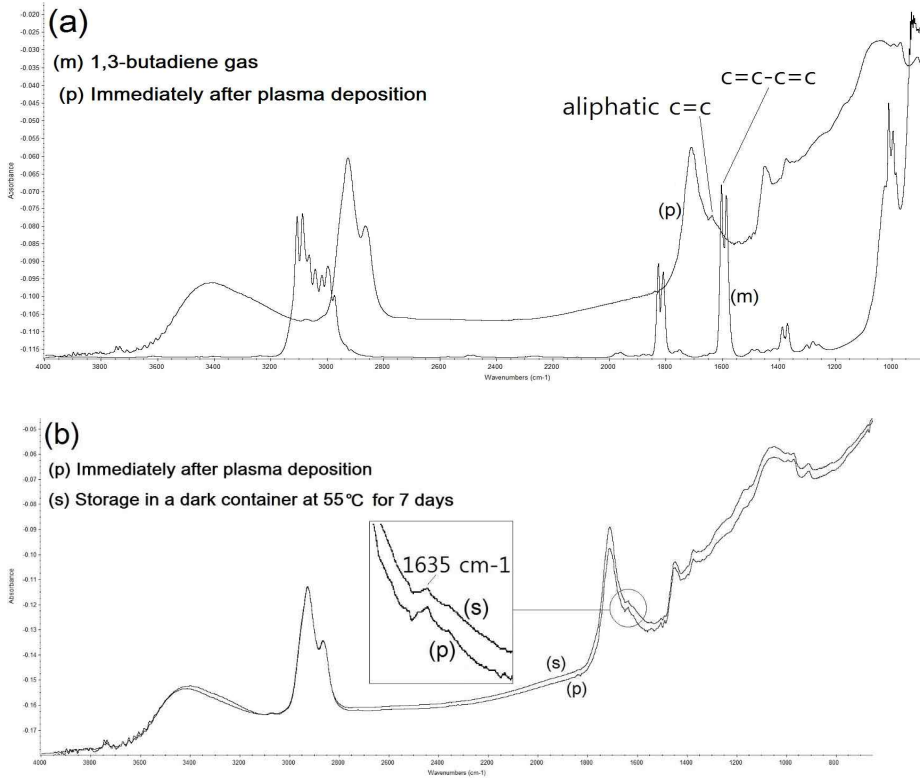

Figure. 19 Fourier-transform infrared spectroscopy (FTIR) spectra of 1,3-butadiene monomer gas (m), plasma-deposited layer of benzene immediately after deposition (p), and the layer after storage in a dark container at 55°C for 7 days (s). (a) Contrary to the spectrum obtained from monomer gas (m), the peak of aliphatic C=C double bonds appeared at 1635 cm^{-1} in the spectrum obtained from the plasma-deposited benzene layer (p); (b) the peak height of aliphatic C=C double bonds slightly decreased after storage in a dark container at 55°C for 7 days (s), which showed a progressive dark-cure.

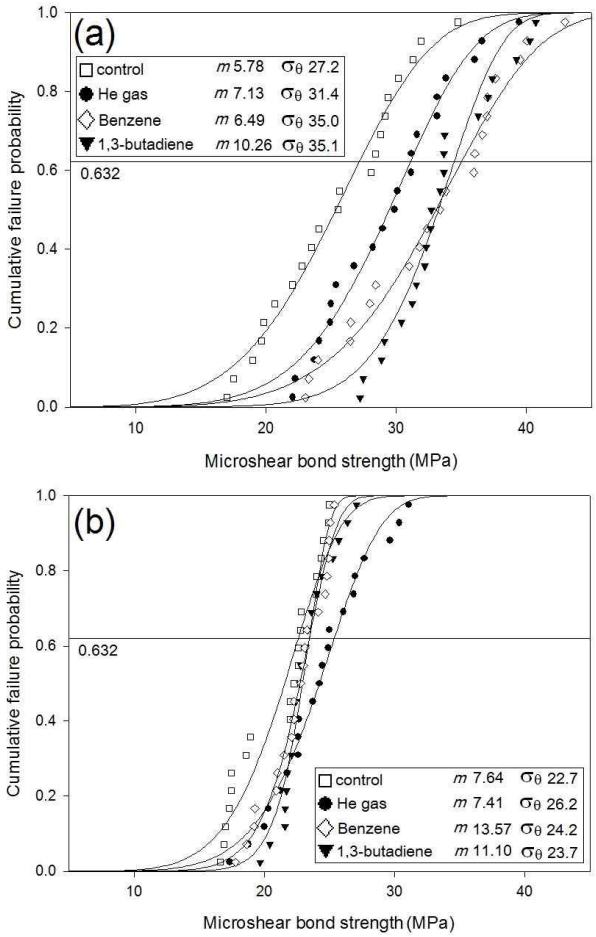

Figure. 20 (a**)** The Weibull modulus, *m*, increased with the plasma treatments. The distribution of the characteristic strengths, σ_θ, at a 63.2% cumulative failure probability was similar to that of the mean values of the experimental groups. However, the *m* of Group 4 using BD was already very high at 24 hours; (b**)** after TC, the *m* values also increased in all groups and especially in Group 3 using BZ as a precursor monomer. This finding indicates that the plasma treatment and TC caused the failure stresses of the enamel adhesion to occur within a narrow range. BZ, benzene; BD, 1,3-butadiene; TC, thermocycling.

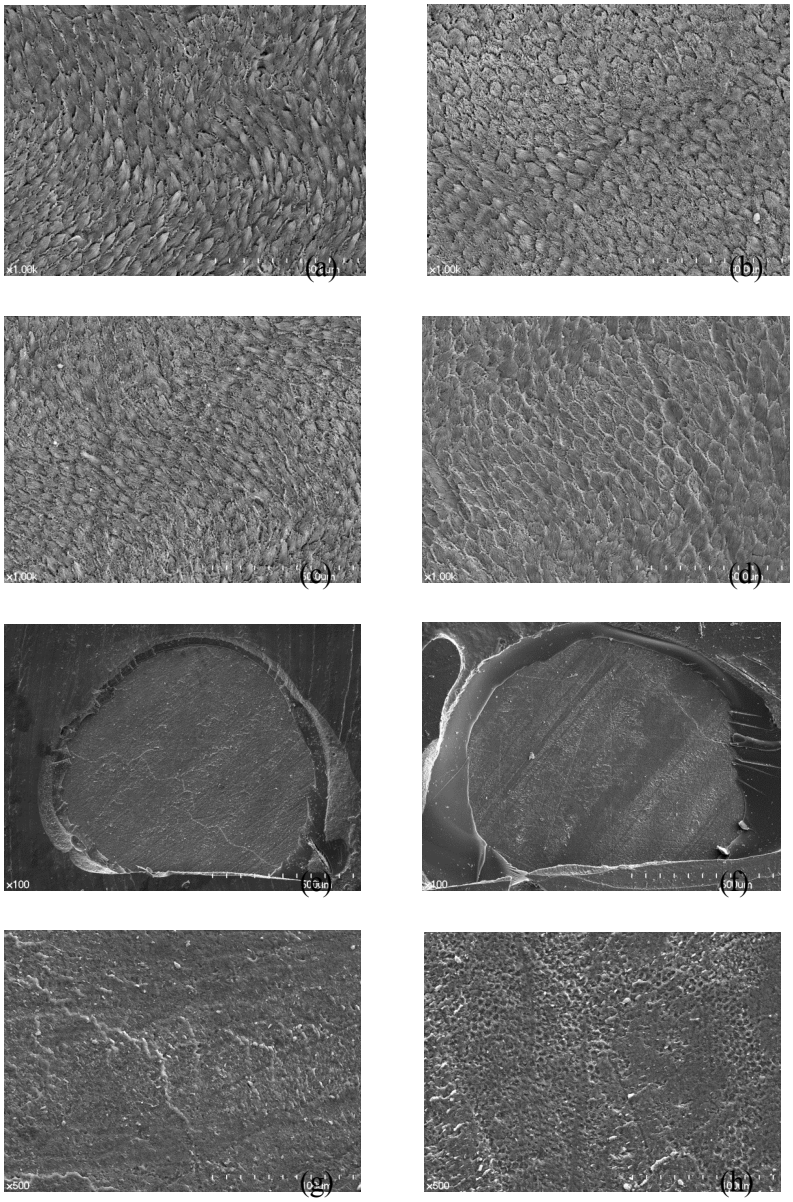

Figure. 21 Scanning electron micrographs show the adhesive modes of the fractures after the micro-shear bond strength measurements. (a**)-(**d**)** Etched enamel surface exposed (x1,000). Because no deposited layer of plasma polymer was observed in any group, the plasma deposition must have been extremely thin. (a**)** After a series of procedures of etching with 32 wt% phosphoric acid for 15 seconds, rinsing with copious amounts of water for 15 seconds, and drying completely with compressed air; (b) after He plasma treatment of the etched enamel surface without

monomer; (c) after plasma deposition of benzene on the etched enamel surface; (d) after plasma deposition of 1,3-butadiene on the etched enamel surface. (e)-(f) debonded enamel surface (x100). (e) Debonded enamel surface of a benzene-deposited specimen; (f) debonded enamel surface of a 1,3-butadiene-deposited specimen. (g)-(h) Although the fracture occurred at the bottom of the adhesive in the images of (e) and (f), magnification of the fractured surface (x500) demonstrated that the characteristic prism structure of the etched enamel was covered with resinous materials. The observation suggested that the fracture occurred in the adhesive mode. (g) Resinous covering on the etched enamel surface treated with plasma deposition of benzene; (h) resinous covering on the etched enamel surface treated with plasma deposition of 1,3-butadiene.

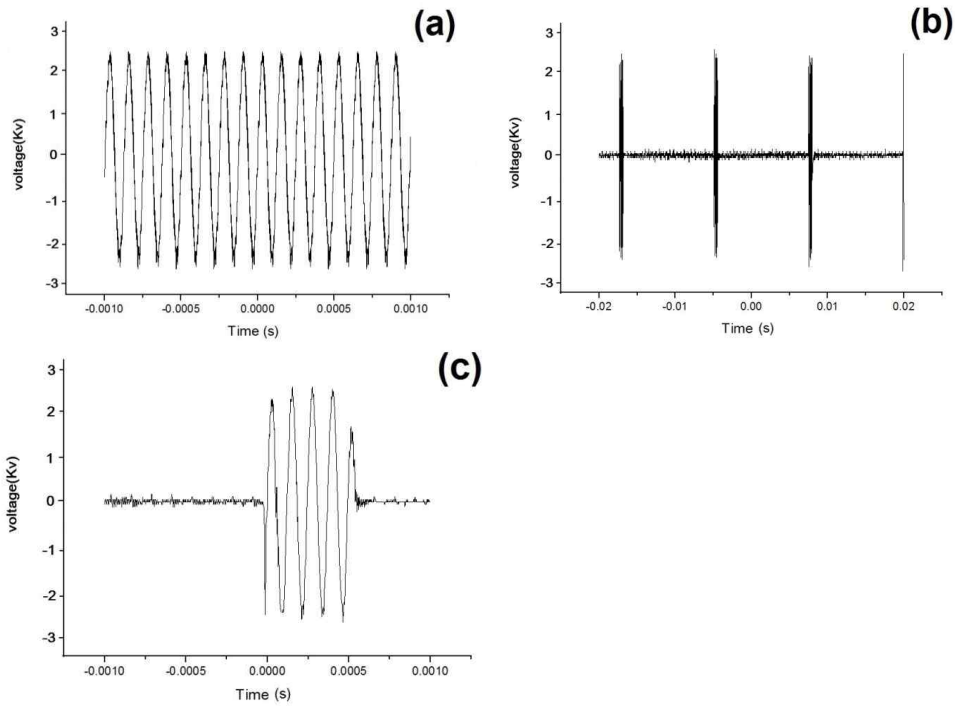

Figure 22. Voltage wave forms of the pulsed and continuous (sinusoidal) discharges used in the audiofrequency plasma equipment. (a) A continuous sinusoidal power source (8.0 kHz) was used to generate a conventional plasma plume, when the pulse was inactived; (b) However, when the pulse was on, a 0.4 kHz pulsed power source generated a pulsed plasma plume; (c) in which each pulse had five voltage peaks (Hz) and lasted for 500 ns at 12.5 ms intervals.

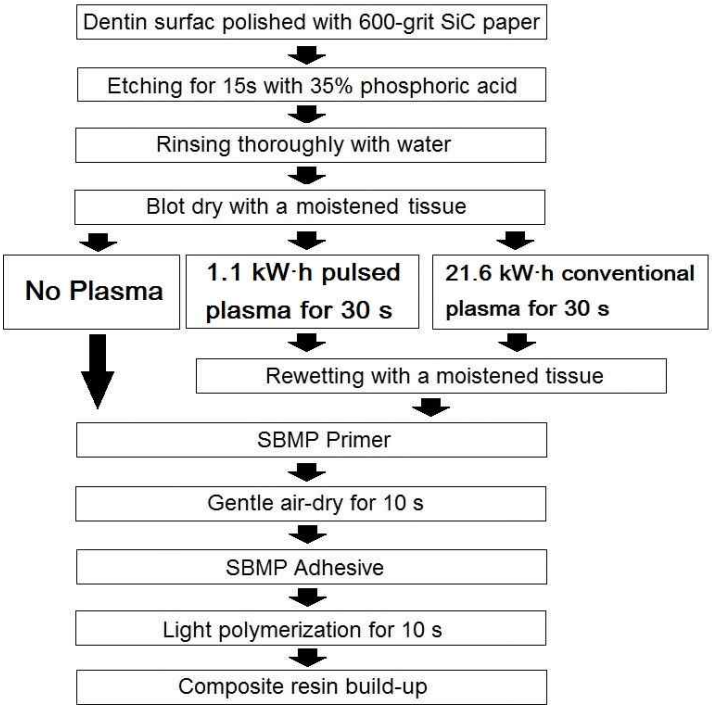

Figure 23. Schematic diagram of the adhesion procedures for the experimental groups.

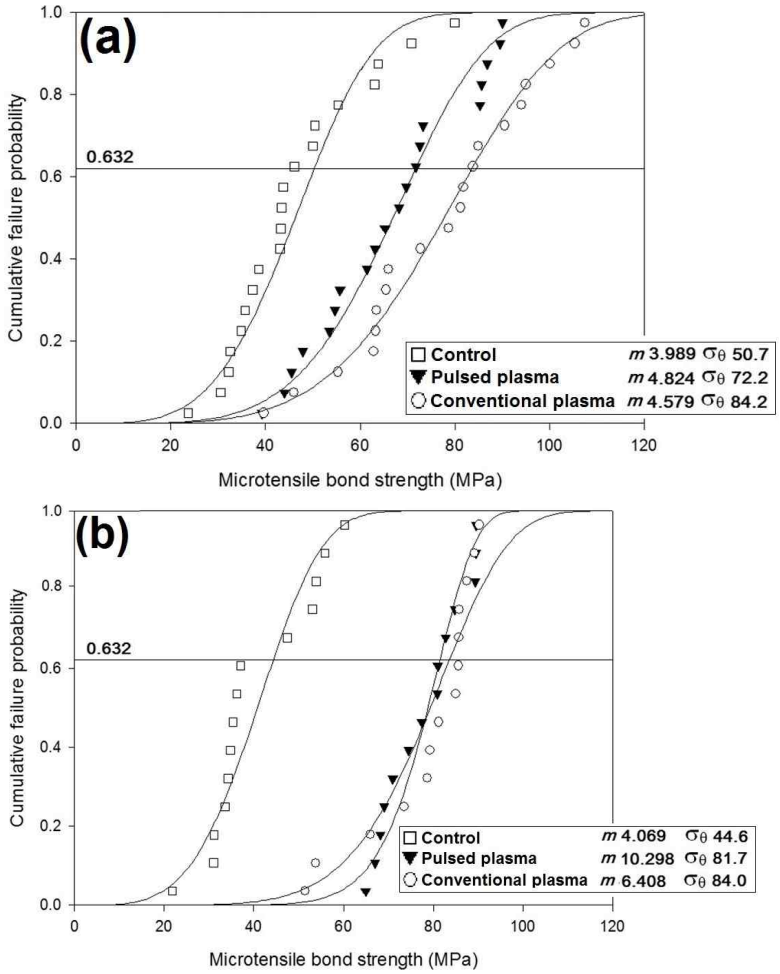

Figure 24. Weibull cumulative failure probability curves for microtensile bond strength. (a) after 24 h; (b) after 5,000 thermocycling.

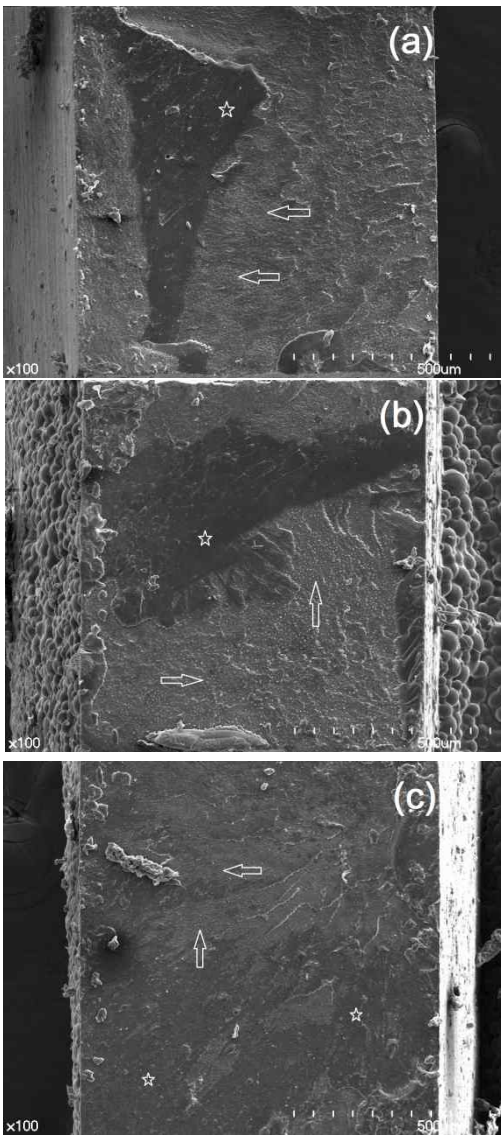

Figure 25. Representative fractured dentin surfaces after microtensile bond strength testing of thermocycled specimens (5,000 thermocycles). Note the shiny surface resulting from adhesive fracture at the interface of the hybrid layer and the adhesive layer (white arrows) and adhesive resin remnants resulting from cohesive fracture of the overlying adhesive layer (asterisks). In the case of adhesive fracture, although tubules and/or fractured resin tags were observed, the intertubular dentin was covered with resinous material (white arrows). (a) control group; (b) pulsed plasma group; (c) conventional plasma group.

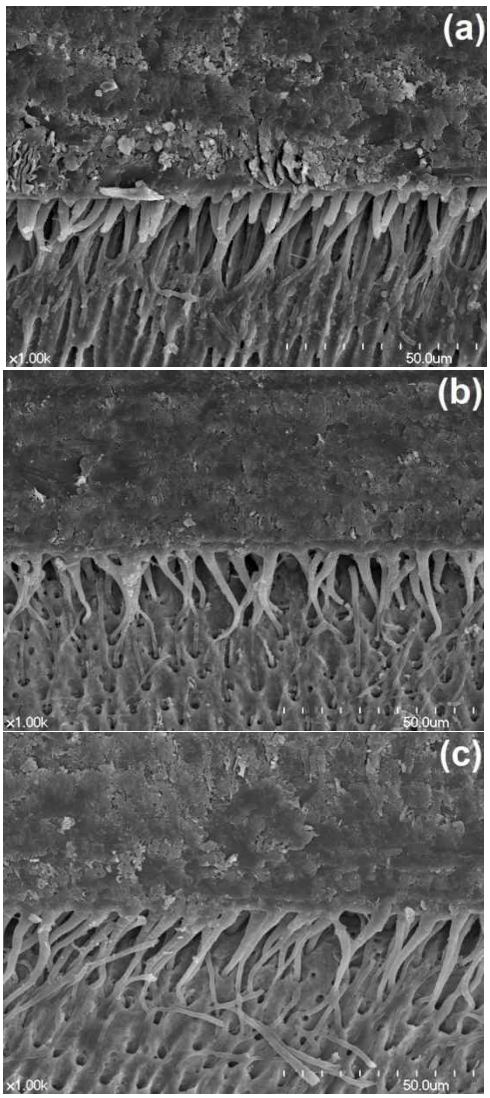

Figure 26. Bonded interface of the sliced specimens selected from each group at 24 h. (a) the bonded interface of the control group; (b) the bonded interface of a specimen treated with pulsed plasma; (c) the bonded interface of a specimen treated with conventional plasma. Note the intimate contact between the layers of composite resin, adhesive layer, and hybrid layer. There was no gap observed at the interfaces. Abundant resin tags observed in the specimens treated with plasma (b & c) appeared longer and more tortuous with lateral projections than those in the control group (a), especially in the specimens treated with conventional plasma (c).

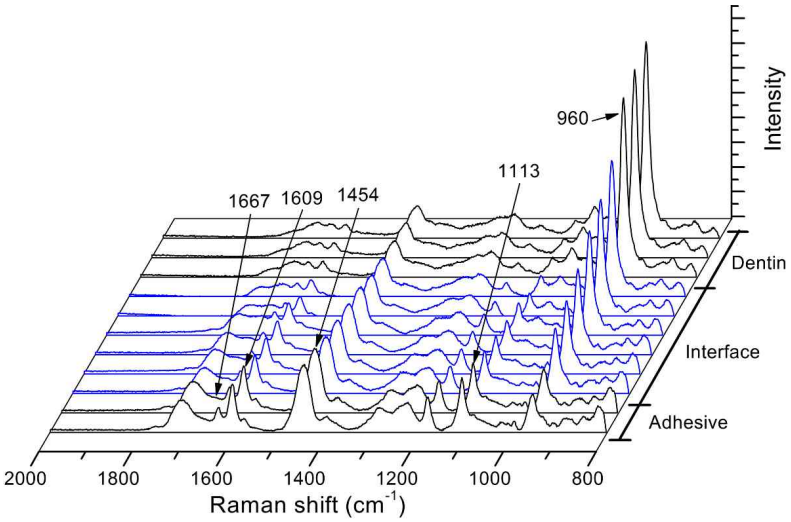

Figure 27. Representative micro-Raman mapping spectra acquired across the adhesive layer, adhesive/dentin interface, and dentin. Spectra corresponding to the adhesive/dentin interface are shown in blue. 960 cm^{-1}, phosphate; 1113 cm^{-1}; phenyl C-O-C of BisGMA; 1454 cm^{-1}, CH_2 deformation, 1609 cm^{-1}, aromatic C=C; 1667 cm^{-1}, amide I of collagen.

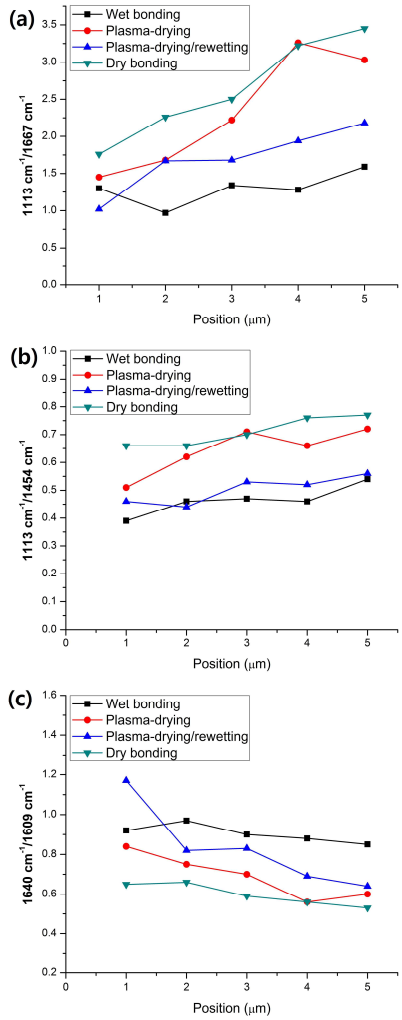

Figure 28. Micro-Raman band ratios as a function of position across the hybrid layer, from the bottom part of the hybrid layer to the adhesive layer. The y-axis represents the distance from the bottom part of the hybrid layer. (a) 1113 cm^{-1} (phenyl C-O-C of BisGMA)/1667 cm^{-1} (amide I of collagen), the degree of BisGMA penetration into the demineralized dentin; (b) 1113 cm^{-1}/1454 cm^{-1} (CH_2 of all monomers), the relative content of BisGMA in the infiltrating adhesive; (c) 1640 cm^{-1} (aliphatic C=C)/1609 cm^{-1} (aromatic C=C), the relative polymerization efficacy of the adhesive.

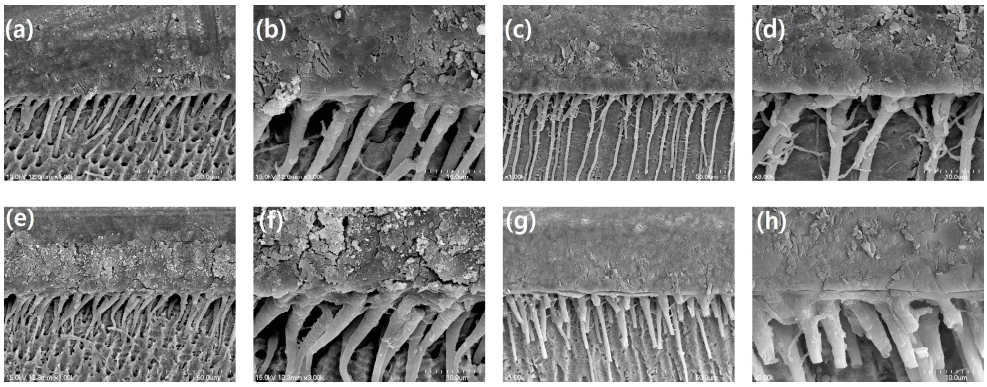

Figure 29. Representative SEM images of the adhesive/dentin interface produced by different adhesion procedures with and without a non-thermal atmospheric pressure plasma treatment. In the plasma-drying group (c, d), abundant and well-developed lateral branches of resin tags were observed as a result of improved penetration of adhesive monomers to dentinal canaliculi. (a, b) Wet bonding group, (c, d) plasma-drying group, (e, f) plasma-drying/rewetting group, and (g, h) dry bonding group.

Tables

Table 1. Experimental groups and procedures used in this study

Groups	Surface treatment	procedures Remarks
Group 1	g	Untreated, negative control group
Group 2	c, g	Plasma polymer coating with TEGDMA
Group 3	a, c, g	Plasma surface cleaning and plasma polymer coating with TEGDMA
Group 4	a, b, c, g	Plasma surface cleaning and plasma polymer coating with HMDSO and TEGDMA, consecutively
Group 5	d, e, f, g	Hydrofluoric acid etching and silane application, routine bonding procedure for feldspathic porcelain

a, plasma surface treatment with vaporized DW in helium gas; b, plasma polymer coating with vaporized HMDSO in helium gas; c, plasma polymer coating with vaporized TEGDMA in helium gas; d, etching with 4% buffered hydrofluoric acid gel for 4 min; e, washing and drying with compressed air from a three-way syringe; f, silane coupling agent coating and drying with compressed air from a three-way syringe; g, sequential bonding procedures after surface treatment of the polished surfaces of ceramic blocks, including the immediate coating of the Adper Scotchbond Multi-Purpose (3M ESPE) adhesive, light-curing for 20 s, composite packing into the inner hole of the iris on the specimen surface, and light-curing for 40 s TEGDMA triethyleneglycol dimethacrylate; HMDSO hexamethyldisiloxane

Table 2. Measurements of water contact angles from various ceramic surfaces prepared according to the plasma surface treatment protocols used in this study

Groups	Surface treatments	Contact angle (°)
Polished ceramic surface	a	12.1 ± 1.7
Polishing/water cleaning	a, b	Less than 10
Polishing/water cleaning/TEGDMA plasma coating	a, b, c	Less than 10
Polishing/TEGDMA plasma coating	a, c	Less than 10
Polishing/water cleaning/HMDSO plasma coating	a, b, d	85.3 ± 8.5
Polishing/water cleaning/HMDSO plasma coating /TEGDMA plasma coating	a, b, d, c	30.8 ± 2.6
Polishing/water cleaning/TEGDMA plasma coating/adhesive light-curing (OIL)	a, b, c, e	45.2 ± 3.5

Surface treatments of each group were performed in a sequential manner designated with the following abbreviations: a, polishing with #500 SiC paper; b, plasma surface cleaning with vaporized water in helium gas; c, plasma polymer coating with vaporized TEGDMA in helium gas; d, plasma polymer coating with vaporized HMDSO in helium gas; e, adhesive coating and light-curing for 20 s OIL, oxygen-inhibited layer, the contact angle of the oxygen-inhibited layer remaining on the cured adhesive was measured to approximate the contact angle measurement of the uncured adhesive itself

*TEGDMA triethyleneglycol dimethacrylate; HMDSO hexamethyldisiloxane

Table 3. Shear bond strength (SBS) of the composite resin to various plasma-treated surfaces of feldspathic porcelain and the distribution of fracture modes observed from the fractures due to shear load

Groups (abbreviation)	SBS	Fracture modes		
		Adhesive	Mixed	Cohesive
Group 1 (PUT)	11.5 ± 2.3a§	9	1	0
Group 2 (T)	14.8 ± 3.7a	7	3	0
Group 3 (WT)	20.0 ± 3.9b	3	7	0
Group 4 (WHT)	14.7 ± 4.0ab	10	0	0
Group 5 (FS)	31.0 ± 6.0c	0	0	10

Fracture modes: adhesive fracture, fracture between the polished ceramic surface and the cured adhesive layer; mixed fracture, fracture meandering from the adhesive interface to the ceramic surface, where, as a result, a small fragment of ceramic was observed on the adhesive surface covering the fractured bottom surface of the composite resin in the iris; cohesive fracture of ceramic, oblique fracture of the ceramic adherend PUT untreated except polishing; T, TEGDMA plasma coating after polishing; WT, after polishing, sequential DW plasma treatment, and TEGDMA plasma coating; WHT, after polishing, sequential DW plasma treatment, and plasma polymer coating with HMDSO and TEGDMA; FS, hydrofluoric acid etching and silane coupling agent coating

_ Values are means ± standard deviations in MPa, and sample numbers are 10

§ The same superscript represents no statistically significant difference ($p > 0.05$)

Table 4. Shear bond strength values between composite resin and dental ceramic and their fracture mode distribution according to surface treatment.

	Ceramic surface treatment		Applied r.f. plasma power			SBS (MPa, mean ± sd, n = 20)	Fracture mode (n)		
			Voltage (kV)	Current (mA)	Applied energy (W)		(A)	(M)	(C)
Group 1	As ground (negative control)					16.1 ± 4.3[a†]	20	0	0 [a†]
Group 2	After grinding, TEGDMA plasma-deposited with an input power of:	9 V	1.13	7.07	8.0	25.8 ± 7.1[b]	7	7	6 [b]
Group 3		15 V	1.70	11.31	19.2	26.6 ± 7.4[b]	6	7	7 [b]
Group 4		18 V	1.98	14.14	28.0	29.5 ± 9.3[b,c]	4	9	7 [b]
Group 5	HF and silane coating (positive control)					35.4 ± 6.3[c]	0	0	20 [c]

† The SBS and fracture mode data were analyzed statistically using one-way ANOVA and Kruskal-Wallis tests, respectively. *Post hoc* tests were performed with the Dunnett T3 multiple comparison test for both data sets. All statistical analyses were done at a 5% level of significance. The same superscripts mean that there is no statistical difference between the groups.

Abbreviations: SBS, shear bond strength; A, adhesive fracture; M, mixed fracture; C, cohesive fracture

Table 5. Contact angles of deionized water to variously treated ceramic surfaces and calculated work of adhesion of each surface.

Surface treatments	G	S	T9	T15	T18
Contact angle (degree)	15.9 ± 3.8	26.3 ± 4.4	<10	<10	<10
Work of adhesion (mN/m)	142.7 ± 1.4	137.9 ± 2.6	>144.5	>144.5	>144.5

Abbreviations for surface treatments: G, ceramic surface as ground; S, HF etching and silane coating; T9, TEGDMA plasma-deposited with an input power of 9 V after grinding; T15, TEGDMA plasma-deposited with an input power of 15 V after grinding; T18, TEGDMA plasma-deposited with an input power of 18 V after grinding.

Table 6. Changes in the binding energy (eV) and the sensitivity factor of each peak deconvoluted from the XPS spectra of a narrow scan of each element.

Ceramic surface treatment			Deconvoluted peaks	C1† C1s(C-C)	C2 C1s(C-O-C)	C3 C1s(O=C-O)	O1 O1s(O=C-O)	O2 O1s(C=O‡)
			Sensitivity Factor (SF)	1	1	1	2.93	2.93
Group 1	As ground (negative control)			284.5	286.1	288.2	532.4	531.3
Group 2	After grinding, TEGDMA plasma-deposited with an input power of	9 V		284.5	286.0	288.8	532.4	531.3
Group 3		15 V		284.5	286.0	288.9	532.4	531.3
Group 4		18 V		284.5	286.1	288.7	532.4	531.3
Group 5	HF and silane coating (positive control)			284.5	286.1	288.5	532.4	531.4

† Peak designations: C1, C1s(C-C); C2, C1s(C-O-C); C3, C1s(O=C-O); O1, O1s(O=C-O); O2, O1s(a mixed peak of C=O, -OH, and C-O‡);

‡ a mixed peak of C=O, -OH, and C-O

Table 7. Quantification of the chemical groups present on the ceramic surface after silane coating and plasma treatment at various applied powers using XPS.

Treatment group	Applied voltage (kV)	Atomic concentration(%) of C1s‡			Atomic concentration(%) of O1s		n(O1s)/n(C1s) ratio
		C1§ C1s(C-C)	C2 C1s(C-O-C)	C3 C1s(O=C-O)	O1 O1s(O=C-O)	O2 O1s(C=O¶)	
Group 1		86.0†	9.2	4.8	69.7	30.3	1.76
Group 2	1.13	80.2	13.3	6.4	73.9	26.1	2.30
Group 3	1.70	79.4	14.3	6.4	70.8	29.2	2.39
Group 4	1.98	80.6	12.5	6.8	74.3	25.7	2.04
Group 5		80.1	12.5	7.5	73.2	26.8	1.05

† The area under the photoelectron peak for each element was measured after subtraction of the background intensity using a linear background subtraction method. To compare the area among the peaks and elements, the area was then divided by the sensitivity factor of the peak (Ai/Si).

‡ The atomic concentration (%) of each peak was obtained by dividing each area corrected by the sensitivity factor by the total area of all the peaks of each element ($((Ai/Si/\Sigma(Ai/Si)) \times 100$).

§ Peak designation: C1, C1s(C-C); C2, C1s(C-O-C); C3, C1s(O=C-O); O1, O1s(O=C-O); O2, O1s (a mixed peak of C=O, -OH, and C-O¶);

¶ a mixed peak of C=O, -OH, and C-O

Table 8. Shear bond strength (SBS) between composite resin and dental ceramic and their fracture mode distribution according to various flow rates of 1,3-butadiene gas as plasma-enhanced chemical vapor deposition (PECVD) using an experimental floating electrode dielectric barrier discharge (FE-DBD) jet.

	Ceramic surface treatment		Applied a.f. plasma power			SBS (MPa, mean ± sd, n = 10)	Fracture mode		
			Voltage (kV)	Current (mA)	Applied energy (W)		(A)	(M)	(C)
Group 1	As prepared		−	−	−	$15.6 \pm 3.2^{c\dagger}$	10	0	$0^{b\dagger}$
Group 2	After preparation, PECVD of 1,3-butadiene at flow rates of:	0.5 sccm	1.80	2.86	5.15	20.7 ± 2.9^{b}	9	0	1^{b}
Group 3		2.0 sccm				34.6 ± 5.2^{a}	4	1	5^{ab}
Group 4		3.0 sccm				32.1 ± 7.0^{a}	3	0	7^{a}
Group 5		6.0 sccm				29.8 ± 4.6^{a}	6	0	4^{ab}

† The SBS and fracture mode data were analyzed statistically using one-way ANOVA and Kruskal-Wallis tests, respectively. *Post hoc* tests were performed with the Dunnett T3 multiple comparison test for both data sets. All statistical analyses were done at a 5% level of significance. The same superscripts mean that there is no statistical difference between the groups. Abbreviations: SBS, shear bond strength; A, adhesive fracture; M, mixed fracture; C, cohesive fracture.

Table 9. Quantification of the chemical groups present on the ceramic surface after plasma deposition with various flow rates of 1,3-butadiene using XPS.

Treatment group	Flow rates of precursor gas (sccm)	Atomic concentration (%) of C1s†			O1s		Si2p	n(O1s)/n(C1s) ratio
		C1 C1s(C-C, C=C)	C2 C1s(C-O-C)	C3 C1s(O=C-O)	O1 O1s(-OH)	O2 O1s(-Si-O-)	Si1 Si2p(-Si-Si-)	
Group 1	-	21.1†	3.2	1.2	37.6	12.1	24.8	1.96
Group 2	0.5	20.3	5.2	2.3	28.3	14.8	29.1	1.54
Group 3	2.0	58.5	15.1	4.0	15.2	1.2	6.0	0.21
Group 4	3.0	64.0	17.6	4.8	12.5	0.0	1.1	0.15
Group 5	6.0	65.1	15.3	4.3	12.6	0.0	2.7	0.15

† The area under the photoelectron peak for each element was measured after subtraction of the background intensity using a linear background subtraction method. To compare the area among the peaks and elements, the area was then divided by the sensitivity factor of the peak (A*i*/S*i*). The atomic concentration (%) of each peak was obtained by dividing each area corrected by the sensitivity factor by the total area of all the peaks of each element (($A_i/S_i/\Sigma(A_i/S_i)$) x 100) (Clark and Thomas, 1978; Chan, 1994).

Table 10. Shear bond strength (SBS) between composite resin and dental ceramic and their fracture mode distribution according to various precursor monomers for plasma-enhanced chemical vapor deposition (PECVD) using an experimental floating electrode dielectric barrier discharge (FE-DBD) jet.

Ceramic surface treatment	Contact angle measurement (degree, n = 5)	Work of Adhesion (*Wa,* x 10^{-2} N/m)	SBS† (MPa, n = 20)	Fracture mode‡		
				(A)	(M)	(C)
Group 1 (negative control)	15.4 ± 1.2	143.0 ± 0.4	20.3 ± 5.2^{c}	20	0	0
Group 2 (H_2O)	< 10.0	>144.5 ± 0.0	26.3 ± 6.3^{b}	12	6	2
Group 3 (HMDSO)	101.3 ± 3.4	58.5 ± 4.3	11.5 ± 2.7^{d}	20	0	0
Group 4 (benzene)	63.3 ± 1.4	105.5 ± 1.6	28.4 ± 5.4^{b}	14	1	5
Group 5 (HMDSO/benzene)	73.5 ± 2.3	93.5 ± 2.8	32.4 ± 3.5^{a}	10	1	9

† The SBS data were analyzed statistically using one-way ANOVA. *Post hoc* tests were performed with the Duncan's multiple comparison test at a 5% level of significance. The same superscripts mean that there is no statistical difference between the groups.

‡ The fracture mode data were statistically analyzed using Chi-square test at a 5% level of significance. There was a statistically significant difference in the fracture modes among the groups (Pearson $x^2 = 38.707$; p = 0.000).

Abbreviations: HMDSO, hexamethyldisiloxane; A, adhesive fracture; M, mixed fracture; C, cohesive fracture.

Table 11. Quantification of the chemical groups present on the ceramic surface using X-ray photoelectron spectroscopy (XPS), after plasma-enhanced chemical vapor deposition (PECVD) of water, benzene, and hexamethyldisoloxane (HMDSO) using an experimental floating electrode dielectric barrier discharge (FE-DBD) jet.

Ceramic Surface Treatment†	Atomic concentration‡ (%) of									n(O1s) /n(C1s) ratio
	C1s				O1s			Si2p		
	C1 (C-C or C=C)	C2 (C-O)	C3 (C=O)	C4 (O-C=O)	O1 (Si-OH)	O2 (O-Si-O)	O3 (C=O or C-O)	Si1 (Si-O-C)	Si2 (O-Si-O)	
Group 1	21.36	2.33	0.62	1.44	12.14	31.59	4.76	0	25.77	1.75
Group 2	16.91	5.47	1.87	3.98	15.64	36.60	3.16	0	22.37	1.75
Group 3	29.34	2.63	0	0	0	32.83	3.53	0	31.67	1.14
Group 4	49.75	21.7	6.97	4.02	0	13.79	2.21	1.12	0.44	0.19
Group 5	50.27	14.09	9.5	3.67	0	16.48	4.35	1.11	0.53	0.27

† In each group, the ceramic surface was treated with the PECVD of the assigned monomers, such as, Group 1 (negative control group), no treatment; Group 2, H_2O; Group 3, HMDSO; Group 4, benzene; Group 5, HMDSO/benzene.

‡ The area under the photoelectron peak for each element was measured after subtraction of the background intensity using a linear background subtraction method. To compare the area among the peaks and elements, the area was then divided by the sensitivity factor of the peak (A*i*/S*i*). The atomic concentration (%) of each peak was obtained by dividing each area corrected by the sensitivity factor by the total area of all the peaks of each element ((A*i*/S*i*/Σ(A*i*/S*i*)) x 100).

Table 12. Microshear bond strength of resin composites to plasma polymer-deposited enamel surface, and the failure modes of the fractured specimens according to the surface treatment and the measurement time

Treatment group		Measurement time†		Two-way ANOVA results		Failure mode‡	
		24 hour	TC			24 hour	TC
Control	Group 1 : (-) control	25.2 ± 5.1^{aA}	21.3 ± 3.1^{aB}	Main effect:		2/21	0/22
Plasma Treatment	Group 2 : No monomer	29.4 ± 4.9^{abA}	24.6 ± 4.0^{bA}	Treatment TC	$p = 0.000$ $p = 0.000$	1/21	0/22
	Group 3 : Benzene	32.6 ± 5.9^{bA}	23.3 ± 2.0^{abB}	Interaction effect:		1/21	0/22
	Group 4 : 1,3-butadiene	33.4 ± 3.9^{bA}	22.6 ± 2.4^{abB}	Treatment x TC	$p = 0.000$	0/21	0/22

† Bond strength measurements were performed at two measurement times, at 24 hours from bonding and after thermocycling

‡ Numbers in the failure mode indicate the number of the enamel cohesive fracture over the total number of the specimens tested.

Table 13. Changes in the contact angle measurements of the etched enamel surface after plasma surface treatments with or without monomers

Surface conditions		Contact angle (degree)
Etched enamel surface†	(Group 1)	10 >
Etched enamel surface† after treatment with	He plasma (no monomer, Group 2)	10 >
	He plasma and benzene (Group 3)	56.6 ± 4.2
	He plasma and 1,3-butadiene (Group 4)	65.0 ± 8.5

† Etched enamel surface was prepared consistently using the same procedure of etching with 37 wt% phosphoric acid (SBMP etchant, 3M ESPE) for 15 seconds, rinsing with copious amounts of water for 15 seconds, and drying completely with compressed air.

Table 14. Quantification of the chemical groups present on the etched enamel surface after plasma surface treatments with or without monomers

Surface Treatment		Atomic concentration of C1s (%)				Atomic concentration of O1s (%)			n(O1s) /n(C1s) ratio
		C1† C1s(C-C, C=C, C-H)	C2 C1s(C-O)	C3 C1s(C-O-C)	C4 C1s(C=O)	O1 O1s(O=C)	O2 O1s(-OH)	O3 O1s(O-C-O)	
	Binding energy (eV)	284.5	285.9	287.2	288.8	531.5	532.5	533.7	
Etched enamel surface		48.8	0	1.8	0	14.0	21.9	13.5	0.98
Plasma deposition	Benzene	54.8	18.0	5.9	2.0	5.2	12.1	2.2	0.24
	1,3-butadiene	62.4	15.7	5.3	2.0	2.8	10.0	1.9	0.17

† Peak designation: C1, C1s(C-C, C=C, and C-H) at 284.5 eV; C2, C1s(C-O) at 285.9 eV; C3, C1s(C-O-C) at 287.2 eV; C4, C1s(C=O) at 288.8 eV; O1, O1s (O=C) at 531.5 eV; O2, O1s (-OH) at 532.5 eV; O3, (O-C-O) at 533.7 eV.

Table 15. Degree of Conversion (Unit, %; n = 5) of the plasma-polymerized layers between two potassium bromide (KBr) pellets measured using FT-IR

Monomer used for deposition of plasma polymer layer†	Degree of Conversion‡	
	Plasma-polymerized for 15 minutes	Matured in a dark room at 55°C for 7 days
Benzene	18.3 ± 14.4	82.6 ± 13.2
1,3-butadiene	0 ± 11.8*	49.3 ± 15.6

* The absorbance of the plasma-deposited layer of 1,3-butadiene was too weak to calculate the degree of conversion.

† Due to the nanometer-scale of the plasma deposition, each precursor monomer was deposited on a KBr pellet for an extremely long deposition time of 15 minutes for FT-IR detection.

‡ The spectra were obtained as uncured, cured, or matured after TC. The uncured spectrum was obtained from a special accessory in which a gas mixture of He and the assigned monomer was filled without plasma. The cured one was obtained from a KBr pellet on which the gas mixture was deposited with activated plasma, and the matured one from a KBr pellet matured in a dark container at 55°C for seven days in order to simulate thermal aging.

Table 16. Microtensile bond strengths (in MPa) of resin composite to the dentin surfaces treated with different plasma jets at 24 h and after 5,000 thermocycles

	At 24 h (n = 20)	After thermocycling (*5,000 cycles,* n = 14)
Control (no plasma treatment)	45.9 (14.5)^{Aa}	40.4 (11.5)^{Aa}
Pulsed plasma (1.1 kW·h)	66.2 (16.0)^{Ab}	77.9 (8.8)^{Bb}
Conventional plasma (21.6 kW·h)	76.9 (20.0)^{Ab}	78.1 (12.6)^{Ab}

The numbers in the parentheses are standard deviations.

Mean values with the same upper case superscript letters indicate no significant difference within the same column, and those with the same lower case superscript letters indicate no significant differences within the same row.

Table 17. Weibull moduli (*m*) and characteristic strengths (σ_θ in MPa) with corresponding 90% confidence intervals (CI) of resin composite bonded to the dentin surfaces treated with different plasma jets at 24 h and after 5,000 thermocycles

	At 24 h (*n* = 20)			After thermocycling (*5,000 cycles, n* = 14)		
	m [CI]	σ_θ [CI]	*r**	*m* [CI]	σ_θ [CI]	*r**
Control (no plasma treatment)	3.99 [3.45 - 4.34]	50.7 [23.7 - 67.2]	0.963	4.07 [3.35 - 4.79]	44.6 [21.5 - 58.4]	0.946
Pulsed plasma (1.1 kW·h)	4.82 [4.48 - 5.17]	72.2 [39.0 - 90.7]	0.978	10.30 [8.63 -11.96]	81.7 [61.2 - 90.9]	0.954
Conventional plasma (21.6 kW·h)	4.58 [4.33 - 4.83]	84.2 [44.0 - 107.0]	0.991	6.41 [5.27 - 7.55]	84.0 [55.2 - 99.8]	0.945

* Coefficient of correlation

Table 18. Weibull parameters (*m*, Weibull modulus; σ_θ, characteristic strength in MPa) of the microtensile bond strength of resin composite to dentin for different adhesion procedures with and without a non-thermal atmospheric pressure plasma treatment.

Group	*n*	*m* (90% CI)	σ_θ (90% CI)	*r*
Wet bonding	24	3.45 (3.26-3.65)	58.1 (24.6-79.8)	0.988
Plasma-drying	24	4.93 (4.53-5.33)	66.8 (36.5-83.4)	0.976
Plasma-drying/rewetting	24	4.50 (4.25-4.75)	64.3 (33.2-82.0)	0.989
Dry bonding	24	3.39 (3.17-3.60)	32.2 (13.4-44.5)	0.985

CI, confidence interval; *r*, correlation coefficien

국문초록

플라즈마 처리가 세라믹 및 치질의 표면 특성과 접착력에 미치는 효과 분석

한 금 준

서울대학교 대학원 치의과학과 치과생체재료과학 전공

(지도교수 조 병 훈)

목 적 *:* 대기압 플라스마는 저렴한 비용의 환경 친화적인 건식 공정을 사용하는 비교적 간단한 시스템을 이용하여 코팅된 표면의 성질을 쉽게 변화 시킬 수 있다. 접착을 위해, 플라즈마는 극성 작용기를 유도하거나 이온결합의 변화를 통해 시료 표면상에 다양한 화학적 활성을 구현하는 데 사용될 수 있다. 본 연구에서는 플라즈마를 이용한 폴리머 코팅의 효과가 세라믹과 복합 레진의 접착력에 미치는 영향을 평가하였고, 플라즈마를 치질에 직접 적용하여 치질과 복합 레진의 접착력 및 내구성에 미치는 효과를 평가하였다.

방 법 : 전단접착강도(Shear bond strength, SBS) 및 마이크로 전단접착강도(Micro-shear bond strength, MSBS) 시험을 사용하여 플라즈마 중합체 코팅이 접착에 미치는 효과를 평가하였다. 플라즈마 코팅된 표면

은 Fourier transform infrared spectrophotometer (FTIR)과 X-ray photoelectron spectroscopy (XPS) 및 접촉각 측정을 사용하여 특성을 확인하였고, 파단 된 표면을 Scanning electron microscopy (SEM) 및 Energy dispersive spectroscopy (EDS)를 사용하여 평가하였다. 또한, Focused ion beam (FIB), Transmission electron microscopy (TEM) 및 EDS를 사용하여 표면의 화학적 구조 및 조성을 각각 검증 하였다.

열순환처리 (Thermocycling, TC) 전과 후에 상아질과 복합 레진 사이의 접착력과 내구성은 마이크로 인장강도(Micro-Tensile bond strength, MTBS)로 시험하였다. 측정값은 Weibull 분석으로 해석하였다. 상아질 계면에 형성된 하이브리드 층은 Mirco-Raman Spectroscopy 및 SEM으로 분석하였다.

결 과 : 플라즈마 폴리머 코팅으로 처리 된 그룹 중, 헬륨 가스에서 water와 triethyleneglycol dimethacrylate (TEGDMA) 플라즈마를 순차적으로 증착한 세라믹 표면의 접착력이 아무 처리되지 않은 접착력 보다 현저히 높았다 ($p < 0.05$). 또한, 가장 높은 전압에서 플라즈마 증착으로 얻어진 SBS는 HF acid 과 Silane coupling agent에 의해 얻은 접착력 결과와 통계적으로 유사했다. 1,3-butadiene의 플라즈마 증착은 유속이 2 sccm 이상의 그룹에서 대조군 보다 접착력에서 효과가 있었다. Benzene의 증착 전에 HMDSO의 플라즈마 증착한 군에서는 HF acid와 Silane coupling agent에 의해 얻은 접착력 결과와 통계적으로 차이가 없었다. 지르코니아 표면에 플라즈마를 이용한 Tetramethylsilane (TMS)와 Benzene의 순차적 증착은 통상적인 방법의 Z-Prime Plus

적용의 접착력에 비해 약 2 배 높은 전단접착강도(SBS)를 보였다.

법랑질 표면에 benzene과 1,3-butadiene의 플라즈마 폴리머 증착은 복합 레진과의 접착력(MSBS)을 향상시켰다 ($p < 0.05$). 이 증착은 법랑질의 접착력을 향상 시켰지만, 내구성은 향상시키지 못했다. 그러나 플라즈마 증착 후 폴리머의 독성에 대한 용해도 평가는 향후에 연구가 필요할 것이다.

상아질에서는 재 습윤 여부와 상관없이 플라즈마 건조 그룹은 임상적 습윤접착 방법 및 건식접착 방법보다 유의하게 높은 접착강도를 나타냈다 ($p < 0.05$). Micro-Raman spectroscopy 분석을 통해 플라즈마 건조가 접착제의 침투력 및 중합 효능을 향상시키는 것으로 나타났다. 그리고 플라즈마 건조는 TC 후 접착강도를 감소시키지 않았다

결 론 : 본 연구에서 플라즈마 폴리머 코팅 기술이 세라믹 및 치질의 접착력을 향상시키는데 기여할 수 있다는 것을 확인하였다. 특히, 1,3 부타디엔 또는 벤젠과 같은 모노머를 이용한 플라즈마 코팅은 C=C 이중결합의 증착을 통해 복합 레진과의 접착력을 향상시켰다. 상아질 표면에서는 재 습윤 여부와 상관없이 He gas를 사용한 플라즈마를 직접 적용하여 건조한 그룹은 상아질과 복합 레진과의 접착력과 내구성을 향상시켰다. 복합 레진을 세라믹 및 치질에 접착시키는데 플라즈마 적용은 유망한 방법 일 것이다.

주요어 : 플라즈마 처리, 세라믹, 치질, 접착, 폴리머 증착, 내구성

학 번 : 2013-21808